CONTOUR Imagers Characterization Report SRO-02M-30

Mary Ruth Keller & Bruce Gotwols

12th December 2002

Page intentionally left blank.

Contents

Chapter 1

Introduction and Methodology

The goal of this analysis is to provide quantitative information on the properties and calibration of the CONTOUR (COmet Nucleus TOUR) visible imaging sensors, CRISP (Contour Remote Imaging SPectrograph) and CFI (Contour Forward Imager). CRISP could also be operated as a spectrometer in the infrared, but that analysis is contained in a separate report by a different contributor. The data used are from an extensive set of pre-mission calibration tests conducted in the JHU/APL Optical Calibration Facility (OCF). Its physical lay-out and capabilities have been described in numerous publications by various contributors in the open literature (see References # 1, 6, and 7).

The sensors measure light intensity in engineering units referred to as image data numbers. These data numbers (DN) are generally converted to radiance, R, with physical units $W - m^{-2} - \mu m^{-1} - sr^{-1}$, using the well-known calibration equation (Reference # 7):

$$R_{x,y,f,T,\tau_e} = \frac{100.0 * [DN_{x,y,f,T,\tau_e} - Dark_{x,y,f,\tau_e,T}] - Smear_{x,y,\tau_e}}{Flat_{x,y,f} * Coef_f * Resp_{f,T} * \tau_e} \tag{1.1}$$

where: $DN_{x,y,f,T,t,c}$is raw DN measured in the pixel in column x, row y, through filter f at exposure time τ_e and temperature T,

$Dark_{x,y,f,T}$ is the dark level in DN modeled for this pixel at column x, row y at exposure time τ_e and temperature T,

$Smear_{x,y,\tau_e}$is the scene-dependent readout smear for the pixel with exposure time τ_e,

$Flat_{x,y,f}$ is the flat field for filter f,

$Coef_f$ is the coefficient for converting dark-removed, flat-field, and smear-corrected DN from filter to radiance, for a baseline exposure time of 1 second,

$Resp_{f,T}$ is the responsivity for this filter at temperature T, relative to a baseline, and,

τ_e is the exposure time in milliseconds.

In this analysis, the quantities above were characterized by first, extracting data from the ASCII, and, when necessary, the binary, headers in the calibration images collected during the pre-environment, post-environment, and in the case of CFI, the 'final' post-environment calibrations conducted prior to instrument integration and testing. Second, statistics on the dark columns and the imagery itself were calculated in IDL and stored in associated binary data files along with the header information. By examining the results of tests conducted for dark currents, filter response, flat-field linearity, temperature dependence, instrument characteristics were derived.

The report itself is divided into two main sections, one to characterize the dark columns, and one for the imager properties. Dark column dependencies on exposure time, temperature, row number, and the relationship between dark columns and dark images are derived. A final dark column section examines noise and corruption encountered in the calibration data. The image characteristics of frame transfer smear, responsivity, noise, problems with sub-sampling the images (binning), and sub-system calibrations are detailed in the imager section. Finally, some conclusions and lessons learned are presented.

Chapter 2

Dark Column properties

2.1 Dark column properties

2.1.1 CRISP

Dark series data were acquired during post-environmental calibrations using the OCF (Optical Calibration Facility) Monochromator/Collimator (M/C) Point source. Throughout this set of tests, the CRISP filter wheel was set at 6, where the center wavelength was 610 nm with a bandwidth of 40 nm. Calibration data were acquired for four different sizes of images: full size, 2 by 2 binning, 4 by 4 binning, and 8 by 8 binning. Exposure times were varied from 0-512 milliseconds. Figure 2.1 shows the dependence of dark column mean on exposure time. The line through the data connects the mean values for each exposure time, with the spread in values due to the differences in the images sizes, although there was no clustering at each exposure time for image size. As a function of exposure time, the mean dark level could be approximated as uniform below 16 milliseconds at a value of 219.56 DN. Above 16 milliseconds, the mean dark level can be approximated as linear in log of time, with a slope of 0.2019 DN/log(millisecond) and an intercept of 219.298 DN. Unlike CFI, the small dynamic range of the dark column means for CRISP (0.4 DN over 500 milliseconds) made it difficult to derive a linear fit to the data. After many attempts, the best results were obtained by fitting to the 100 to 500 millisecond range of exposure times for the unbinned imagery, which the vast majority of the images generated in the calibrations were. As shown in figure 2.2, over this limited range of exposure times (τ_e, in milliseconds), the mean dark level can be approximated as:

$$DN(darkcolumn) = 0.00012293\tau_e + 219.78 \tag{2.1}$$

Regardless of the length of exposure time, the average dark column value never rose above 219.9 DN. Examination of saturated data obtained when viewing the white integrating sphere indicated that except in case of dark column corruption (see Section 2.5.1), the mean dark column value remained below this value.

Finally, although the standard deviations for the four dark columns had a lower average value than the mean of the dark image standard deviations, the dark column standard deviations were more variable than the standard deviation of the corresponding dark images. This is not surprising, since there were two orders of magnitude fewer points in the dark columns than in the dark images. Figure 2.3 shows the standard deviations for the image portion and the dark columns in each image in this dark series.

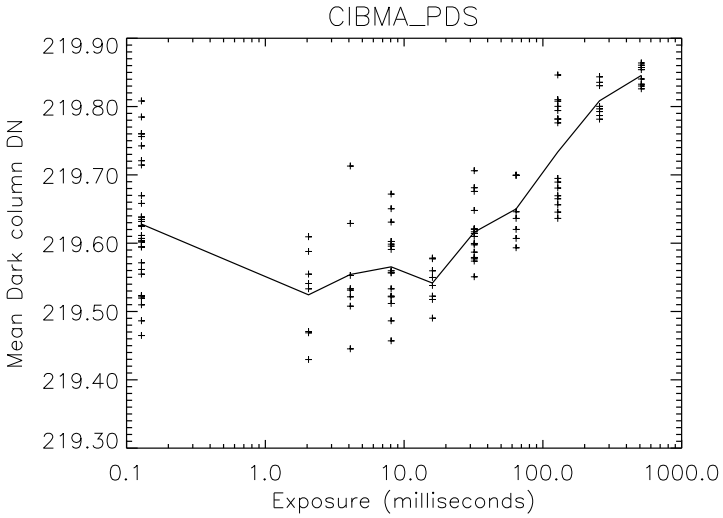

Figure 2.1: Dark column mean as a function of exposure time for the CRISP post-environment dark series tests plotted with exposure time as semi-log. Line connects mean of dark values for each exposure time.

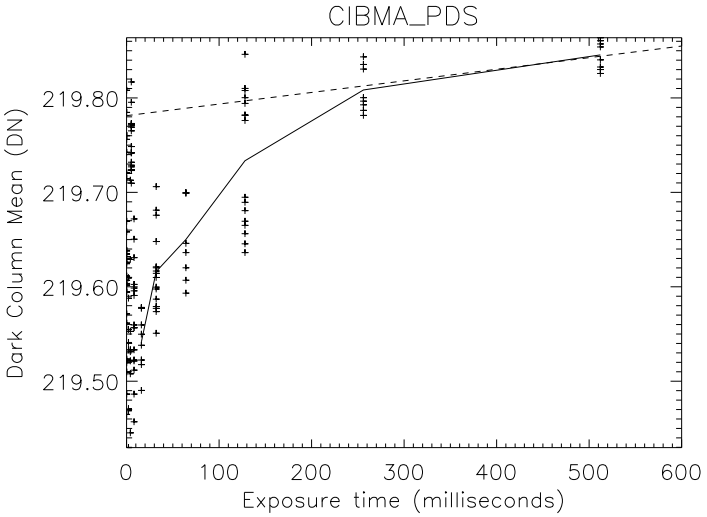

Figure 2.2: Dark column mean as a function of exposure time for the CRISP post-environment dark series tests plotted linearly. Solid line connects mean of dark values for each exposure time. The dashed line is the linear fit for data between 100 and 500 milliseconds.

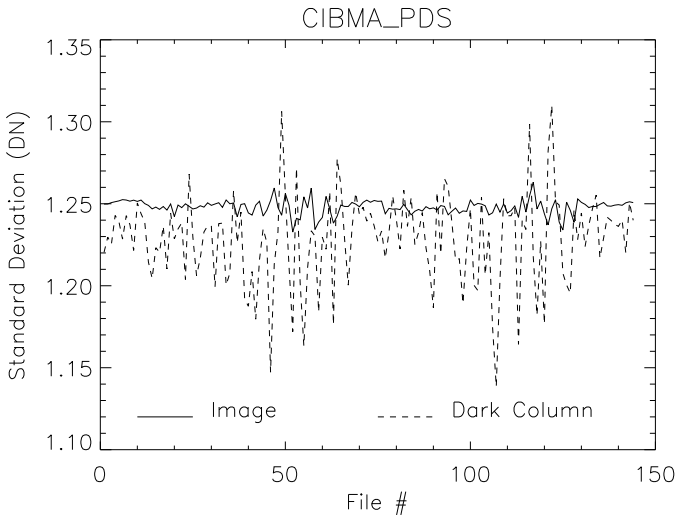

Figure 2.3: Image portion standard deviations (solid line) and dark column standard deviation (dashed line) for the CRISP post-environment dark series tests.

2.1.2 CFI

As with CRISP, dark series data were acquired for CFI during post-environmental calibrations in tests using the OCF M/C point source. Throughout this set, the CFI filter wheel was set at 4, where the center wavelength was 620 nm with a bandwidth of 4 nm. The light from the Halogen and Xenon lamps was fully attenuated, but this did not mean there was a total absence of light. About 6 DN of room illumination was still sensed by the imager in the OCF. Exposure times were varied from 0-5002 milliseconds. The OCF vacuum chamber was set to three different temperatures: -30 °, 0°, and 30°. Figures 2.4, 2.5, and 2.6 show the effects of temperature and exposure time on the mean dark columns. Fits to all three data sets are as follows (where τ_e is the exposure time in milliseconds):

$$Cold(-33°C) : DN(darkcolumn) = 0.000033036 * \tau_e + 232.93 \tag{2.2}$$

$$Intermediate(-7°C) : DN(darkcolumn) = 0.00031871 * \tau_e + 224.64 \tag{2.3}$$

$$Warm(26°C) : DN(darkcolumn) = 0.013678 * \tau_e + 221.94 \tag{2.4}$$

The warm data were acquired at a temperature much higher than would ever have been encountered had the instrument been used in space and are being reported here for completeness.

2.2 Comparison of Dark column properties with dark image properties

2.2.1 CRISP

The dark series data discussed in Section 2.1.1 provided a comparison of the dark column properties and the dark image properties. Figure 2.7 shows the dark column average plotted against the dark image mean for this test. A linear

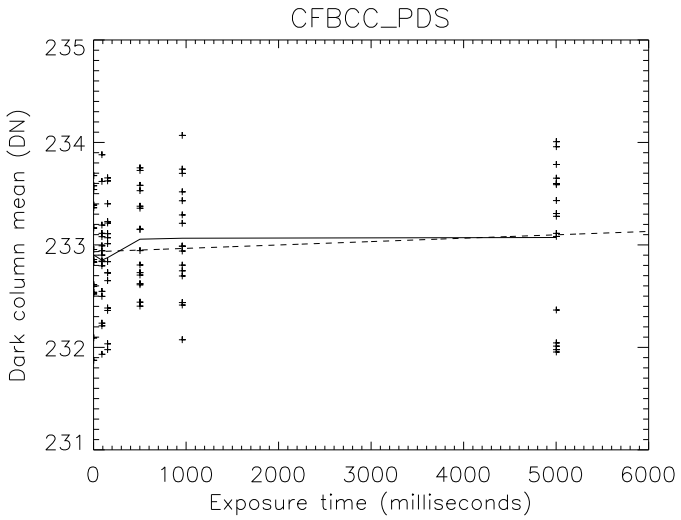

Figure 2.4: Dark column means versus exposure time in milliseconds for CFI post-environment dark series tests under 'cold' conditions. The solid line is the mean value for that exposure time, and the dashed line is a linear fit to the data. The average detector temperature for the run was -33 °C.

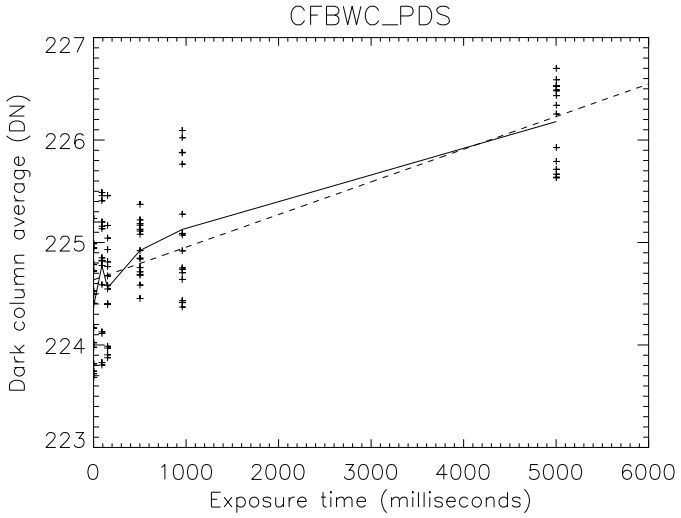

Figure 2.5: Dark column means versus exposure time in milliseconds for CFI post-environment dark series tests under 'intermediate' conditions. The solid line is the mean value for that exposure time, and the dashed line is a linear fit to the data. The average detector temperature for the run was -7 °C.

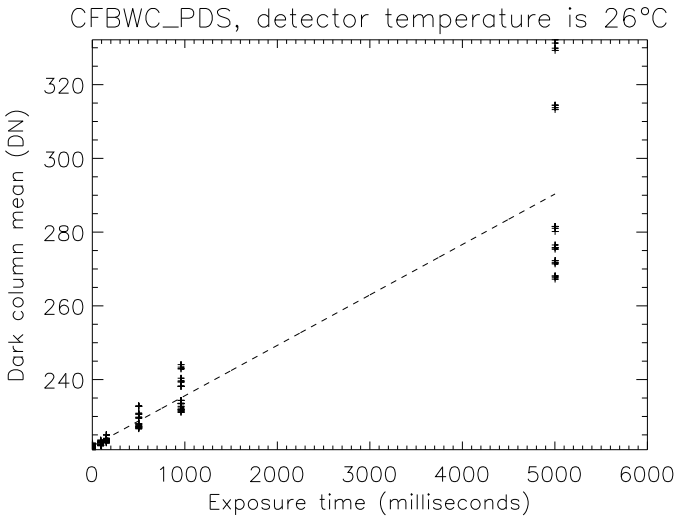

Figure 2.6: Dark column means versus exposure time in milliseconds for CFI post-environment dark series tests under 'warm' conditions. The dashed line is a linear fit to the data. At these scales, the line connecting the mean values lies on the data fit, so is not shown separately here. The average detector temperature for the run was 26 °C.

regression between the two was not calculated because the dark column mean distribution was so highly parabolic at least a third-order fit would be required to describe the data.

A more meaningful calculation is the difference between the image mean and the dark column mean plotted as a function of image mean (see Figure 2.8). The different symbols refer to separate exposure times, with the asterisks indicating 512 millisecond (points cluster above 220.1 DN image mean and 0.2 DN image minus dark difference) and the diamonds 256 millisecond (points cluster above 219.9 DN image mean and 0.08 DN image minus dark difference) exposure times. The remaining exposure time clusters overlap on this linear plot, so are not differentiated with separate symbols. With the exception of the longest exposure time, the difference between the image mean and the dark column mean never exceeded 0.2 DN. The average difference between the dark columns and the dark images was found to be 0.0557 DN with a standard deviation of 0.0660 DN. In practice, the dark column DN's may be treated as equivalent to the dark image DN's, with a error of <0.3 DN. If the difference values are plotted against exposure time (see Figure 2.9), the data show a slight dependence on exposure time above 16 milliseconds, but remain constant below that. A polynomial fit to the data is as follows (where τ_e is exposure time in milliseconds):

$$DN_{image-darkcolumn} = 0.00000076320\tau_e^2 + 0.000049064\tau_e + 0.049198 \tag{2.5}$$

2.2.2 CFI

The post-environment dark series tests for CFI discussed in Section 2.1.2 may also be used to determine the relationship between dark image means and dark column means. While the CRISP imager exhibited essentially no linear trend and had variability less than 1 DN, the CFI imager had a larger dynamic range in both dark image mean and dark column mean, which increased with temperature. Figures 2.10, 2.11, and 2.12 show the effects of temperature on the dependence of image mean on dark column mean. Fits to all three data sets are as follows:

$$Cold(-33°C) : I_{mean}(DN) = 1.0070DC_{mean}(DN) - 3.3911 \tag{2.6}$$

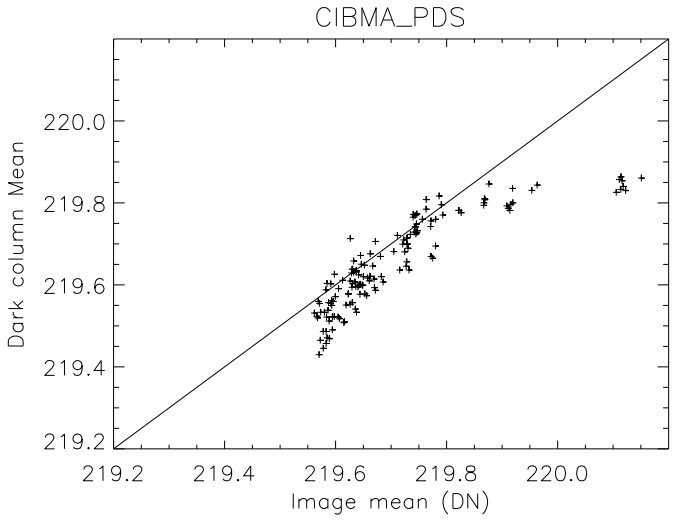

Figure 2.7: Plot of image mean versus dark column mean for different exposures for the CRISP post-environment dark series tests. The line indicates perfect agreement between the two parameters.

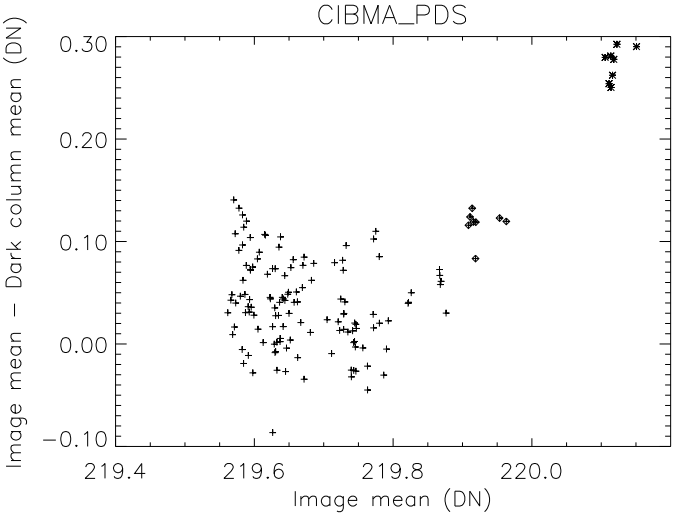

Figure 2.8: Difference between image mean and dark column mean as a function of image mean for the CRISP post-environment dark series tests. The different symbols indicate different exposure times.

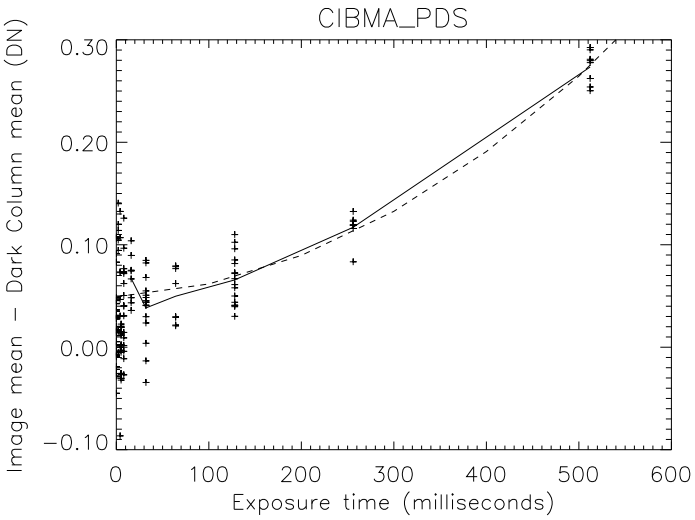

Figure 2.9: Difference between mean of dark image and mean of dark columns plotted for different exposures for the CRISP post-environment dark series tests. Solid line connects mean of difference values for different exposure times, the dashed line a second-order fit to the data.

$$Intermediate(-7°C) : I_{mean}(DN) = 1.0717 DC_{mean}(DN) - 17.9004 \tag{2.7}$$

$$Warm(26°C) : I_{mean}(DN) = 0.9813 DC_{mean}(DN) + 2.2983 \tag{2.8}$$

The warm data fail to follow the same trend as the intermediate and cold data, but, as these were acquired at a much higher temperature than would ever have been encountered in space, they are reported only for completeness.

2.3 Dark Column Properties as a function of Temperature

2.3.1 CRISP

Figure 2.13 shows the the final test of the post-environment calibrations, a set of dark series runs collected from the CRISP sensor over the expected operating range of temperatures. The dark column average is plotted in the figure as a function of detector temperature, since this was the calibrated (and functional) heat sensor nearest the CCD itself.

According to the master calibration record, three exposure times were intended for this data series test: 10 milliseconds, 500 milliseconds, and 980 milliseconds. However, data were acquired at only two exposure times: 10 and 500 milliseconds. But, given the already-demonstrated slight dependence of dark column average on exposure time, temperature effects should exceed those due to exposure time for dark series data. Also according to the master calibration record, nine runs were acquired during this test. For the first run, the chiller temperature was set to -55 $°C$. For the second run, it was set to -40$°C$. For the remainder of the runs, it was raised in 5$°C$ or 10$°C$ increments until, for the final run (#9), the chiller temperature was 0$°C$. Even though the target chamber was given 30 minutes and more to come to equilibrium after each chiller temperature change, the coldest measured temperature was -37.4 $°C$, and this only with the second run. The first run, supposedly conducted at the coldest temperature setting, actually yielded slightly higher dark column values (Figure 2.13). It may have been that the CCD was still slightly warmer

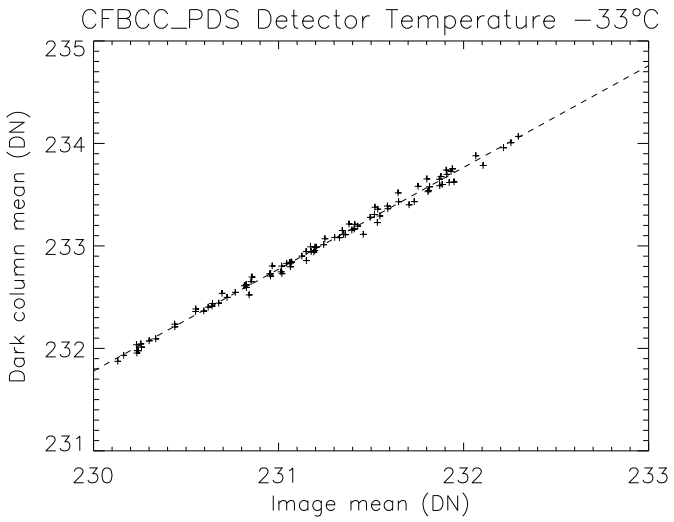

Figure 2.10: Dark column mean as a function of image mean for the cold temperature CFI post-environment dark series tests. The dashed line is a linear fit to the data, collected at a mean temperature of -33 °C.

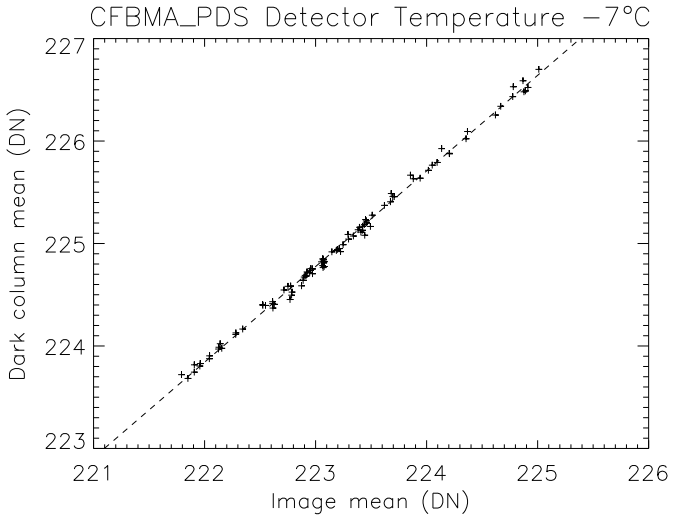

Figure 2.11: Dark column mean as a function of image mean for the intermediate temperature CFI post-environment dark series tests. The dashed line is a linear fit to the data, collected at a mean temperature of -7 °C.

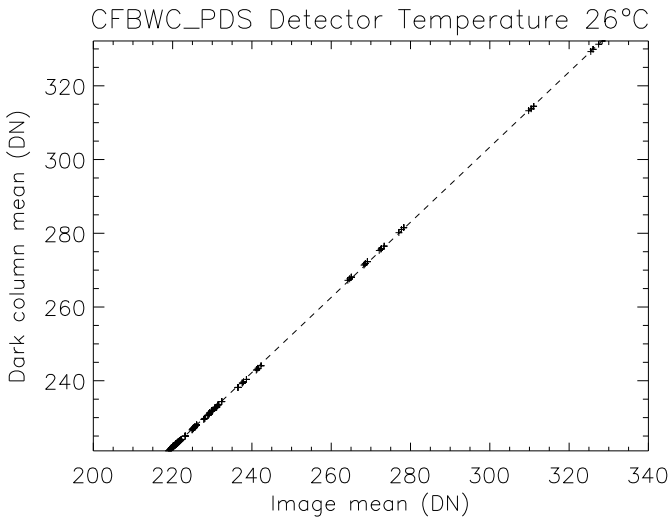

Figure 2.12: Dark column mean as a function of image mean for the warm temperature CFI post-environment dark series tests. The dashed line is a linear fit to the data, collected at a mean temperature of 26 °C.

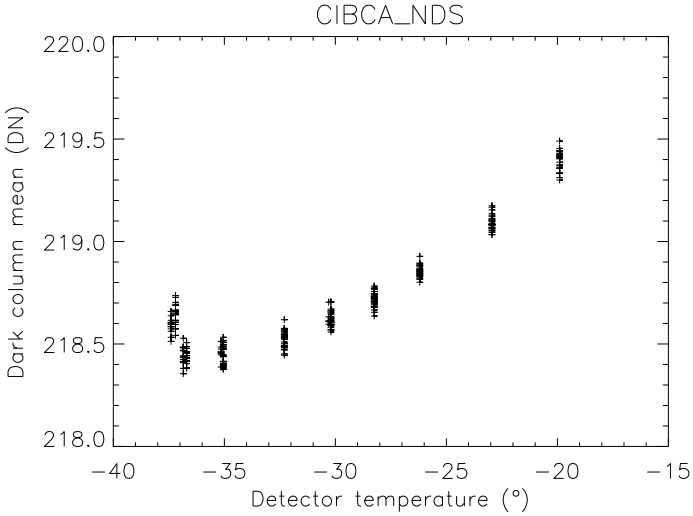

Figure 2.13: Dark column mean as a function of detector temperature for the CRISP post-environment dark series temperature tests.

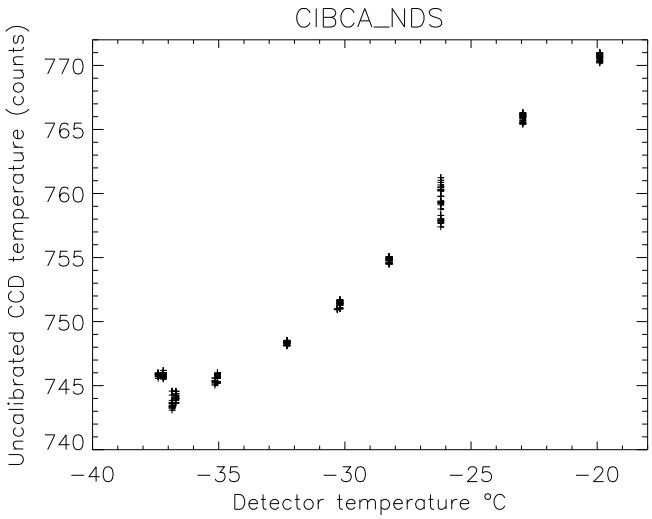

Figure 2.14: Uncalibrated CCD temperature sensor counts versus detector temperature for the CRISP post-environment dark series temperature tests.

than the rest of the chamber, since the detector temperature sensor was close to, but not on the CCD itself. To check that these measurements are actually from a slightly warmer CCD condition, temperature sensors closer to or on the CCD are required, and, fortunately, there were two such instruments available. There was a separate temperature sensor mounted closer to the CCD, which, when functional, was calibrated to give readings as accurately as the detector temperature sensor would. In addition, the Thomson TH7888A CCD has a temperature sensor on the CCD which was uncalibrated during the OCF tests. For this series, the calibrated temperature sensor closer to the CCD was not functioning; however, the uncalibrated temperature sensor directly on the CCD was. Figure 2.14 shows the uncalibrated CCD temperature sensor data plotted against the detector temperature and verifies that this first run was acquired with the CCD at a slightly higher temperature than the second (2 uncalibrated counts higher).

Since the calibration from counts to temperature is unknown for the on-board CCD temperature sensor, other than that the counts increased with temperature, the higher uncalibrated values for the first run were taken to have verified that the chamber was hotter at that time. Thus, the anomalously warmer first run was excluded from further analysis for the present (see Figure 2.15).

Once the set containing accurate temperature-dependent data was determined (Runs 2-9), a simple parabolic relationship between the dark column average and detector temperature emerges that is essentially independent of exposure time, as shown in Figure 2.15. Here, the crosses indicate data for exposure times of 10 milliseconds, and the asterisks data for 500 millisecond exposures. The 500 millisecond exposure data have been displaced in temperature by 0.5 $^{\circ}C$ to show the overlap in data. The maximum variation in any run at a given temperature is 0.15 DN, with little exposure time dependence. Figure 2.16 shows the dark column averages plotted against the uncalibrated CCD temperature sensor. Here, too, the dark column mean is a parabola independent of exposure time.

Using the detector temperature sensor, then, the dependence of dark column mean (DN) on detector temperature (T_d), is calculated to be:

$$DN = 222.61 + 0.21804T_d + 0.0028419{T_d}^2 \tag{2.9}$$

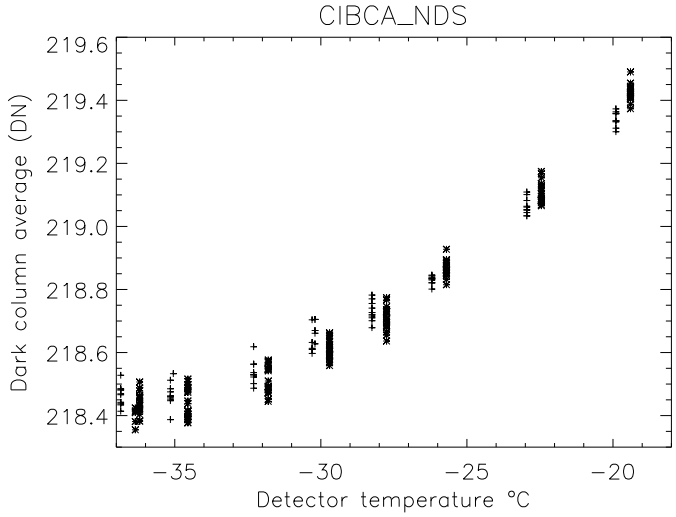

Figure 2.15: Dark column mean as a function of detector temperature for the CRISP post-environment dark series temperature tests. The crosses are for 10 millisecond exposure time, the asterisks are for 500 millisecond exposures. The 500 millisecond exposure data have been displaced in temperature by 0.5 $°C$ to show the overlap in data.

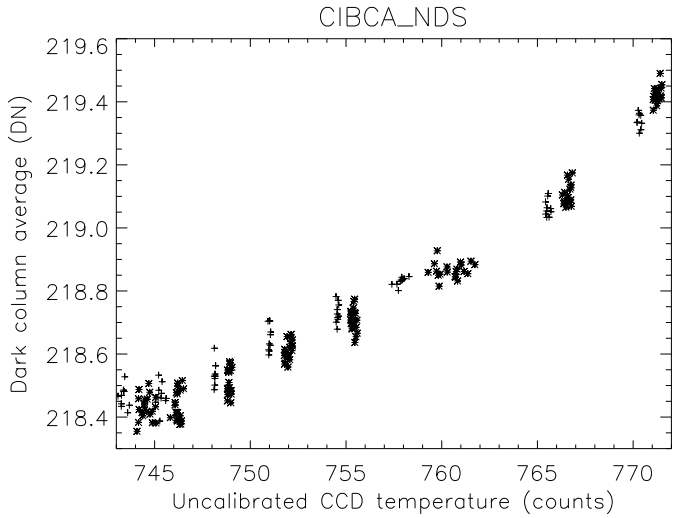

Figure 2.16: Dark column mean as a function of uncalibrated CCD temperature for the CRISP post-environment dark series temperature tests. The crosses are for 10 millisecond exposure time, the asterisks are for 500 millisecond exposures. The 500 millisecond exposure data have been displaced in temperature by 0.5 $°C$ to show the overlap in data.

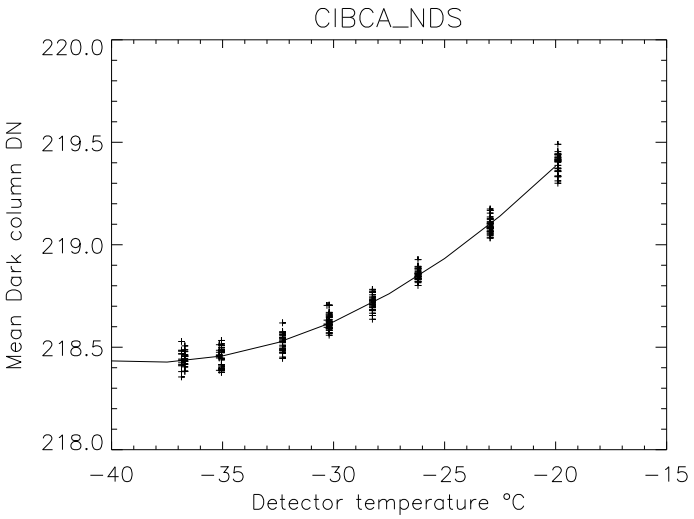

Figure 2.17: Calculated data fit (line) plotted on dark column mean values (crosses) for the CRISP post-environment dark series temperature tests. No separation of data due to exposure time is shown here.

Figure 2.17 shows the fit plotted on the data, which are no longer segregated by exposure time, since the exposure time effect is so much less than the temperature effects.

2.3.2 CFI

The CFI imager was tested over a larger temperature range than the CRISP imager, and showed unexpected increases in noise in the dark columns as a result. Figure 2.18 shows the response of the CFI dark columns from a 'final' flat-field warm-up test with the white sphere as a source. The exposure time was fixed at 958 milliseconds, the CFI filter wheel setting was alternated between 2 (933 nm center wavelength with a 13 nm bandpass) and 3 (840 nm center wavelength with a 4 nm bandpass), and the Halogen and Xenon attenuators alternated between a 220 and a 240 setting (98.5% and 99.95% attenuated). Imagery were acquired in a sequence that rotated between 'darks' (255 attenuator settings), filter 2 with a 240 attenuator setting, filter 3 with a 220 attenuator setting, and several more darks, as the chamber temperature was stepped from -40$°C$ to +40$°C$. As mentioned above, because of the exponential increase in thermal noise at temperatures far above what would be encountered in space, the relationship between dark column signals and image values becomes increasingly problematic. However, in the intended operating range of the sensor (see Figure 2.19) the CFI dark column mean has a linear dependence on temperature that may be fitted as:

$$DN(darkcolumn) = -0.6067 T_{CCD} + 203.42 \tag{2.10}$$

Dark column data acquired for the same conditions in the CFI final calibrations had temperature dependence in the operating range nearly identical to that reported here.

2.4 Imager Properties as a function of Row and Temperature

Thermal noise as sensed on a CCD is a function of temperature, exposure time, and frame transfer time (FTT). FTT can be described simply as how long it takes to transfer all the charge accumulated in the charge wells (individual CCD

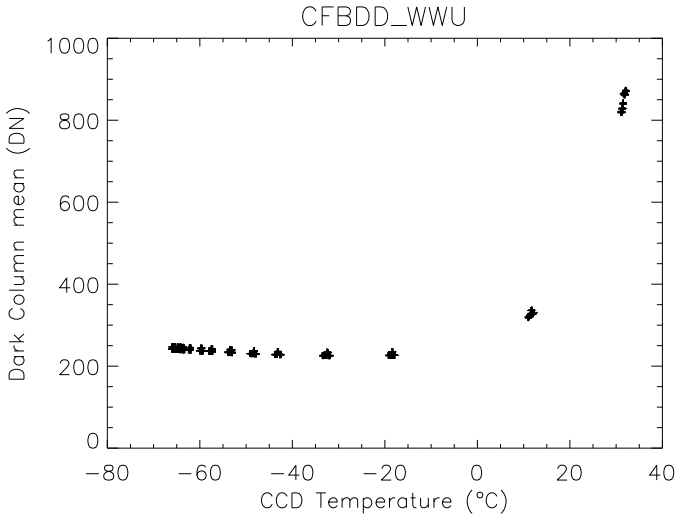

Figure 2.18: Dark column mean versus temperature for a post-environment white sphere test. Note the exponential increase with thermal noise once the temperature rises above freezing ($0\,^{\circ}C$).

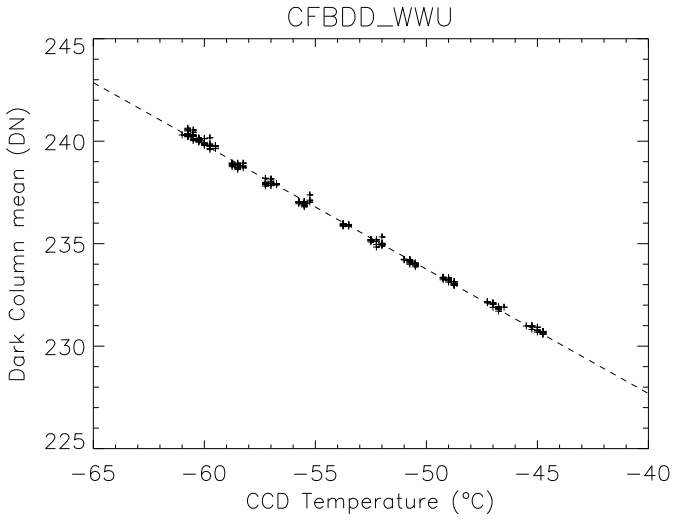

Figure 2.19: Dark column mean versus temperature for a post-environment white sphere test. The dashed line is a linear fit to the data.

elements) off the CCD chip and into charge accumulators to be counted digitally. The longer this process takes, the larger the charge, and the higher the resulting noise in the digitally sampled signal. Since charge is transferred from the bottom row to the first row above to the second row above, and so on to the end of the CCD before it transfers into the read-out registers, the signal levels in the dark columns should increase with increasing row number. There is a similar, but much smaller, effect with increasing column number, since the charges are transferred off the read-out registers one column at a time. But, that effect is usually too small to be significant, except in very specific applications. The imaging portion of the CCD will have a similar increase as a function of increasing row number, which is measurable for dark images, images where there is no source to impact the light wells and where the attenuators are set to full (to block out, insofar as possible, stray light).

2.4.1 CRISP

FTT can be deduced for the CRISP imager from the post-environment dark series collected as a function of temperature, as described in the previous section.

Dark Images

Figure 2.20 shows the dependence of image intensities on the row number as a function of temperature for exposure times of 10.112 milliseconds. For clarity, the clouds of data points to which these lines were fit are not plotted. The data are, however, distributed uniformly 0.125 DN above and below the lines shown. The fits to the data are as follows (where R is row number, with the image origin at the lower left corner):

$$-19.9°C : DN(darkimage) = 0.00025679 * R + 219.25 \tag{2.11}$$

$$-26.2°C : DN(darkimage) = 0.00014093 * R + 218.87 \tag{2.12}$$

$$-32.3°C : DN(darkimage) = 0.000085941 * R + 218.63 \tag{2.13}$$

$$-36.85°C : DN(darkimage) = 0.000067553 * R + 218.57 \tag{2.14}$$

Dark Columns

A similar set of expressions can be derived for the dark columns (R, as above, is row number):

$$-19.9°C : DN(darkcolumns) = 0.00030324 * R + 219.18 \tag{2.15}$$

$$-26.2°C : DN(darkcolumns) = 0.00019064 * R + 218.70 \tag{2.16}$$

$$-36.85°C : DN(darkcolumns) = 0.00010495 * R + 219.38 \tag{2.17}$$

2.4.2 CFI

The data described in Section 2.3.2 can also be used to quantify the dependence of the sensor dark data as a function of row and temperature. By selecting representative dark images over the expected operating temperature of the instrument (-50$°C$ to -35$°C$), we can derive expressions for the row dependence (R):

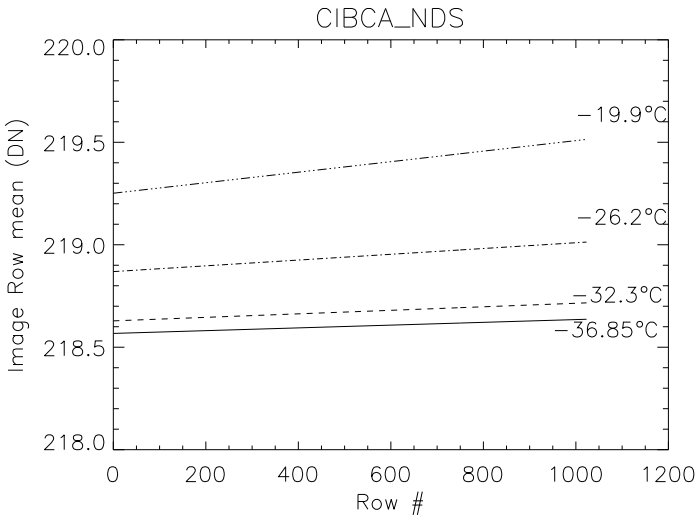

Figure 2.20: Dark image row mean as a function of row number for the CRISP post-environment dark series temperature tests. The actual data are not over-plotted on these fits for the sake of clarity, however, they fluctuate uniformly 0.125 DN above and below the fits.

Dark Images

$$-50.0°C : DN(darkimage) = 0.000024546 * R + 229.33 \tag{2.18}$$

$$-44.0°C : DN(darkimage) = 0.000035902 * R + 227.03 \tag{2.19}$$

$$-35.0°C : DN(darkimage) = 0.00018052 * R + 224.25 \tag{2.20}$$

Dark Columns

$$-50.0°C : DN(darkcolumns) = 0.00050439 * R + 225.25 \tag{2.21}$$

$$-44.0°C : DN(darkcolumns) = 0.000036194 * R + 223.24 \tag{2.22}$$

$$-35.0°C : DN(darkcolumns) = 0.000035021 * R + 225.55 \tag{2.23}$$

2.5 Dark Column Corruption

2.5.1 CRISP

The effects of increasing exposure on the dark column averages was initially examined using the data from the post-environment linearity series collected with the white integrating sphere as a source. Exposure times ranged from 0 to 900 milliseconds, the CRISP filter wheel was set to value 6 (where the center wavelength was 610 nm with a bandwidth of 40 nm), and the Halogen and Xenon lamp attenuators were set to either 255 (minimum light) or

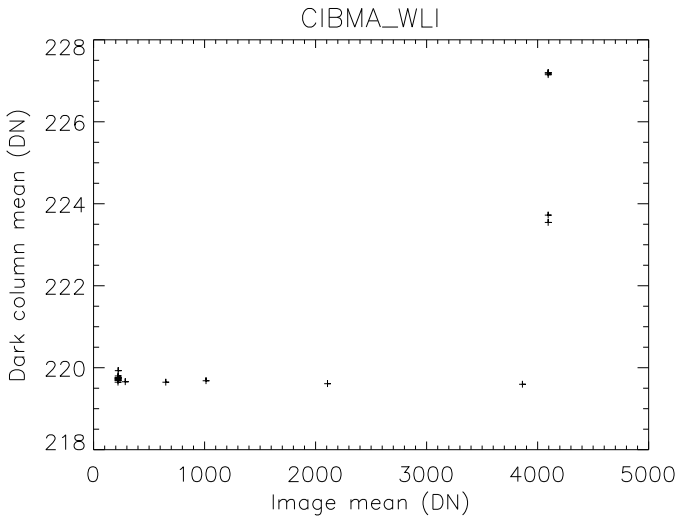

Figure 2.21: Dark column means as a function of image means for the CRISP post-environment white sphere linearity series. The average dark column mean is 221.22 DN with a standard deviation of 2.8325 DN.

140 (65% attenuated). The image mean values ranged from 200 DN to complete saturation (4095 DN). Figure 2.21 shows the dark column means plotted against the image means for these data. It was initially thought the increased dark column means for the saturated images were the result of light leakage that caused an overall increase in the dark column average. On further examination, the increase was found to be the result of fully saturated values appearing, for a few rows, in the dark columns. Figure 2.22 shows one of the images with the saturations on the dark columns, visible in the lower left of the image. The appearance of these saturated dark column rows is uncorrelated with exposure time, filter wheel number, or attenuator setting. The suspected cause is anti-blooming overload, where accumulated charge from the saturated imagery overloads the anti-bloom correction during read-out. It is, however, infrequent, and occurs in only a few initial rows of the CCD in fewer than 20 of the hundreds of images in the calibration set. Other than these saturated values, no pinholes or other problems were found with the dark columns in these data. Further, when the saturated rows were excluded from the dark column average, the numbers remained below 219.9 DN in the post-environment calibrations, as shown in Figure 2.23. We thus conclude that the dark columns in the CRISP imager provide a highly stable calibration point, once saturated rows are excluded by a simple threshold.

2.5.2 CFI

Dark column corruption in the CFI imager was not a result of dark columns being overwritten with data columns due to anti-bloom overload, but from two other sources. First, the dark columns were corrupted during the acquisition of binned (i.e. reduced size) imagery and, second, in dark imagery when horizontal banding occurred in the imagery itself.

Binning problems

Binned images were acquired for CFI as part of a dark series, and when both the M/C point source and the white sphere were used as targets. The standard image size is 1024 by 1024 pixels, with four additional 'dark' columns to track the shot noise. Four binning modes could be selected, for image sizes of 1024 by 1024, 512 by 512, 256 by 256,

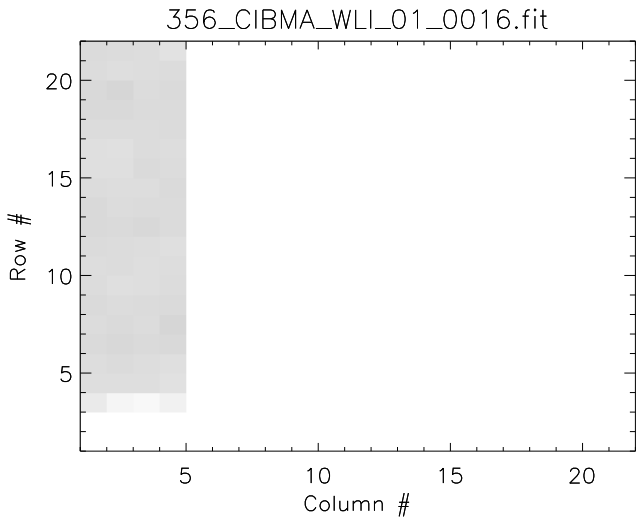

Figure 2.22: Lower left corner of image number 16 from CRISP post environment test for linearity with the white sphere showing saturated data overwriting the dark columns in rows 1-3. The Halogen and Xenon attenuators are both set to 140, the CRISP filter wheel is at 6, and the exposure time is 200 milliseconds.

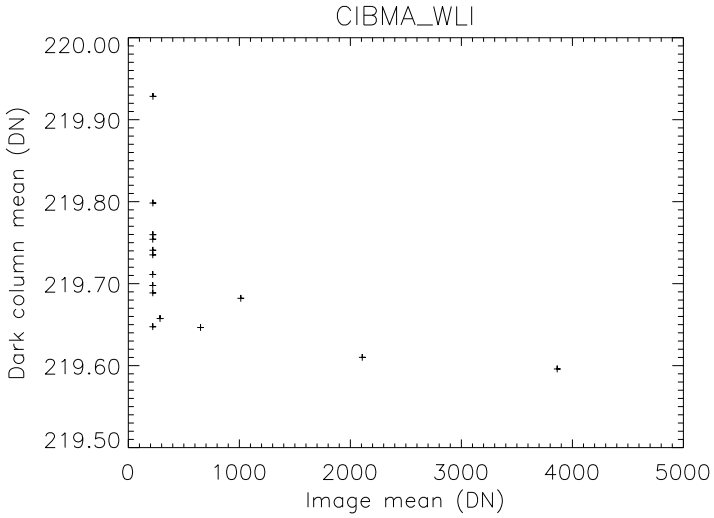

Figure 2.23: Dark column means with the saturated rows excluded as a function of image means for the CRISP post-environment white sphere linearity series. The average dark column mean is 219.71 DN with a standard deviation of 0.08307 DN.

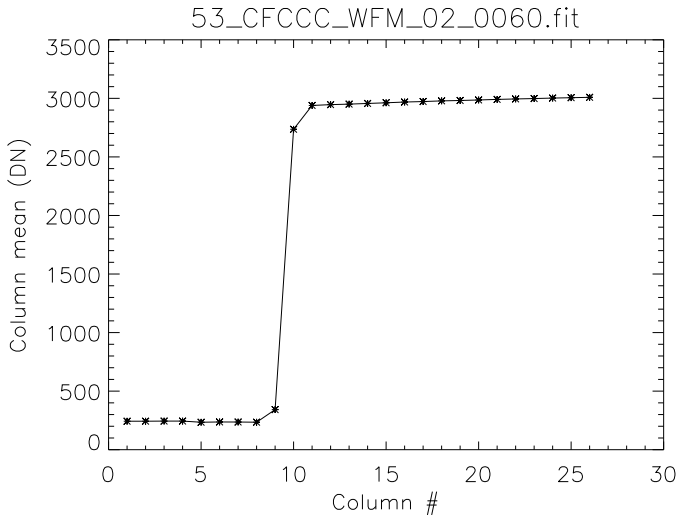

Figure 2.24: Extra dark columns resulting from binning errors in CFI. These 'final' calibration data are from a formatting test with the white sphere as a source. The exposure time is 51.2 milliseconds, the CFI filter number is 4 (center wavelength of 620 nm, with a 4 nm bandwidth), and the Halogen and Xenon lamps are unattenuated.

and 128 by 128. For all binned modes, the number of dark columns was supposed to remain unchanged. Figure 2.24 shows a row-averaged cut through a white image binned to a size of 256 by 256. Instead of four dark columns, there were eight, with two more columns containing intermediate values between dark and white. More troublesome were cases of binned data collected with the white sphere as a source where the dark columns alternated between being dark, saturated, and dark before simply being saturated (see Figure 2.25). It proved impossible to predict the increase in number of dark columns with binning, since the increase in number of, and signal intensity within, the added columns was random.

If this sensor had been used in space, and if these had been the only binning problems with CFI, the simplest course for dealing with this problem, outside of troubleshooting the cause in hardware/firmware, would have been to assume the first two dark columns of the binned images were truly dark, and the first ten columns of any binned image might contain dark values. At worst, this would have meant ignoring 6 columns, or using a 128 by 122 image. The data loss would have been less severe as the binning was reduced. But, as will be shown later, there were more problems with the binned CFI data than simply this dark column corruption.

Horizontal Banding

Throughout the CFI calibrations, imagery were acquired that split itself into two different horizontal fields. One would, on average, be a DN or so brighter than the other, and this banding would persist into the dark columns (see Figure 2.26). Here, the CFI filter number is 7 (center wavelength of 526 nm with bandwidth of 12 nm), the exposure time is 551 milliseconds, and both the Halogen and Xenon bulbs are fully attenuated (setting of 255). The average difference between the two fields is 0.7 DN. As with the binning problems, the occurrence of banding and the magnitude and direction of the mean offset between the bands were random, and, thus, unpredictable. A more detailed discussion of the horizontal banding are given in Section 3.3.3.

Deriving a banding correction to the CFI imagery from the dark columns is challenging because, although the difference is clearly visible, it is only by averaging all the image columns together that an unequivocal offset is

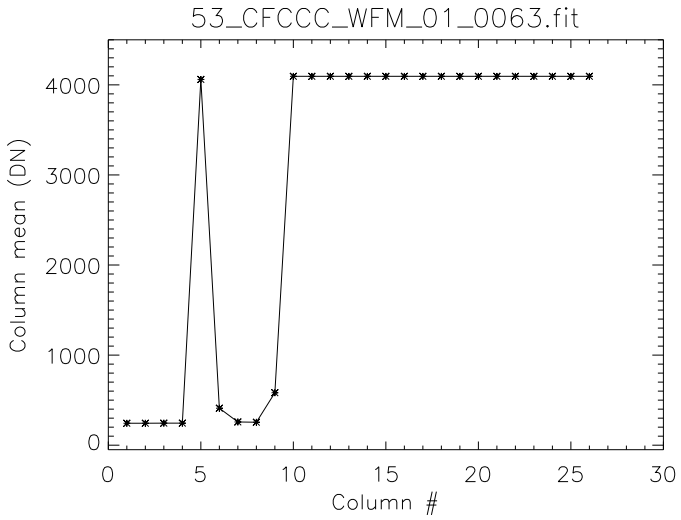

Figure 2.25: Ringing in binned saturated CFI imagery. These 'final' calibration data are from a formatting test with the white sphere as a source. The exposure time is 901.12 milliseconds, the CFI filter number is 4 (center wavelength of 620 nm, with a 4 nm bandwidth), and the Halogen and Xenon lamps are unattenuated.

quantitatively distinguishable (see Figure 2.26). With only four dark columns (in unbinned data) to average over, given the wide dynamic range of the dark columns in CFI (25 DN), neither smoothing nor subsampling yielded a reliable measure of the occurrence or location of horizontal banding in the dark columns.

If this sensor had been used in space, the existence of horizontal banding could be detected from the imagery itself (not the dark columns) by using a first difference calculation (see Section 3.3.3). When a large first difference occurred, the two halves of the imagery could be stitched together by calculating a mean in each band and removing the difference.

NOTE ON CRISP

In fewer than 10 cases during a single post-environment dark test, horizontal banding smaller than that discussed here were seen in CRISP imagery. But, these bands were not present in the dark columns, as was true for CFI. An approach similar to that used on CFI for locating and correcting the bands could be used on this sensor, or sensors using a similar CCD, in the future, if it was required.

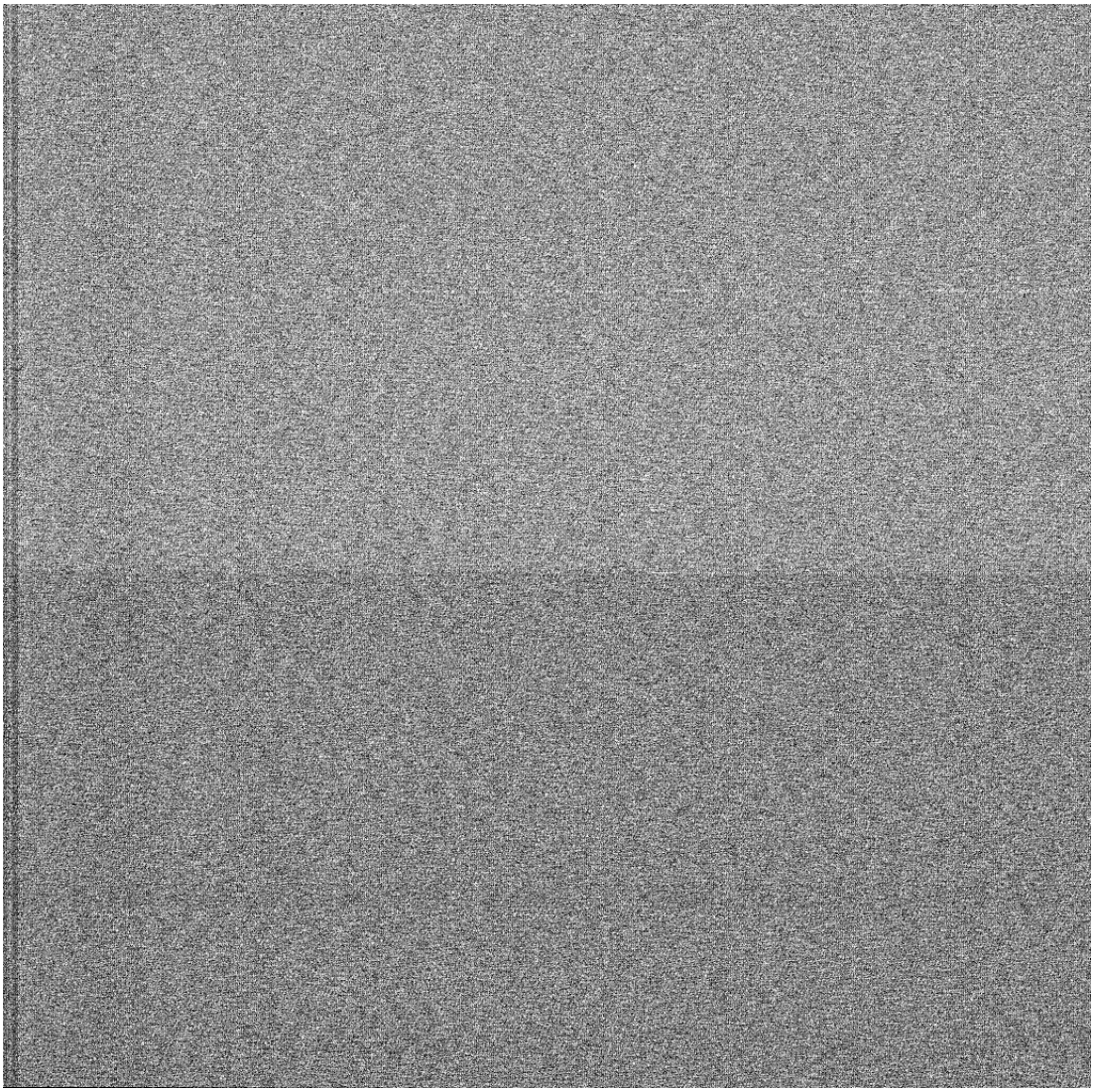

Figure 2.26: Dark image from a 'final' flatfield calibration run, with the horizontal band transition at row 485 (counted from origin at lower left corner). The CFI filter number is 7, the exposure time is 551 milliseconds, and both the Halogen and Xenon bulbs are fully attenuated. The average difference between the two fields is 0.7 DN. The handing persists into the four dark columns at the left of the image. (Other bands may appear if the image is viewed in a print-out from a printer with a old toner cartridge, but do not exist in the electronic version.)

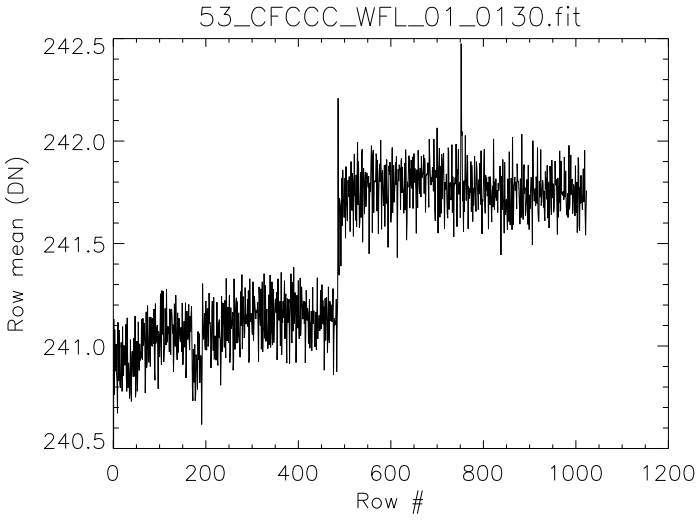

Figure 2.27: Average of all columns of image data (not including dark columns) plotted against row number for the image in Figure 2.26. The 0.7 DN offset is distinctly visible at row 484.

Chapter 3

Image Properties

3.1 Frame Transfer Smear Removal (FTSR)

3.1.1 CRISP

Since the CCD used in CRISP has been employed several times before, the FTSR for the chip is well known. The few cases of FTSR used in the responsivity calculations for the imager appeared to provide correct results. Figure 3.1 is from the CRISP post-environmental white sphere linearity test, and shows image means as a function of exposure time for CRISP filter wheel setting #6 (center wavelength of 610 nm with a bandpass of 40 nm), with the Halogen and Xenon attenuators at 140 (65% attenuated). The FTSR image means (indicated by an asterisk) have a fixed mean offset of 260.66 DN from the raw, uncorrected image means (indicated by the crosses), but, show the same responsivity (slope between dark and white).

3.1.2 CFI

The same is not true for CFI. Figure 3.2 shows two errors in the FTSR for CFI. First, for exposure times shorter than the frame transfer time (FTT), there is no apparent increase in image mean. Second, for long exposure times, the FTSR over-corrects, and data that should be saturated, are not. This changes the dependence of image mean on exposure time needed to calculate image responsivities, as can be seen by comparing the fits to the raw and corrected data between 12 and 32 milliseconds (where τ_e is the exposure time in milliseconds).

$$DN(raw) = 113.67\tau_e + 195.53 \tag{3.1}$$

$$DN(corrected) = 100.33\tau_e - 576.14 \tag{3.2}$$

For exposure times shorter than the FTT (11.47 milliseconds for CFI), the mean image values are constant. It would appear as if the instrument were actually not acquiring data at all. For exposure times longer than the frame transfer time, the image means increase with increasing exposure time. The data appear as if the frame transfer time and exposure time are incorrectly summed when clocking the CCD to acquire data. For exposure times shorter than the frame transfer time, it appears as if only frame transfer of dark charge is occurring. For exposure times longer than the frame transfer time, it appears as if the frame transfer begins before full exposure has been completed. The true exposure time, $\tau_e(true)$ (in milliseconds), may be written (where $\tau_e(commanded)$ is the commanded exposure time in milliseconds):

$$\tau_e(true) = 0.0[\tau_e(commanded) \leq FTT] \tag{3.3}$$

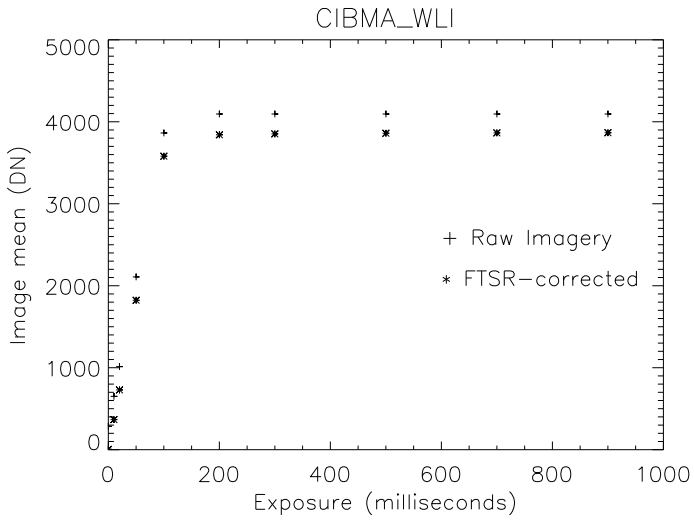

Figure 3.1: Raw and FTSR-corrected image means from the CRISP post-environmental white sphere linearity test. The CRISP filter wheel setting is #6 (center wavelength of 610 nm with a bandpass of 40 nm) and the Halogen and Xenon attenuators are at 140 (80% attenuated). The crosses are the raw data and the asterisks are the FTSR-corrected vales.

$$\tau_e(true) = \tau_e(commanded) - FTT[\tau_e(commanded > FTT] \tag{3.4}$$

While there was not sufficient time to rerun the FTSR corrections for this shorter 'actual' exposure time for this write-up, several actions are recommended to correct this problem should a follow-on instrument be proposed.

(1) Check the clocking firmware in CFI. From the documentation for the CFI hardware and software (Reference # 2), the exposure time is calculated by counting backward from a 1 Hz pulse. The CFI software should be checked to ensure the proper back-counted time (frame transfer time plus exposure time, and not just the longer of the two) is actually being used to calculate when the exposure begins.

(2) Use the 'actual' exposure time (0 milliseconds for exposure times shorter than the frame transfer time, or $\tau_e(commanded) - FTT$ for longer exposure times) and re-calculate the FTSR for these calibration data. Once the FTSR-corrected data for CFI behave as do the CRISP data, the CFI FTSR will be correct.

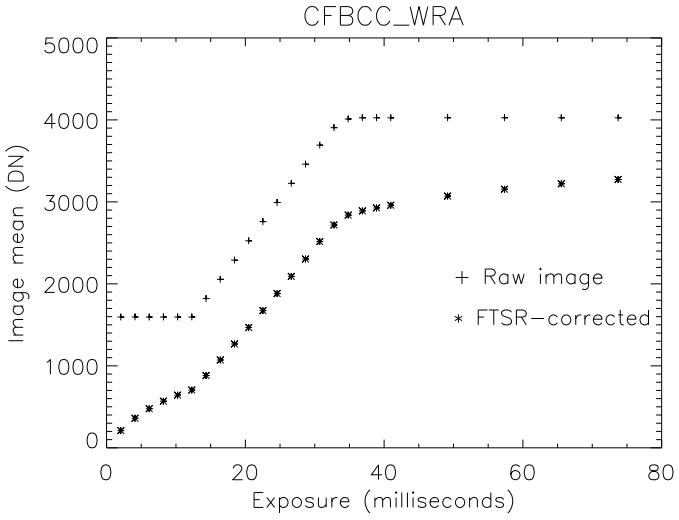

Figure 3.2: Raw and FTSR-corrected image means from the CFI post-environmental white sphere linearity test. The CFI filter wheel setting is #2 (center wavelength of 920 nm with a bandpass of 13 nm) and the Halogen and Xenon lamps are unattenuated. The crosses are the raw data and the asterisks are the FTSR-corrected vales.

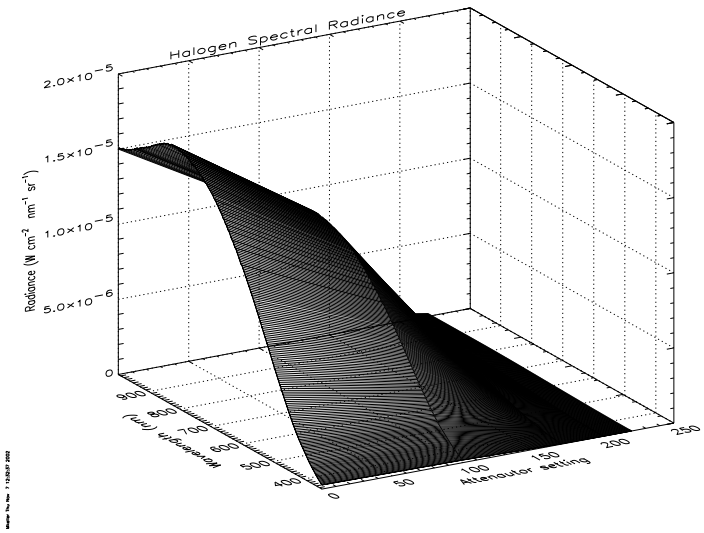

Figure 3.3: Halogen radiances as calibrated by Optronic Labs. The 3-D plot shows the radiance (z axis) as a function of attenuator position (x axis) and wavelength (y axis).

3.2 Responsivity

3.2.1 White Sphere Calibrations

Extensive calibrations of the dual lamp (Halogen and Xenon) white sphere were performed by Optronic Labs in August of 2002. The spectral radiances, in $W - cm^{-2} - sr^{-1} - nm^{-1}$, of the Halogen and Xenon lamps were measured at 1 nm intervals over the range 300 nm to 2500 nm for five attenuator settings: 0, 100, 170, 200, and 220. Figures 3.3 and 3.4 show the calibrations plotted as a function of attenuator setting over the wavelengths of interest for the imagers. In addition, the attenuators themselves were calibrated over their entire 0-255 setting range against an OLI monitor photometer, since it had been learned that the attenuators did not necessarily return to the same metered level unless the attenuators were reset to zero before every adjustment (Reference # 5). The calibrated spectral radiances were reported in a series of spreadsheets that listed unattenuated radiance, ratios of the attenuated radiances to the unattenuated value, and gave coefficients for a series of polynomial fits that permitted the retrieval of radiances for any wavelength/attenuator combination. However, these fits proved unwieldy for use on a Linux-based system. For this study, the ratios at the four attenuated settings were used to calculate radiances for each lamp at each measured attenuator setting. Fits were calculated in IDL for the retrieved data (see the Appendix), once the radiances were corrected for the aged Halogen bulb used during the OCF tests and the differences in the attenuated data (Reference # 5). No attempt was made to fit across the spectral lines encountered with the Xenon lamp. Figure 3.5 shows the quality of fit for all attenuations for the Halogen lamp as a difference between the calibrations and the fit. Note that the differences are always two orders of magnitude less than that of the calibrated radiances, for an error of less than 1%.

3.2.2 CRISP

Since the CCD manufactured by Thomson and used in CRISP has been characterized and used before, little time was spent performing radiance measurements for the different filter wheel settings. In fact, for the clear filter wheel setting

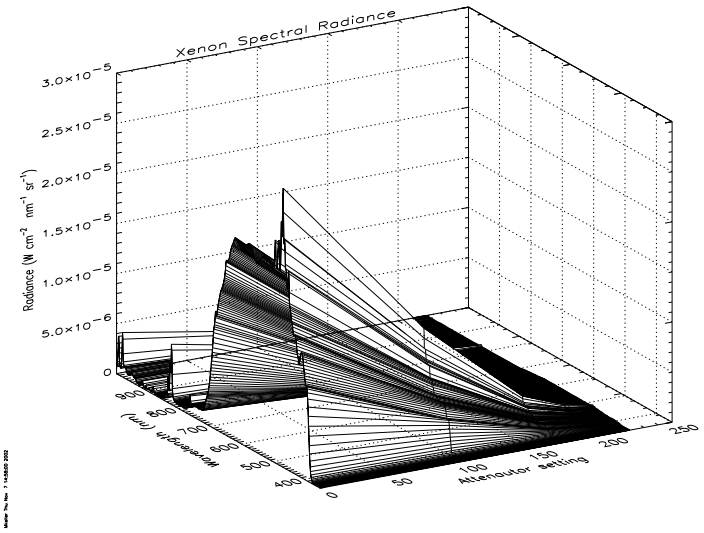

Figure 3.4: Xenon radiances as calibrated by Optronic Labs. The 3-D plot shows the radiance (z axis) as a function of attenuator position (x axis) and wavelength (y axis).

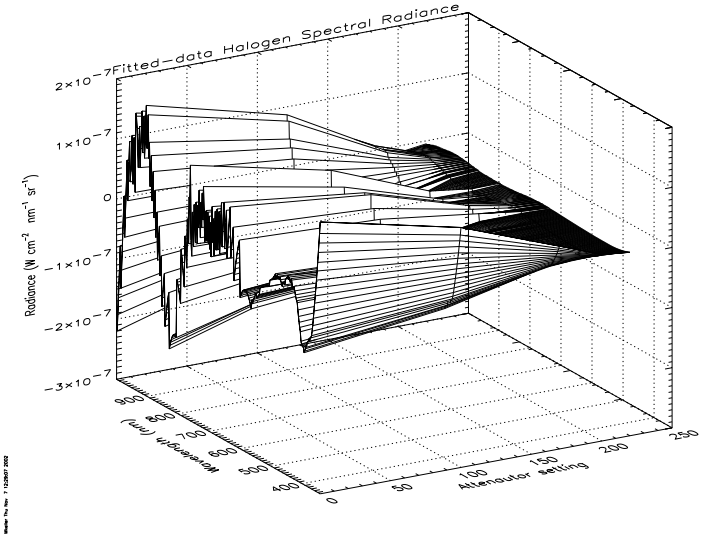

Figure 3.5: Difference between the derived fit of the Halogen radiance at all attenuations plotted as a function of attenuation and wavelength for the Imager range of interest.

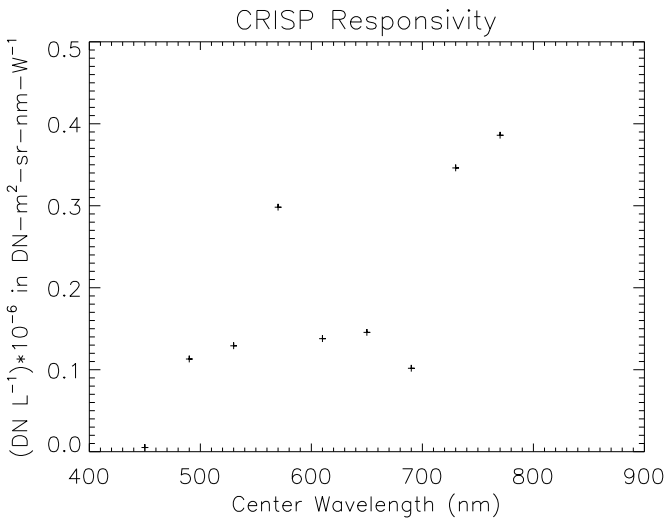

Figure 3.6: Responsivity of filter wheel settings 2-10 used on CRISP, converted to 1 second. All settings have bandwidths of 40 nm.

(#1), no data were acquired from the white sphere at any attenuator setting that had exposure times greater than 1.3 milliseconds (or, greater than half the frame transfer time). As has been shown in the previous section, the FTSR calculations were correct for CRISP, so even data where the white sphere was used at only a few exposure times, as long at the FTSR-corrected data were available, were useful for a responsivity calculation. The data used, thus, came from post-environment white sphere tests for linearity (Filter wheel #6) , flat/radiometry (Filter wheels #7-10), and mirror test (#2-5). All the CRISP measurements were acquired from attenuated data in the "cold" chamber (-30$°C$), and through the OCF optical window. They will have a less than 1% error from the fitting process, and have been corrected for losses due to the non-unity transmissivity of the window. Figure 3.6 shows the responsivity, after conversion to 1 second, as derived.

3.2.3 CFI

An extensive set of radiometry measurements were acquired from the white sphere for nine attenuator settings from 0 to 255, all filter wheel numbers, and for exposure times from 5 to 40 milliseconds. Since there were questions about the FTSR corrections, the responsivities were calculated from the uncorrected longer exposure times. Without an accurate measure of the magnitude of the true FTSR corrections, errors in the responsivity calculations cannot be estimated fully. Let it simply be stated that these numbers will need to be recalculated in the future should a similar instrument be developed once the FTSR is correct. Figure 3.7 shows the responsivities, after conversion to 1 second, calculated from the slopes of image means as a function of center wavelength for the unattenuated and uncorrected imagery.

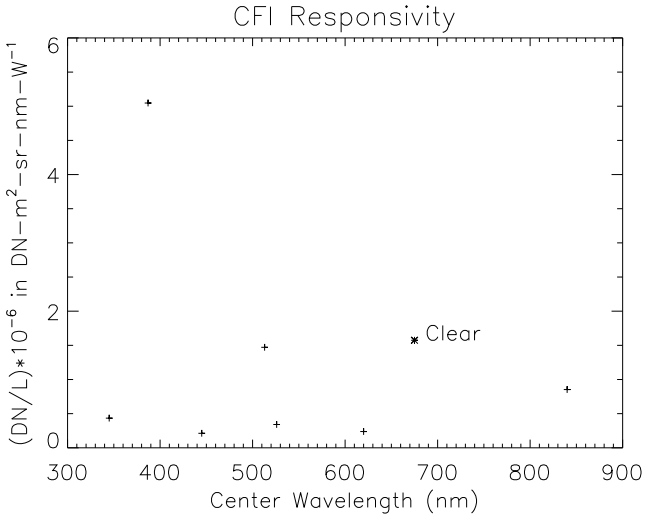

Figure 3.7: Responsivity of filter wheel settings 1-10 used on CFI, converted to 1 second. The bandwidths are variable between 4 and 13 nm. The 'clear' filter wheel setting (labeled as 'Clear') is plotted at the center of the nominal visible band (675 nm) for completeness, not because the wavelength has any quantitative significance.

3.3 Noise Analysis

3.3.1 CRISP

The last day of post-environment calibrations for the CRISP imager was December 25, 2001. The plan for the day was to conduct a series of tests with the Master/Collimator (M/C) point source as the signal. However, difficulties were encountered keeping the point source in the image, and, during the wavelength test, data acquisition was interrupted after image 122 (Figure 3.8) so the point signal could be recentered, a single frame (image 123, Figure 3.9) snapped, the test script resumed (image 124, Figure 3.10), and the test concluded. Since the M/C point signal had not been visible in the imagery, all tests conducted on that day to that point were repeated, including the on-going wavelength test. However, something was modified during the stop and restart that initiated herringbone noise (see Figure 3.9) in the CRISP imagery. The other CRISP imager repeat tests from that day also exhibit the same problems, as can be demonstrated by a comparison of the imagery from before and after the re-zeroing. These included: CIBMA_PVV (the CRISP imager vacuum pump vibration test), CIBMA_PSL (the infield scattered light test for the CRISP imager), CIBMA_PW2 (the CRISP imager wavelength test), CIBMA_PRL (the CRISP imager red leak test), CIBMA_PFO (the CRISP imager focus test), and possibly several CRISP spectrometer runs that are not examined here (see Reference # 4). The aim of this section is to suggest possible causes for the herringbone noise in the imagery.

CIBMA_PW2

Constant quantities for the wavelength test are listed in Table 3.1. The exposure time was 979.968 milliseconds throughout, and the filter wheel settings were stepped from 1 to 5. The exposure time is longer than the frame transfer time for the CRISP imager by a factor of three, but, these were Master/collimator (M/C) point source runs, so the data were essentially 'dark' images (overall image mean of 219.41 DN versus 219.30 DN for an overall dark column mean). Although the CCD temperature for the runs was measured as 138.75 °C, this must be an error due to a non-working monitor channel. It should be noted that whatever effect the vacuum pump vibrations were postulated to have on the CRISP imager or the OCF systems were undetectable in either Vacuum Pump Vibration run. Also remaining unchanged over the course of the run were the chamber and detector temperatures, which had values of -30.51 °C and -30.65°C, respectively. As Figures 3.8-3.10 show, it was after the interruption and restart that the herringbone noise appeared in the CRISP imagery. Figure 3.11 shows that the CRISP mirror changed position by approximately 45 at the time of the recentering of the M/C point signal. Table 3.2 and Figures 3.12-3.22 show CRISP current statistics and how they were modified after the restart. The mirror pointing shows simple offsets between the two sections of the run. The lack of variability in the temperature sensors within the run is due to its short duration in time. It should be noted that only the DPU (Figure 3.14) and Cooler converter current (Figure 3.16) were unchanged after the stop and restart. The Spectrometer primary motor current (Figure 3.18), the Filter Wheel motor primary current (Figure 3.21), and the Filter Wheel motor converter current (Figure 3.22) were only slightly, if at all, affected by the stop and restart.

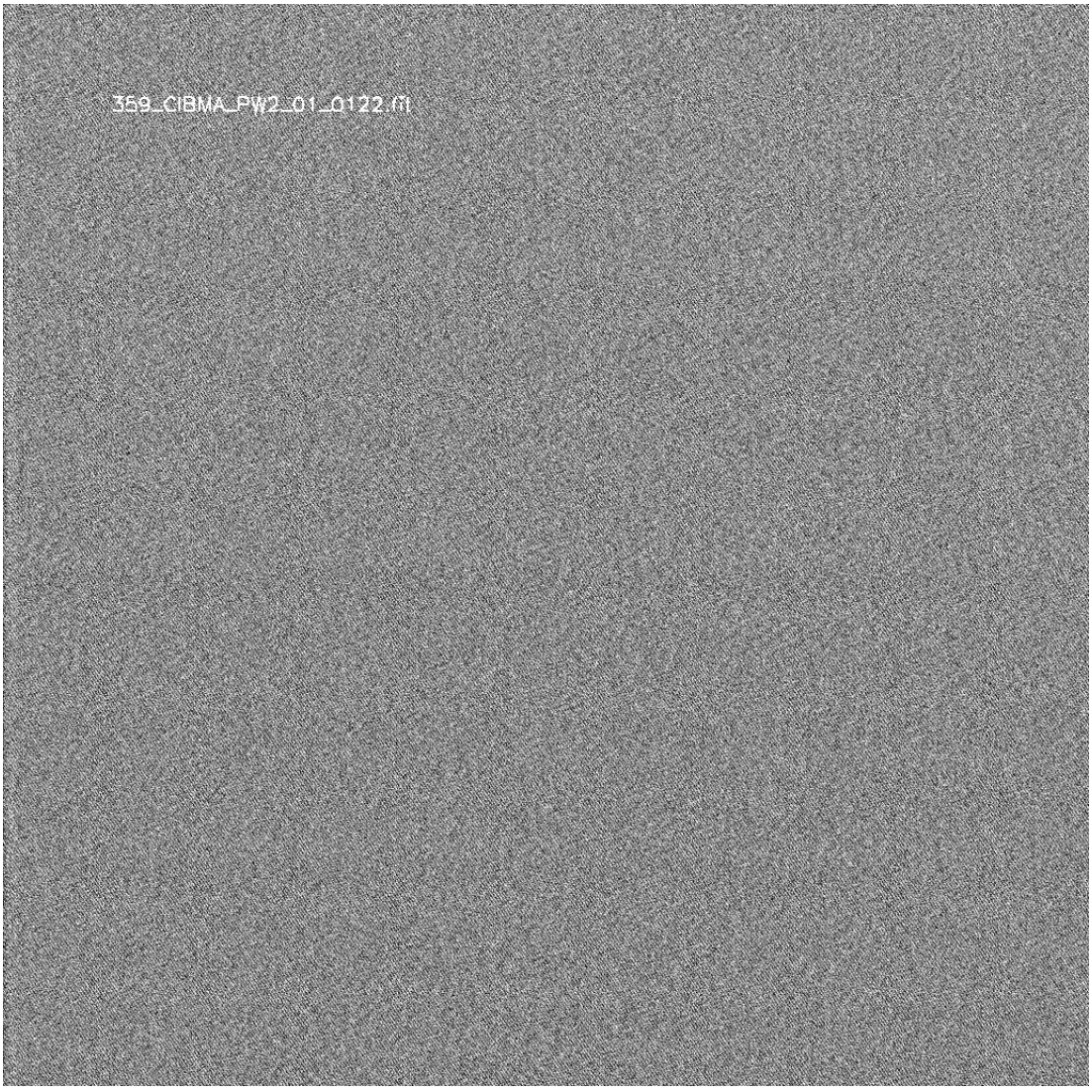

Figure 3.8: Image 122 from Wavelength test. This is the last image before the restart. There is no herringbone noise in this dark image. The peak to peak signal in this image is slightly less than 6 DN.

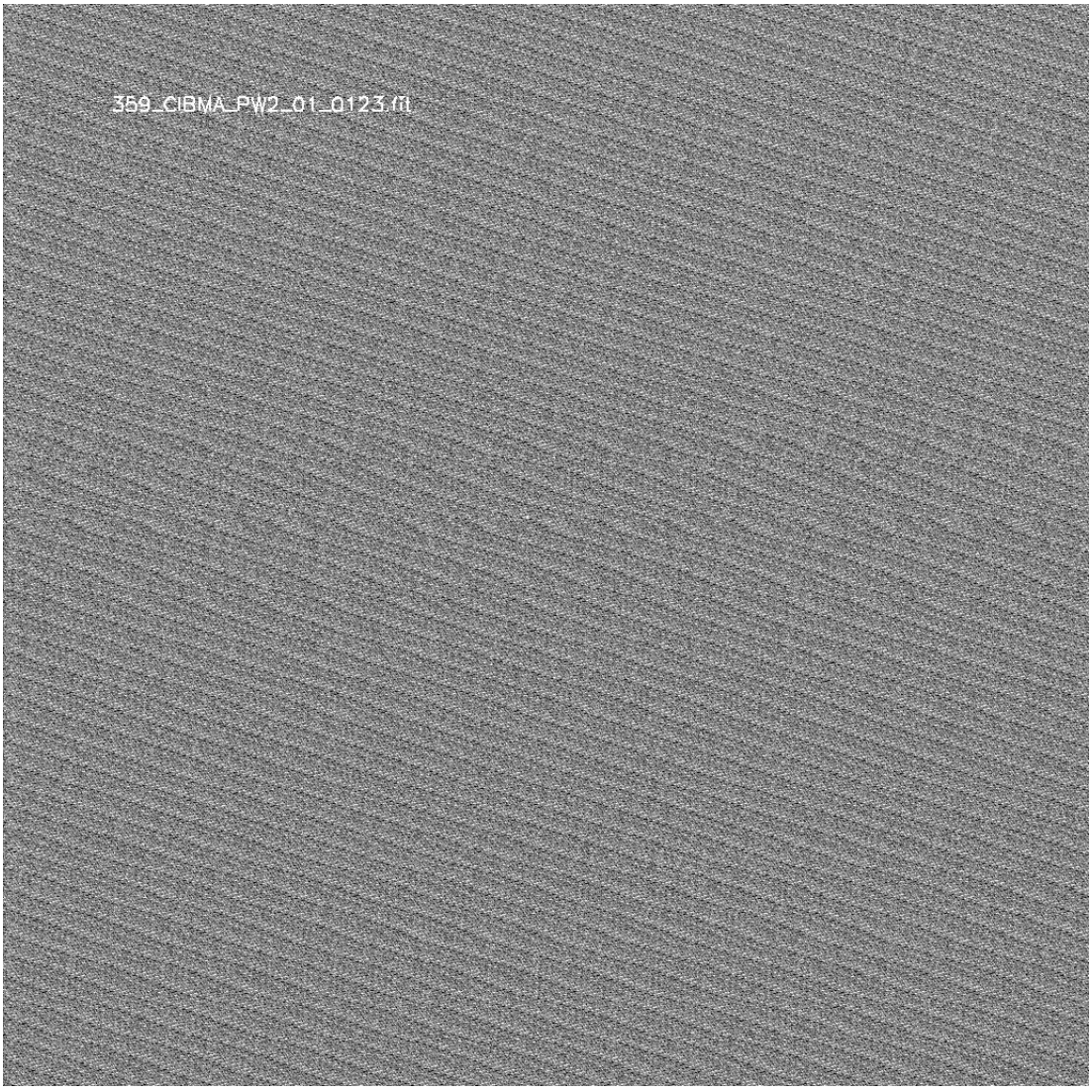

Figure 3.9: Image 123 from Wavelength test. This is the first image after the restart. Note the presence of herringbone noise with a peak-to-peak amplitude of 12 DN.

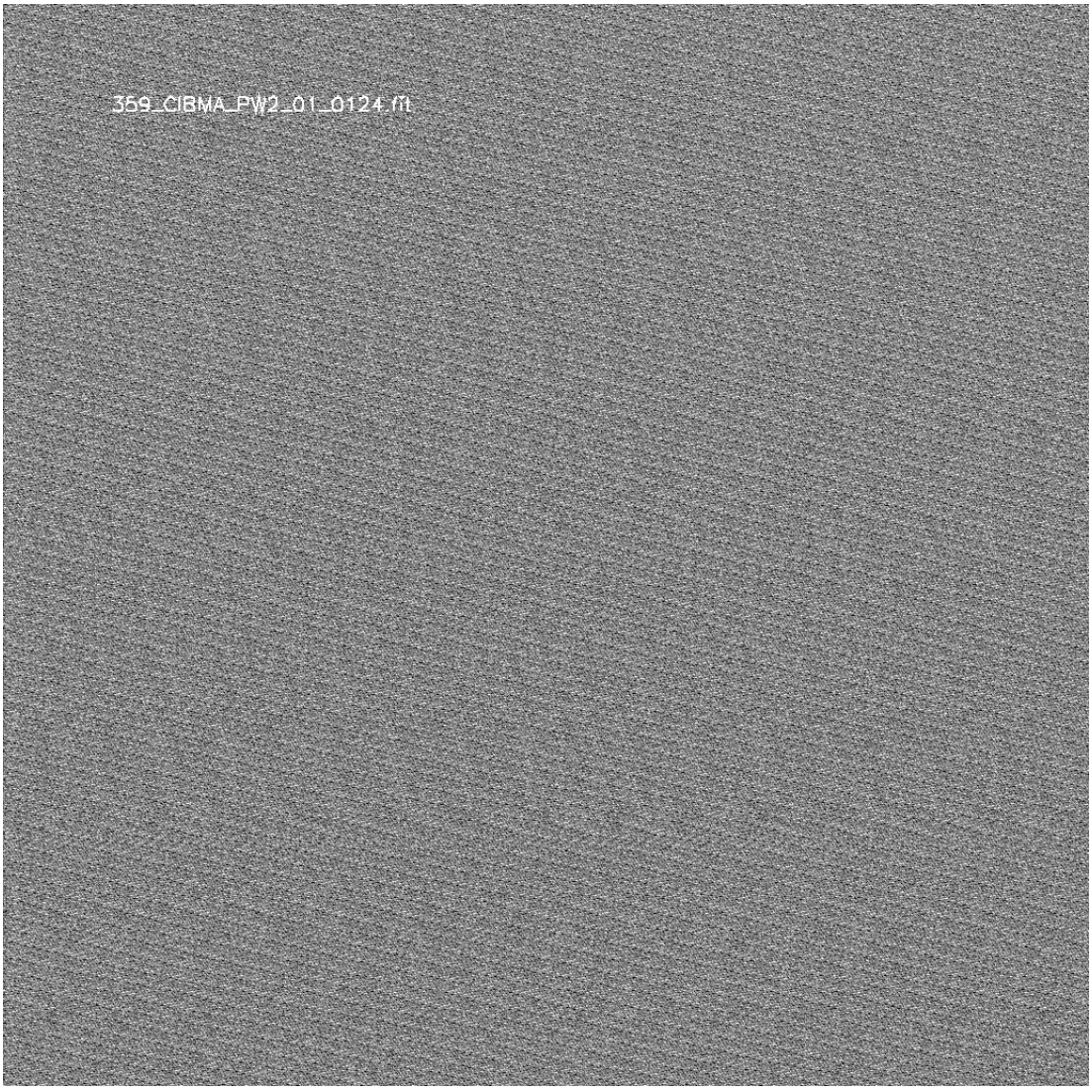

Figure 3.10: Image 124 from Wavelength test. This is the second image after the restart and the first image run with the test script. It shows significant herringbone noise persisting regardless of how image generation was commanded.

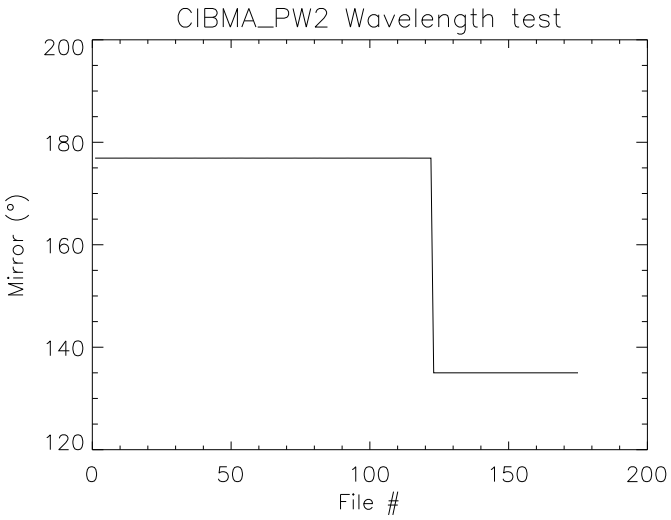

Figure 3.11: Mirror pointing (in degrees) for Wavelength tests

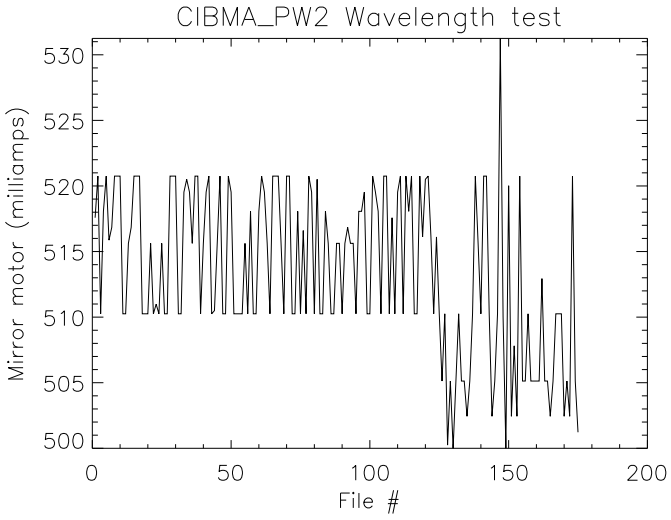

Figure 3.12: Mirror motor current for Wavelength test

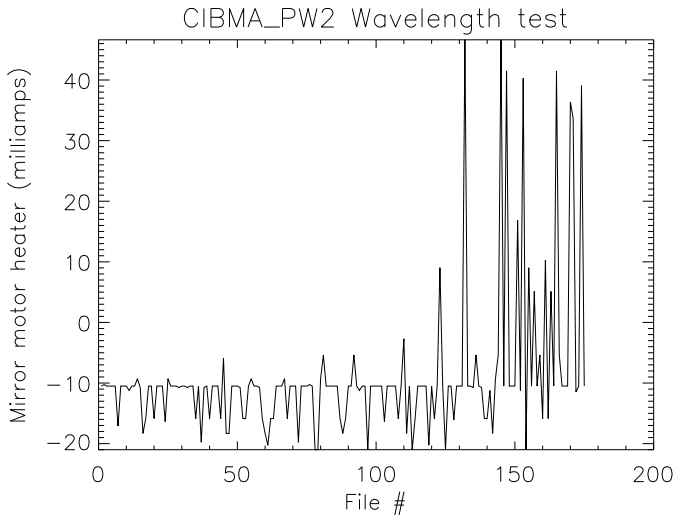

Figure 3.13: Mirror motor heater current for Wavelength test

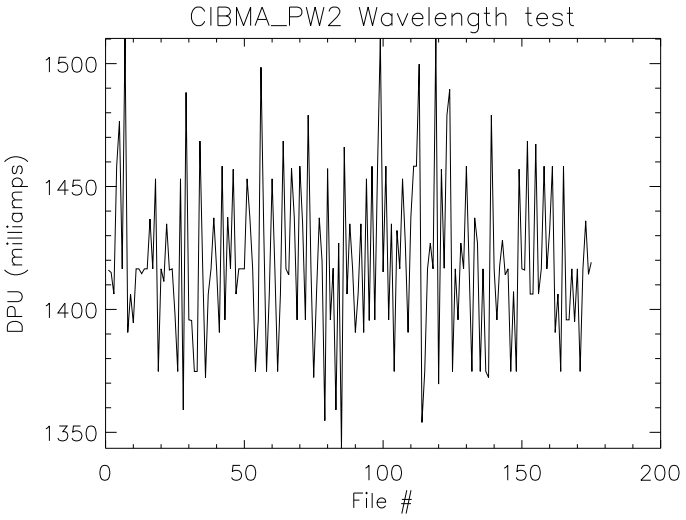

Figure 3.14: DPU current for Wavelength test

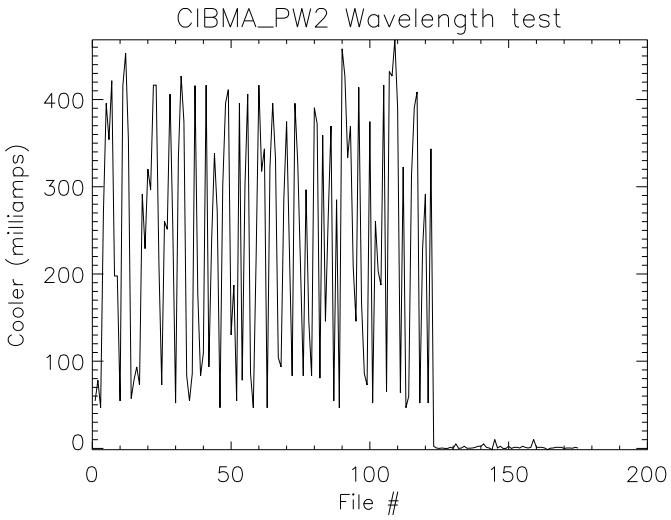

Figure 3.15: Cooler current for Wavelength test

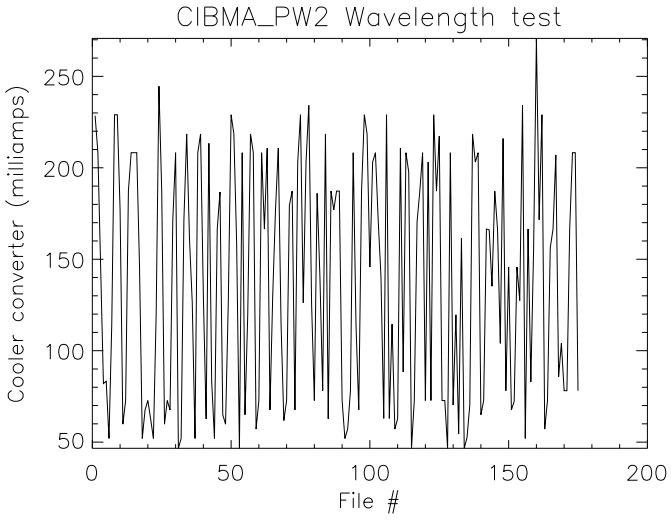

Figure 3.16: Cooler converter current for Wavelength test

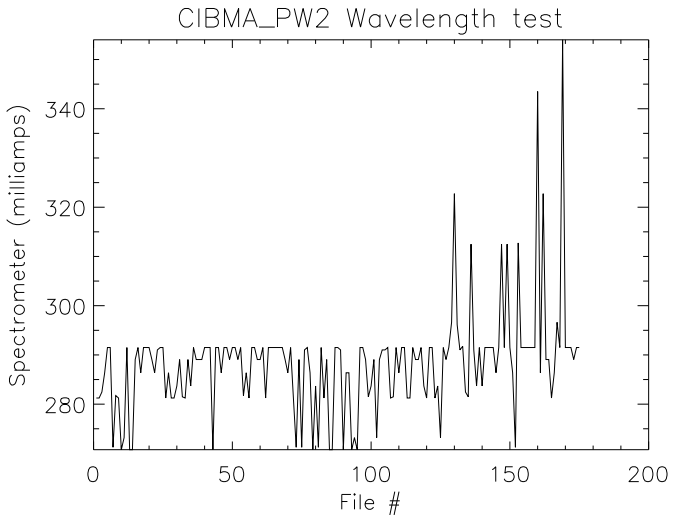

Figure 3.17: Spectrometer current for Wavelength test

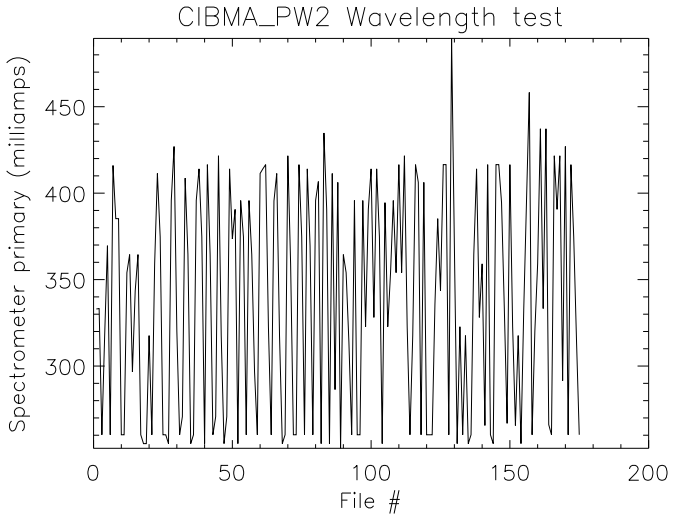

Figure 3.18: Spectrometer primary current for Wavelength test

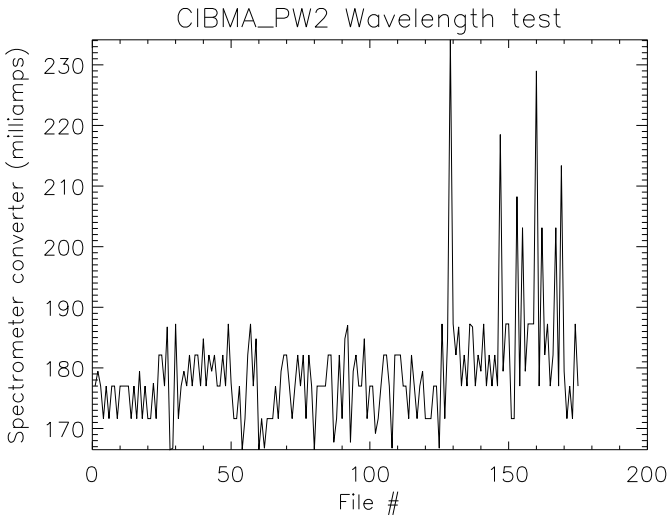

Figure 3.19: Spectrometer converter current for Wavelength test

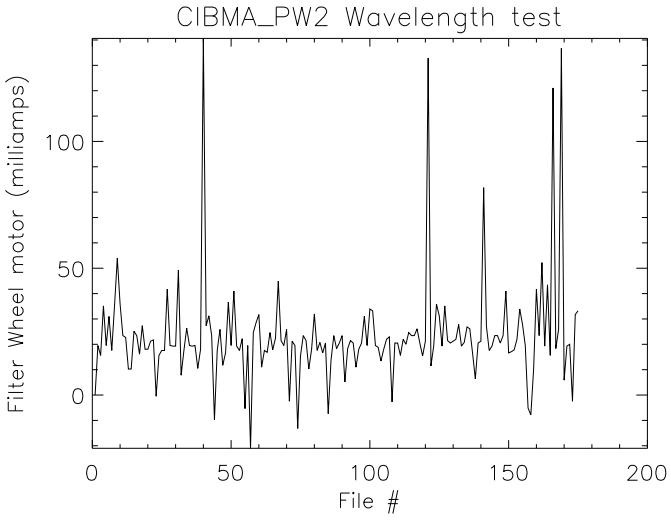

Figure 3.20: Filter wheel motor current for Wavelength test

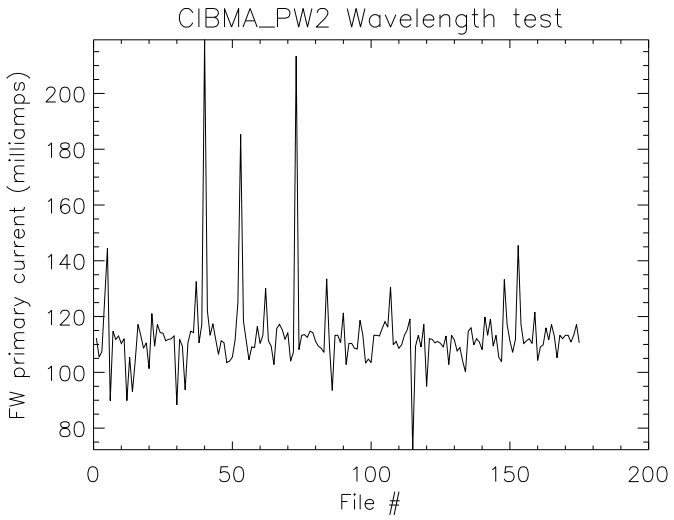

Figure 3.21: Filter wheel motor primary current for Wavelength test

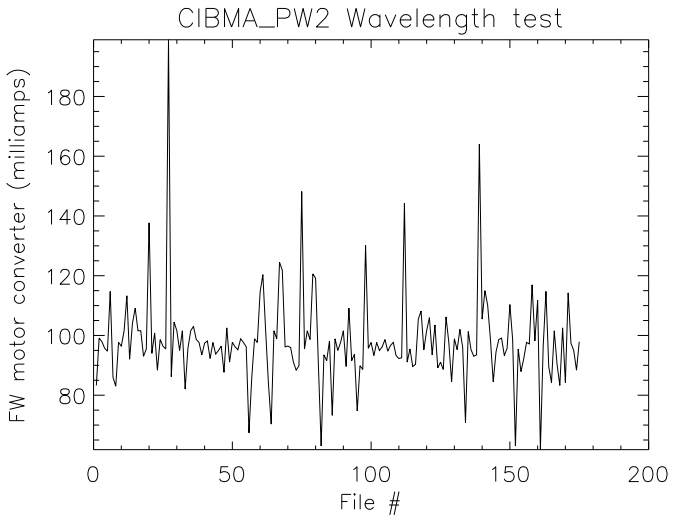

Figure 3.22: Filter wheel motor converter current for Wavelength test

For the CRISP currents, the effects of the restart are most obvious as an increase in signal variability (standard deviation) between the two runs. Several show increases in variability by between a factor of three (Spectrometer converter, see Table 3.2 and Figure 3.19) and a factor of five (the Mirror Motor heater, see Table 3.2 and Figure 3.13). The major significant exceptions to this conclusion are the DPU, the cooler converter current, and the spectrometer primary current. The DPU (Table 3.2 and Figure 3.14) shows essentially no change between the two runs. One puzzle with these data is how the cooler current could be turned off without simultaneously terminating the cooler converter

Table 3.1: OCF / CCD Quantities

Quantity (units)	Value
Exposure (milliseconds)	979.968
Filter Wheel (#)	1-5, stepped
Attenuator 1 (Halogen) setting	0 (no attenuation)
Attenuator 2 (Xenon) setting	255 (full attenuation)
Azimuth (°)	-1.04
Elevation (°)	1.12
Stage Motor on/off	On through both runs
CCD (°C)	138.75 (must be bad)
Mirror side	0
Mirror offset (°)	0.0
Reference detector	0.0

current, since it was standard procedure to turn the cooler current on for ten minutes prior to activating the cooler converter (Reference # 3).

Predominantly, the effect of the restart on the imagery is to introduce herringbone noise into the imagery itself. The M/C point source is missing in the first image (Figure 3.8); however, it is visible in the second and third images (the single snapped image and the first script restart image, Figures 3.9 and 3.10) as a small white dot in the center of the image, or just above and to the right of center. While the noise leaves the image mean relatively unchanged (219.03 DN for image 122 and 219.79 DN for image 123), the peak to peak DN of the imagery doubles from image 122 to image 123 (5.99 DN versus 12.03 DN). A similar increase occurred in all imagery with the herringbone noise for any of the affected calibration tests on December 25, 2001.

Table 3.2: CIBMA PW2 current statistics for CRISP

Quantity	Units	Before recenter: Mean	SD	After recenter: Mean	SD
Mirror Motor (M. M.)	milli-amps	515.579	4.46088	508.517	6.64525
M. M. Heater	milli-amps	-12.1790	3.57412	-1.23452	19.3845
DPU	milli-amps	1420.67	34.4337	1417.20	30.2880
Cooler (C.)	milli-amps	241.175	139.347	1.31283	2.15631
C. Converter	milli-amps	139.660	65.2839	135.572	63.7731
Spectrometer (S.)	milli-amps	285.765	6.92039	294.212	14.8538
S. Primary	milli-amps	335.887	63.4250	343.335	68.3543
S. Converter	milli-amps	176.740	5.17930	185.404	13.9791
Filter Wheel (FW) Motor	milli-amps	27.2977	18.4848	27.2977	24.5220
FW Motor Primary	milli-amps	113.523	17.3150	112.406	7.01084
FW Motor Converter	milli-amps	98.5728	15.3623	96.9100	14.6360

When the instrument integrated into the satellite and taken to Goddard Space Flight Center for system testing, the herringbone noise was not seen again. This suggests the noise is a result of the specific configuration of the sensor and OCF on that day.

Possible noise sources in CRISP

While no one candidate has emerged from the noise analysis as the conclusive cause of the herringbone in the CRISP imagery, several anomalies remain to be investigated.

(1) Stage Motor Noise: The stage motor is known to be a source of noise in the OCF. However, it was on both before and after the stop and restart, and the stage itself was not moved. So, unless some unknown source induced increased noise in the stage motor, it is unlikely to be the source of the herringbone noise.

(2) Cooler current/Cooler converter current disconnect: According to the data recorded in the FITS header for the images in the Wavelength test, the cooler current was turned off when the M/C Point Source was refocused. Yet, the cooler converter current shows no change in mean or standard deviation. This violates operating procedure for the cooler, since the converter cannot run while the cooler is off. The handwritten calibration log for this day indicates nothing about changing the state of the cooler at this time. Without more information about the state of the test, it will be nearly impossible to duplicate what effect may have caused this anomaly, or to determine whether or not it is related to the herringbone noise in the imagery.

(3) Mirror motor noise: When the M/C point was refocused, the mirror motor current both dropped in mean and increased by a factor of three in standard deviation. Whether this then fed-back into the sensor can only probably be determined by duplicating the test conditions with a new instrument.

It is thus strongly recommended that, should a new CRISP sensor be built for a second CONTOUR mission or if a similar instrument is used in the future, an attempt be made to duplicate the experimental conditions of the tests on this day to see if the herringbone noise can be caused to recur.

3.3.2 CFI

A portion of the analysis of dark columns discussed the lack of correlation of the major source of noise in CFI, horizontal bands of two distinct mean levels in the imagery, with variations in the dark columns. The occurrence of the horizontal bands was, unfortunately, frequent enough that the location of the band discontinuity could be analyzed. When the banding appeared, its location in row number (R, where the image origin is in the lower left corner) was dependent on exposure time (τ_e) in milliseconds as follows:

$$R = 1160.21 - 1.2240 * \tau_e \tag{3.5}$$

However, no relationship could be found to predict the direction of the band mean change (low mean to high mean, or vice versa). As has already been noted, the dark columns contained insufficient data to be used to measure the direction of the band mean change.

3.3.3 First Differences (FD) Analysis

A different approach to quantify and correct the banding is that of calculating first differences (FD). This first difference approach is less sensitive to gradients and variations in the image than a technique based on simple mean comparisons would be. The steps in the technique are five. (1) Each row in the image is averaged. (2) Each row average is subtracted from the following row average and an absolute value is applied to this first difference. (3) The maximum first difference is located. (4) The mean and standard deviations of the first differences are calculated. (5) The maximum is compared to the mean plus five standard deviations of the first difference. If the maximum first difference is greater than the mean plus five standard deviations, the image may be considered to be split into horizontal bands, and the technique has located the boundary between the two bands.

Now that the boundary has been located, it is straightforward to calculate a mean of the two bands, adjust one band to the other by subtracting the difference of the means, and stitch together a uniform image. Using image 130 of the 'final' flatfield linearity test using the white sphere as a target, we begin with the raw image (Figure 3.23).

A similar analysis could be used on the few CRISP images that had horizontal bands, especially as the dark columns show no zoning for that sensor.

The average of all non-dark columns on a row by row basis is shown in Figure 3.24. The calculated first differences, with the threshold of mean plus five standard deviations, are plotted on Figure 3.25. The boundary can be spotted easily at row 485. After applying the first difference correction, the average rows now appear as in Figure 3.26 and the image as in Figure 3.27.

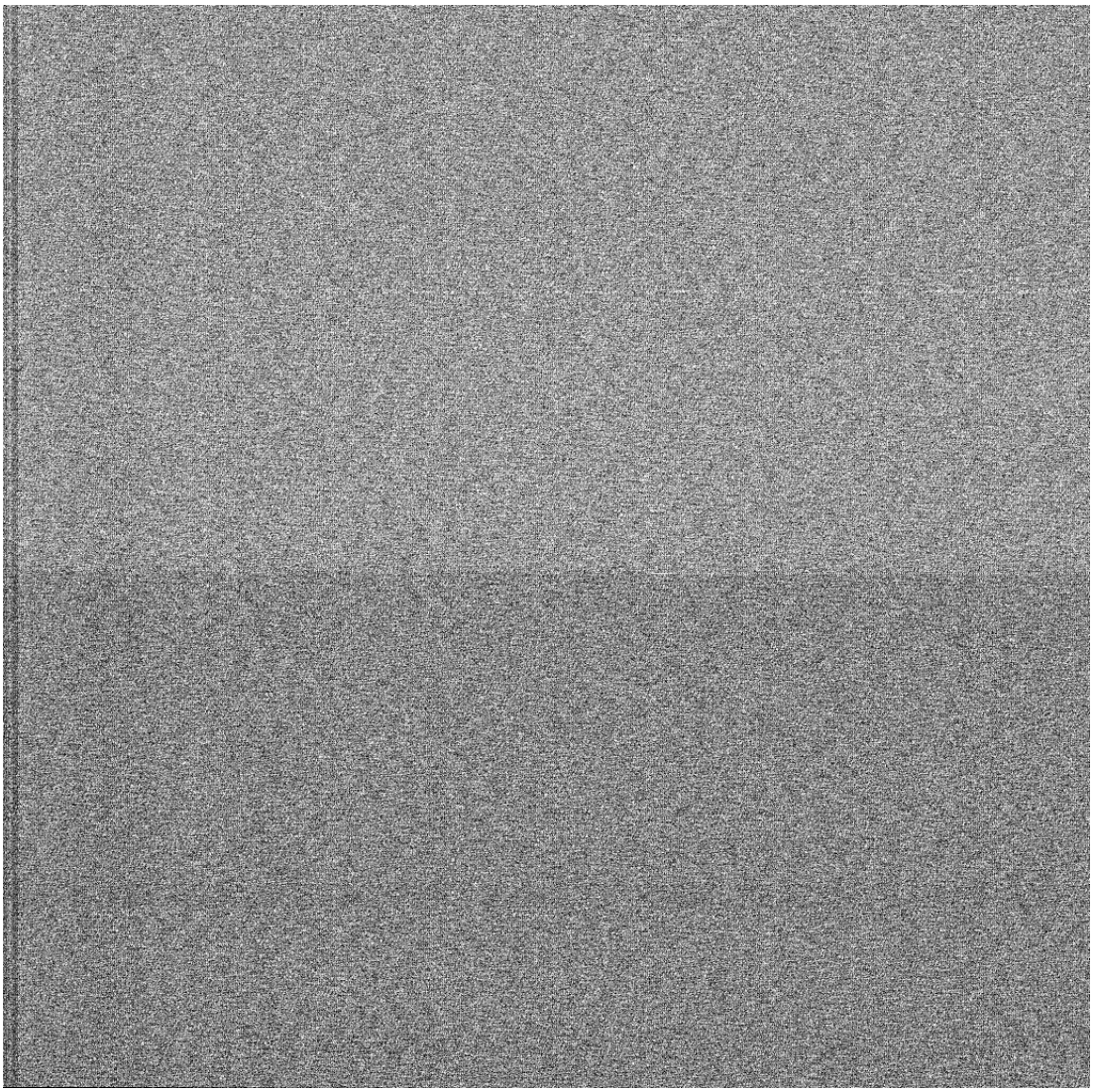

Figure 3.23: Dark image from a 'final' flatfield calibration run. The filter number is 7, the exposure time is 551 milliseconds, and both the Halogen and Xenon bulbs are fully attenuated. The average difference between the two fields is 0.7 DN. If the image is viewed in a printed copy, any other bands present are due to toner differences when printed.

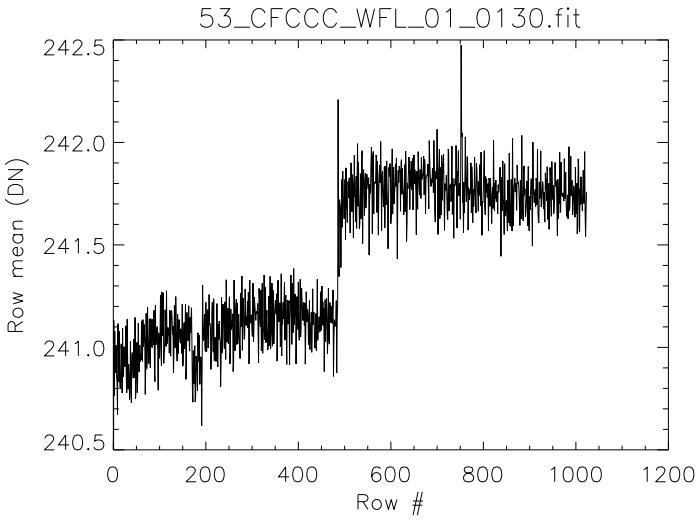

Figure 3.24: Average of all columns of image data (no dark columns) for image 130 described above.

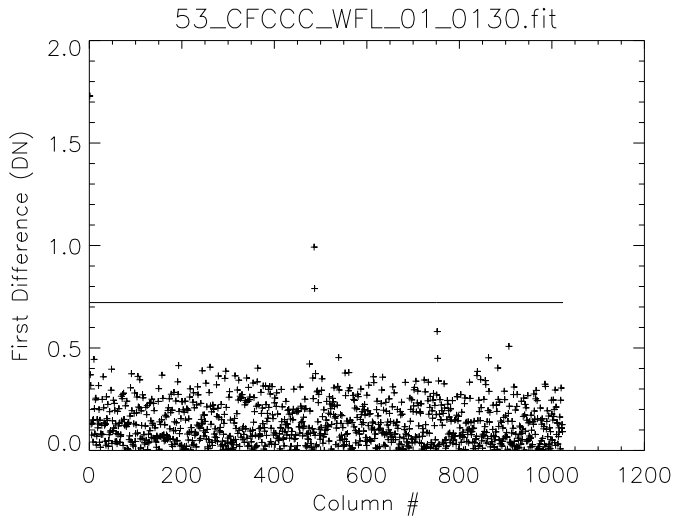

Figure 3.25: First differences with threshold for the image above.

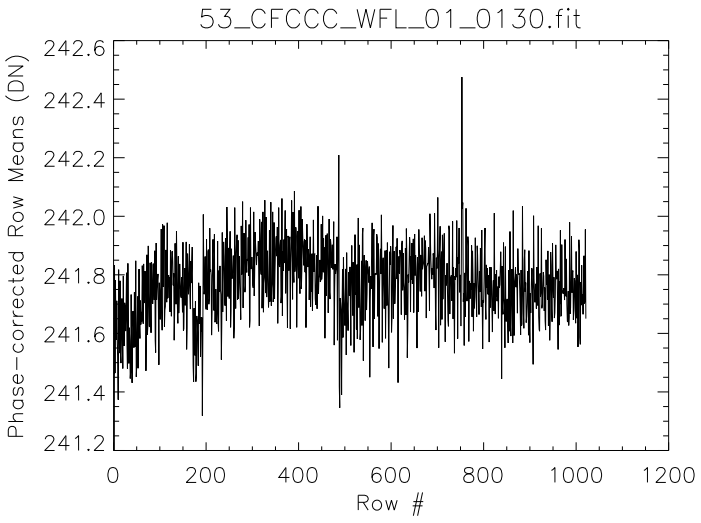

Figure 3.26: First difference-corrected row averages for image 130.

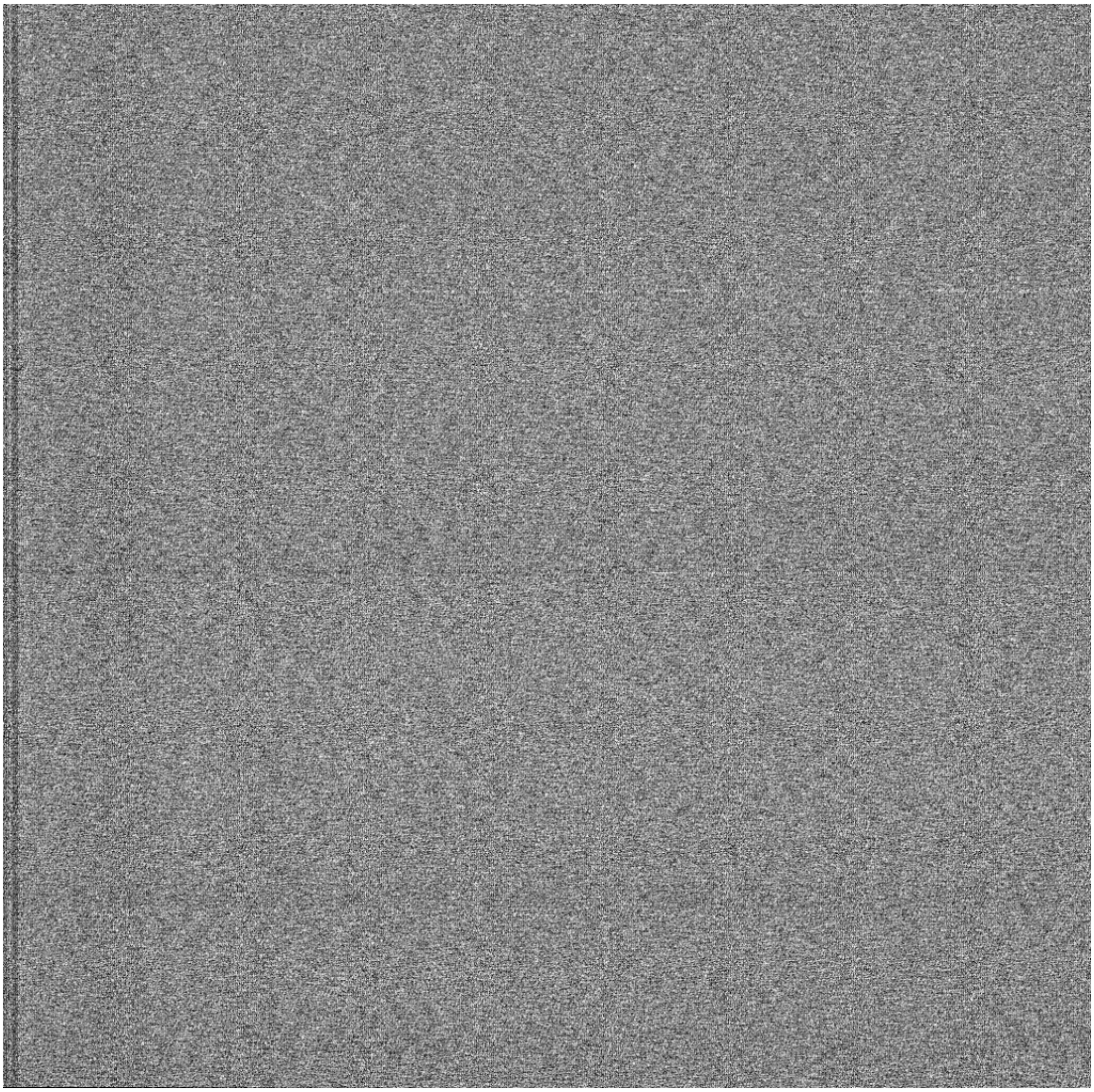

Figure 3.27: Image 130 with horizontal banding removed. If the image is viewed in a printed copy, any bands present are due to toner differences when printed.

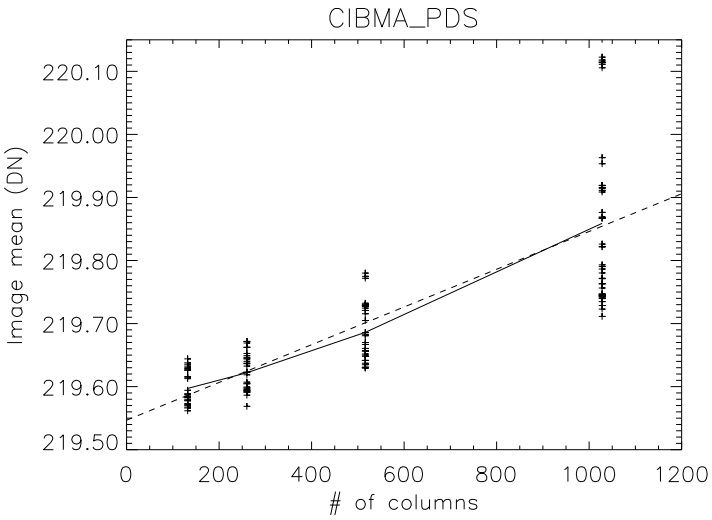

Figure 3.28: Dependence of dark series image mean on binned size of image for CRISP. The solid line connects the mean of each data set, and the dashed line is the fit to the data as given above.

3.4 Binning Anomaly

3.4.1 CRISP

A small dependence on binning was discovered in CRISP that should be documented here. Specifically, the image mean for dark series images was found to depend slightly on the degree of binning, with a linear decrease in image mean from 219.86 for unbinned data to 219.59 for 128 by 128 binned data. A linear fit to the data is as follows (where R is the number of rows in the binned image, counting from an image origin at the lower left of the image):

$$DN(mean) = 0.00029012 * R + 219.55 \tag{3.6}$$

Figure 3.28 shows the data and the fit to the data given above. The fit deviates only slightly from the mean at each bin level.

3.4.2 CFI

Since the effects of binning on the dark columns in CFI has been discussed earlier in this report, that material will not be repeated. Neither will the well-known problem of point smear with binning be, since corrections are already in-place to remove the effect. Instead, problems with significant distortion in both the dark and saturated imagery will be presented. The binning effects were examined in formatting tests in both post-environment and 'final' calibrations. Imagery were acquired at full scale (1024 by 1024), 512 by 512 , and 256 by 256 pixels, for filter wheel setting #4 (620 nm center wavelength with 4 nm bandwidth). Figure 3.29 shows 'dark' data binned to 512 by 512 pixels. While the image mean eventually reaches a level of ~245 DN, it is clear from the figure that at least one quarter to one half of the data are adversely affected. Ringing at the transition from dark column to image is also present in an initial spike of 3.7 DN dynamic range. Figure 3.30 shows that the problem is worse at greater binning levels. There are two transition spikes, and the rise to a mean level takes nearly all the columns in the image. Odd-even variations on the

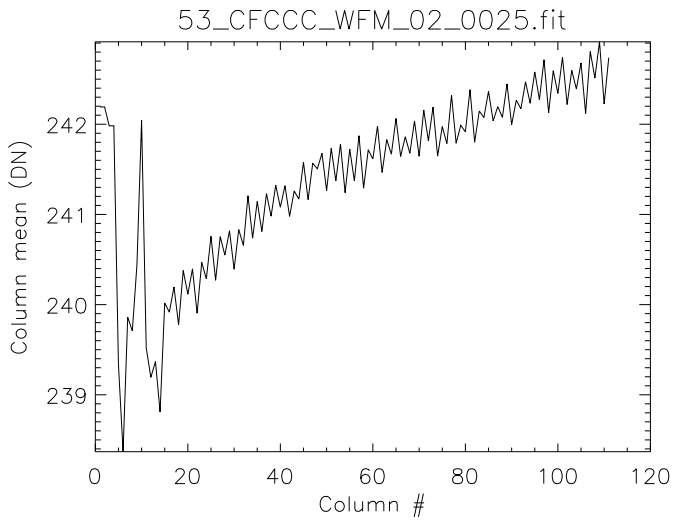

Figure 3.29: Ringing and undershoot/recovery in a binned image. The exposure time for this 512 by 512 binned dark image is 204.8 milliseconds. The Halogen and Xenon lamps were fully attenuated (255 setting).

order of one DN are present in all binned images, although this is no worse than what is encountered in other noisy CFI data. Figure 3.31 shows an example of ringing in a saturated binned image.

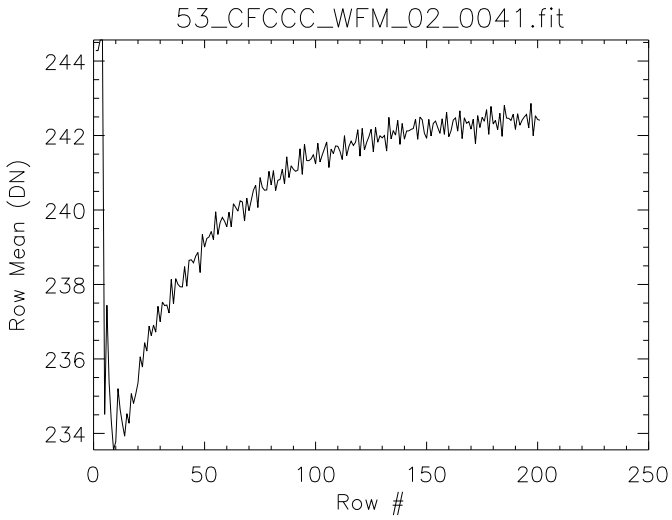

Figure 3.30: Ringing and undershoot/recovery in a binned image. The exposure time for this 256 by 256 binned dark image is 51.2 milliseconds. The Halogen and Xenon lamps were fully attenuated (255 setting).

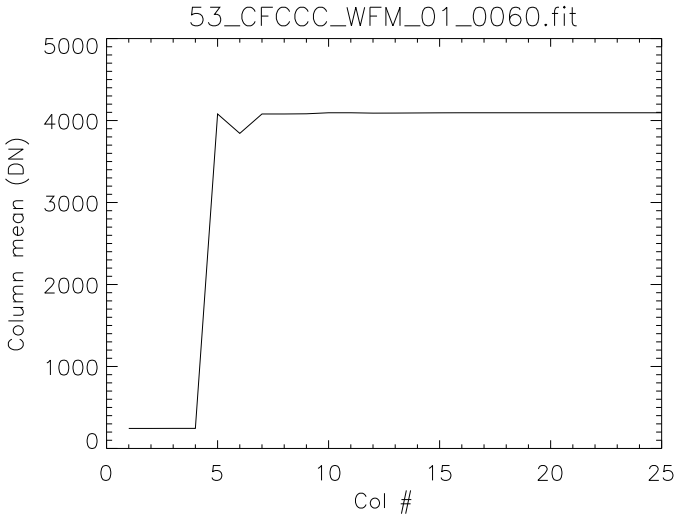

Figure 3.31: Ringing in a saturated, 256 by 256 'binned' image from the CFI 'final' formatting test. The exposure time for this image is 901.12 milliseconds, the filter number is 4 (center wavelength of 610 nm with a bandwidth of 4 nm). The Halogen and Xenon bulbs are nearly fully attenuated (setting 220).

3.5 CRISP Mirror Calibration

3.5.1 CIBMA_WMI

The CRISP sensor was not designed to have a direct line of sight with the comet. Instead, the CCD viewed a mirror reflecting the exterior into its focal plane array (FPA). This shielded the instrument from micrometeorites and radiation without requiring a cover over the sensor. The aim of this test was to use the white sphere optical source to calibrate the intensity reflected off the mirror through all the filter wheel settings and over a large range of exposure times (1.024 milliseconds to 900.096 milliseconds). In the OCF test chamber, rotating the mirror for calibration required rotating the stage position to keep the white sphere in the field of view. Unfortunately, during this calibration test, the camera body itself began occulting the view of the white sphere when the stage angle approached +8 °, making the test unusable for calibration.

3.5.2 CIBMA_PMI

However, a more limited test of the mirror calibration was performed later on the same day as the white sphere test above, for which the M/C point source was used. To view the M/C source, the camera was turned by 180 °, so the camera body could never occult the Field of View, no matter how the stage was turned. During this test the filter number was fixed at 6, with center wavelength of 610 nm and bandwidth of 40 nm, and had a single long exposure time (980 milliseconds). The point itself gave a strong signal over 49 pixels, with a weaker signal for three or four (depending on location) pixels surrounding the strong signature. Thus, the point signal was averaged over these 49 pixels, as shown in Figure 3.32 for Side A and Figure 3.33 for Side B. The data for Side A may be fitted with a Gaussian distribution as follows:

$$DN_{M/Cpoint} = 137.82e^{\frac{-z^2}{2}} + 1236.02 - 2.17\lambda \tag{3.7}$$

where: $z = \frac{\lambda - 4.6065}{3.0769}$, and λ is the line of sight angle in degrees. This is only a relative measure, and it should be noted that the peak is offset from the head-on line of sight by 4 °. The data for Side B may be fitted with a slightly different Gaussian distribution:

$$DN_{M/Cpoint} = 408.088e^{\frac{-z^2}{2}} + 1110.94 \tag{3.8}$$

where: $z = \frac{\lambda - 0.05540}{2.5981}$, and λ is the line of sight angle in degrees. For Side B, the peak of intensity is at a line of sight of 0°. The reason for the difference in peak location between the two sides is unclear.

To be used at other filter wheel settings, the values derived here should be multiplied by a ratio of the responsivities to obtain relative magnitude differences.

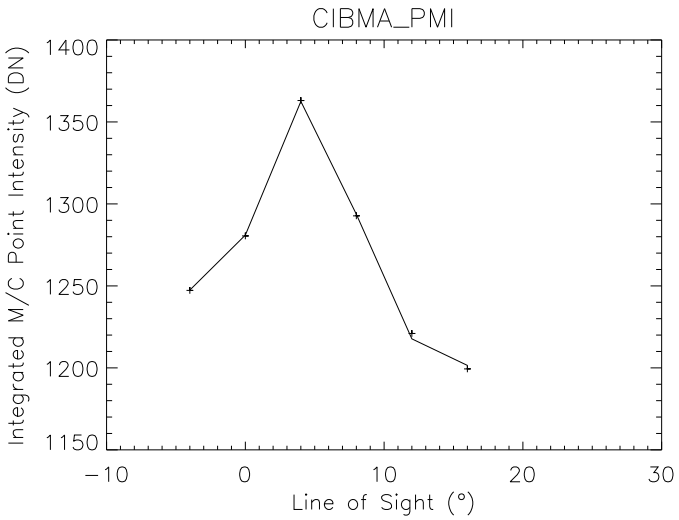

Figure 3.32: Averaged M/C point source intensity as a function of line of sight in degrees for filter wheel #6 and exposure time of 980 milliseconds for Side A of the CRISP mirror. The Halogen lamp was completely unattenuated (setting 0) and the Xenon lamp was fully attenuated (setting 255).

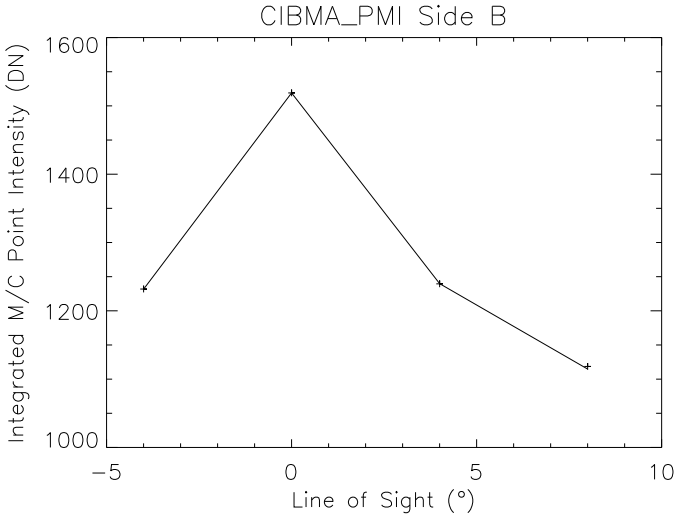

Figure 3.33: Averaged M/C point source intensity as a function of line of sight in degrees for filter wheel #6 and exposure time of 980 milliseconds for Side B of the CRISP mirror. The Halogen lamp was completely unattenuated (setting 0) and the Xenon lamp was fully attenuated (setting 255).

Chapter 4

Conclusions and Lessons Learned

The dark column properties and imager characteristics of the CRISP and CFI sensors were exhaustively tested during the OCF calibrations conducted prior to instrument integration.

(1) CRISP dark column properties: The uncorrupted dark column means of the CRISP sensor remained below 219.9 DN and varied by <1 DN over the range of exposure times and temperatures used in the OCF calibrations. The dark column means may be treated as equivalent to the dark image means, with an error of <0.3 DN. In a few cases of long exposure time white imagery, saturated pixels showed up in the dark columns. It is suspected the the saturated image pixels bled over into the dark columns during read-out.

(2) CFI dark column properties: The uncorrupted dark column means of the CFI sensor were more variable as a function of exposure time and temperature, varying by <5 DN with exposure time at temperatures expected in space, and by tens of DN for $26°C$ or higher. Binning caused the number of dark columns to increase, with columns of intermediate (and even saturated) intensity between the dark levels and the image level appearing as well. Horizontal banding in the imagery persisted in the dark columns; however, because of the variability in the dark column pixel intensities, these could not be used to predict horizontal banding in the imagery itself.

(3) CRISP Frame Transfer Smear Removal: The FTSR for CRISP worked well. Barring future difficulties, no further work should be required on FTSR for follow-on versions of this sensor.

(4) CFI Frame Transfer Smear Removal: The FTSR for CFI under-corrected for short exposure times and over-corrected for long ones. It was unclear from the data whether the problem is due to the algorithm itself or due to errors calculating and directing the exposure time in the CFI firmware. It is recommended that:

(a) the clocking firmware/hardware in CFI be checked to ensure it is calculating the correct start of the exposure time, which should be the exposure time plus frame transfer time, and,

(b) the FTSR be re-calculated using the 'modified' exposure time to check (and revise if necessary) the CFI algorithm.

(5) Responsivity calculations: The problems with the CFI FTSR were so serious that accurate responsivities could not be calculated for the sensor.

(6) White sphere calibrations: An extensive set of calibrations of the dual (Halogen and Xenon) lamp white sphere was conducted by Optronic Labs. Data were collected in one nanometer steps for five attenuator settings for both lamps. These results are invaluable for careful calculation of sensor responsivities. However, when the values were reported to JHU/APL, the measured data were converted to ratios, with fits provided to retrieve calculated radiances at any wavelength and attenuator setting. The MEASURED attenuated radiances were not reported in raw form. While attenuated radiances could be, with some analysis, retrieved from the reported results, uncertainty, beyond that which occurs with any measurement, will remain about the data because the numbers used must, of necessity, be calculated, not reported, quantities. In future, it is suggested that, whatever analysis is performed by the facility calibrating the source, all the raw calibration data AS MEASURED be reported to JHU/APL.

(7) Noise in CRISP: Herringbone noise was seen in the CRISP imagery during post-environment calibrations in the OCF that was not seen when the sensors were integrated into the complete instrument and taken to Goddard Space Flight Center for further testing. Several possible sources were identified, which should be tested should a future instrument be developed.

(8) Noise in CFI: There were two types of noise in CFI, horizontal banding and binning anomalies.

(a) Horizontal banding: While the occurrence of the horizontal banding could not be predicted, nor could the direction of the reversal (low mean to high mean or vice versa), if a band difference did occur, the location of the difference in the image was dependent on exposure time. A first difference analysis is proposed to correct the imagery for the banding.

(b) Binning anomalies: When the CFI imagery was acquired in binning mode, significant image corruption resulted, including ringing, mixing of dark and image intensities, and multiple image intensity spikes at the dark column/image transition. It is recommended that the binning mode be thoroughly examined should a follow-on instrument be proposed.

(9) OCF Calibration procedure: It is recommended that several individuals, knowledgeable in the properties and capabilities of the OCF and the sensors themselves, be on hand during calibrations to examine data as they are acquired. There were several cases during the CONTOUR OCF calibrations (such as during the CRISP mirror test with the white sphere as a source), when immediate inspection of data would have prevented the corruption of valuable test results. This suggestion is being made, even though it well-understood that it is not, by reason (among others) of scheduling difficulties for personnel or simple exhaustion during long test runs, possible to eliminate all errors during the acquisition of experimental results.

Chapter 5

References

(1) Hawkins, S. E. III, E. H. Darlington, S. L. Murchie, K. Peacock, T. J. Harris, C. B. Hersman, M. J. Elko, D. T. Prendergast, B. W. Ballard, and R. E. Gold, “Multi-Spectral Imager on the NEAR Earth Asteroid Rendezvous Mission”, Space Science Reviews #82: 31-100, 1997.
(2) Hayes, J.R. “CFI Software Requirements” SRI-01-DRAFT November 1, 2001, 40 pp.
(3) Hayes, J.R. “CRISP Software Requirements” SRI-01-DRAFT November 1, 2001, 75 pp.
(4) Howser, L.M., “Analysis of Noise in the CONTOUR Spectrograph Images”, A1F(2)02-U-067, October 29, 2002, 16 pp.
(5) Howser, L.M., “Measurements of the Attenuator for the CRISP Test Equipment”, A1F(2))2-U-082, October 29, 2002, 8 pp.
(6) Murchie, S., M. Robinson, D. Domingue, H. Li, L. Prockter, S.E. Hawkins III, W. Owen, B. Clark, and N. Izenberg, “Inflight calibration of the NEAR multispectral imager, II: Results from Eros Approach and Orbit”, Icarus #155, 2002, pp. 229-243.
(7) Murchie, S., M. Robinson, S.E. Hawkins III, A. Harch, P. Helfenstein, P. Thomas, K. Peacock, W. Owen, G. Heyler, P. Murphy. E. H. Darlington, A. Keeney, R. Gold, B. Clark, N. Izenberg, J, F. Bell, III, W. Merline, and J. Veverka, “Inflight calibration of the NEAR multispectral imager”, Icarus #140, 1999, pp. 66-91.

Chapter 6

Appendixes

6.1 White Sphere Calibration fitting code (IDL)

```
;*****************************************************************
    ;+
    ; NAME:
    ; HALOGEN_XENON_FITS
    ; PURPOSE:
    ; Function to calculate spectral radiances from fits to
    ; August 2002 calibrations of Halogen/Xenon white sphere.
    ; CALLING SEQUENCE:
    ; specrad = halogen_xenon_fits(wavel, hatten, xatten)
    ; INPUTS:
    ; wavel = (float) wavelength in nanometers (valid range 350-998nm)
    ; hatten = (float) attenuator setting (0-255) for halogen lamp
    ; xatten = (float) attenuator setting (0-255) for xenon lamp
    ; OUTPUTS:
    ; specrad = (double) spectral radiance value [W / (cm^2-sr-nm)]
    ; KEYWORD PARAMETERS: NONE
    ; USES: Calibration data stored in the text files:
    ; Tungsten_all_atten_radiances.txt (for halogen lamp) and
    ; Xenon_all_atten_radiances.txt.
    ; NOTES: (1) No attempt was made to fit the multiple spectral lines
    ; encountered in the Xenon measurements. (2) Two fits were
    ; required for the Xenon data, the first for 350-724 nm,
    ; the second for 725-999 nm. (3) The fits to the calibration
    ; data are recalculated with each call, since SFIT fits to
    ; the array indicies of the independent variables,
    ; and not to the independent variables themselves.
    ; MODIFICATION HISTORY:
    ; MRK 11/07/02 Created.
    ; MRK 11/29/02 Ratios to accomodate differences in halogen
    ; lamp intensity and variations in attenuator
    ; properties added to include L. Howser’s
```

```
; analysis of the sphere calibrations (c.f.
; "Measurements of the Attenuator for the CRISP
; Test Equipment, #A1F(2)02-U-82, Oct. 29, 2002).
; Copyright (C) 2002, Johns Hopkins University/Applied Physics Laboratory
; This software may be used, copied, or redistributed as long as it is not
; sold and this copyright notice is reproduced on each copy made. This
; routine is provided as is without any express or implied warranties
; whatsoever. Other limitations apply as described in the file disclaimer.txt.
;-
;*****************************************************************
function halogen_xenon_fits, wavel, hatten, xatten, help=hlp
if (n_params(0) lt 1) or keyword_set(hlp) then begin
print,' Function to calculate spectral radiances from fits to '
print,' August 2002 calibrations of Halogen/Xenon white sphere. '
print,' specrad = halogen_xenon_fits(wavel, hatten, xatten) '
print,' INPUTS: '
print,' wavel = (float) wavelength in nanometers (valid range 350-998nm) '
print,' hatten = (float) attenuator setting (0-255) for halogen lamp '
print,' xatten = (float) attenuator setting (0-255) for xenon lamp '
print,' OUTPUTS: '
print,' specrad = (double) spectral radiance value [W / (cm^2-sr-nm)] '
print,' KEYWORD PARAMETERS: NONE '
print,' USES: Calibration data stored in the text files: '
print,' Tungsten_all_atten_radiances.txt (for halogen lamp) '
print,' and Xenon_all_atten_radiances.txt '
print,' NOTES: (1) No attempt was made to fit the multiple spectral '
print,' lines encountered in the Xenon measurements. (2) Two fits '
print,' were required for the Xenon data, the first for 350-724 nm, '
print,' the second for 725-999 nm. (3) The fits to the calibration '
print,' data are recalculated with each call, since SFIT fits to '
print,' the array indicies of the independent variables, '
print,' and not to the independent variables themselves. '
return, 0
endif
; Declare input and calculation parameters.
halsprad = 0.D0
xensprad = 0.D0
fitord = 4
headerstr = ' '
numwl = 0
atten0 = 0
atten1 = 0
atten2 = 0
atten3 = 0
atten4 = 0
iwl = 0
fmthstr = "$(I3,6X,I1,10X,I3,4(9X,I3))"
fmtdstr = "$(I3,5(1X,E11.4))"
```

```
minwavel = 350.0
xenwlbound = 724.0
maxwavel = 998.0
halbaf = 914.0/1998.0 ; Factor added to account for aged Halogen
; bulb during calibrations, while a new bulb
; was used during the Optronics Lab cals.
; L. Howser also derived ratios of attenuator changes between the
; sensor calibrations and the sphere calibrations. The ratios are
; given below for both lamps.
attenset = fltarr(13)
attenset(0) = 0.0
for ivl=1,3 do attenset(ivl) = 130.0 + (ivl-1.0)*10.0
for ivl=4,11 do attenset(ivl) = 170.0 + (ivl-4.0)*10.0
attenset(12) = 255.0
halattrat = [1.00, 1.10, 1.08, 1.06, 1.27, 1.25, $
1.18, 1.69, 1.47, 1.07, 0.47, 1.22, 1.00]
xenattrat = [1.00, 0.95, 0.90, 0.85, 0.91, 0.86, $
0.81, 1.00, 0.92, 0.80, 0.59, 1.26, 1.00]
; ================== Halogen lamp calculations ======================
; Calculate fourth-order fit coefficients for Halogen lamp.
; Valid calibrations cover the wavelength range of 340nm-998nm.
; For consistency with the Xenon measurements, use 350-998nm.
; Open Halogen calibration data file, read in wavelengths,
; attenuator settings, and spectral values.
openr, lundat, 'Tungsten_all_atten_radiances.txt', /get_lun
for ivl=0,1 do readf, lundat, headerstr
readf, lundat, fmthstr, numwl, atten0, $
atten1, atten2, atten3, atten4
attens = [atten0, atten1, atten2, atten3, atten4]
readf, lundat, headerstr
readwavel = intarr(numwl)
readhrad = fltarr(5, numwl)
for ivl=0, numwl-1 do begin
readf, lundat, fmtdstr, iwl, rad0, rad1, rad2, rad3, rad4
rad1 = 1.08 * rad1 ; Ratios to take into account attenuator
rad2 = 1.27 * rad2 ; differences between sensor cal and sphere
rad3 = 1.69 * rad3 ; cal. While not completely correct, these
rad4 = 1.07 * rad4 ; will do for the lateness of the hour.
readwavel(ivl) = iwl
readhrad(0:4,ivl) = [rad0, rad1, rad2, rad3, rad4]
endfor
close, lundat
free_lun, lundat
readhrad = readhrad * halbaf ; Correct intensity for Halogen bulb aging factor.
; Reduce size of wavelength array for ease of calculation.
wantwl = where(readwavel ge minwavel, numwls)
; If valid wavelength range exists, retrieve spectral values.
if (numwls le 0) then begin
```

```
print, 'No valid wavelengths found.'
return, 0
endif else begin
wavelength = fltarr(numwls)
wavelength = readwavel(wantwl)
halrad = fltarr(5, numwls)
halrad(0:4,0:numwls-1) = readhrad(0:4,wantwl)
readwavel = 0.0
readhrad = 0.0
endelse
; Find index values that point into the attenuator dimension
; of the fit coefficients. Example: since the attenuator
; values are 0 at index 0 and 100 at index 1, for an attenuator
; setting of 50, use an attenuator index value of 0.5.
useaind = where(attens eq hatten, numusi)
if (numusi le 0) then begin
diffatten = attens - hatten
negdiffatten = where(diffatten lt 0.0, numneg)
posdiffatten = where(diffatten gt 0.0, numpos)
if (numneg gt 0) then lowint = $
where(negdiffatten eq max(negdiffatten), nlowint)
if (numpos gt 0) then higint = $
where(posdiffatten eq min(posdiffatten), nhigint)
if (nlowint ge 0) and (nhigint gt 0) then begin
useaind = (hatten - attens(negdiffatten(lowint(0)))) / $
(attens(posdiffatten(higint(0))) - $
attens(negdiffatten(lowint(0)))) + negdiffatten(lowint(0))
endif
endif
; Find index values that point into the wavelength dimension
; of the fit coefficients. Example: since the halogen values
; are reported for even nanometers, 350 at index 0, 352 at
; index 1, etc., for a wavelength of 351nm, use a wavelength
; index value of 0.5.
usewind = where(wavelength eq wavel, numusi)
if (numusi le 0) then begin
diffwl = wavelength - wavel
negdiffwl = where(diffwl lt 0.0, numneg)
posdiffwl = where(diffwl gt 0.0, numpos)
if (numneg gt 0) then lowint = $
where(negdiffwl eq max(negdiffwl), nlowint)
if (numpos gt 0) then higint = $
where(posdiffwl eq min(posdiffwl), nhigint)
if (nlowint ge 0) and (nhigint gt 0) then begin
usewind = (wavel - wavelength(negdiffwl(lowint(0)))) / $
(wavelength(posdiffwl(higint(0))) - $
wavelength(negdiffwl(lowint(0)))) + negdiffwl(lowint(0))
endif
```

```
endif
; Use SFIT to calculate fourth-order fit coefficients.
temphres = sfit(halrad, fitord, kx = halfit)
; Calculate spectral radiance from halogen lamp.
halsprad = 0.D0
for j=0, fitord do begin
for i=0, fitord do halsprad = halsprad + $
halfit(j,i) * useaind^i * usewind^j
endfor
; ================== Xenon lamp calculations ======================
; Open Xenon calibration data file, read in wavelengths,
; attenuator settings, and spectral values.
openr, lundat, 'Xenon_all_atten_radiances.txt', /get_lun
for ivl=0,1 do readf, lundat, headerstr
readf, lundat, fmthstr, numwl, atten0, $
atten1, atten2, atten3, atten4
attens = [atten0, atten1, atten2, atten3, atten4]
readf, lundat, headerstr
readwavel = intarr(numwl)
readxrad = fltarr(5, numwl)
for ivl=0, numwl-1 do begin
readf, lundat, fmtdstr, iwl, rad0, rad1, rad2, rad3, rad4
rad1 = 0.94 * rad1 ; Ratios to take into account attenuator
rad2 = 0.91 * rad2 ; differences between sensor cal and sphere
rad3 = 1.00 * rad3 ; cal. While not completely correct, these
rad4 = 0.80 * rad4 ; will do for the lateness of the hour.
readwavel(ivl) = iwl
readxrad(0:4,ivl) = [rad0, rad1, rad2, rad3, rad4]
endfor
close, lundat
free_lun, lundat
; Retrieve data needed to calculate a set of
; fourth-order fit coefficients for the Xenon lamp
; in the wavelength range 350-724nm).
if (wavel le xenwlbound) then wantwl = $
where((readwavel ge minwavel) and $
(readwavel le xenwlbound), numwls)
; Retrieve data needed to calculate a set of
; fourth-order fit coefficients for the Xenon
; lamp in the wavelength range 725-998nm).
if (wavel gt xenwlbound) then wantwl = $
where((readwavel gt xenwlbound) and $
(readwavel le maxwavel), numwls)
; If valid wavelength range exists, retrieve spectral values.
if (numwls le 0) then begin
print, 'No valid wavelengths found.'
return, 0
endif else begin
```

```
wavelength = fltarr(numwls)
wavelength = readwavel(wantwl)
xenrad = fltarr(5, numwls)
xenrad(0:4,0:numwls-1) = readxrad(0:4,wantwl)
readwavel = 0.0
readxrad = 0.0
endelse
; Find index values that point into the attenuator dimension
; of the fit coefficients. Example: since the attenuator
; values are 0 at index 0 and 100 at index 1, for an attenuator
; setting of 50, use an attenuator index value of 0.5.
useaind = where(attens eq xatten, numusi)
if (numusi le 0) then begin
diffatten = attens - xatten
negdiffatten = where(diffatten lt 0.0, numneg)
posdiffatten = where(diffatten gt 0.0, numpos)
if (numneg gt 0) then lowint = $
where(negdiffatten eq max(negdiffatten), nlowint)
if (numpos gt 0) then higint = $
where(posdiffatten eq min(posdiffatten), nhigint)
if (nlowint ge 0) and (nhigint gt 0) then begin
useaind = (xatten - attens(negdiffatten(lowint(0)))) / $
(attens(posdiffatten(higint(0))) - $
attens(negdiffatten(lowint(0)))) + negdiffatten(lowint(0))
endif
endif
; Find index values that point into the wavelength dimension of
; the fit coefficients. For Xenon, every integer nm value was
; measured, but the interpolation code was retained in case non-
; integer values of wavelengths are required in future analysis.
usewind = where(wavelength eq wavel, numusi)
if (numusi le 0) then begin
diffwl = wavelength - wavel
negdiffwl = where(diffwl lt 0.0, numneg)
posdiffwl = where(diffwl gt 0.0, numpos)
if (numneg gt 0) then lowint = $
where(negdiffwl eq max(negdiffwl), nlowint)
if (numpos gt 0) then higint = $
where(posdiffwl eq min(posdiffwl), nhigint)
if (nlowint ge 0) and (nhigint gt 0) then begin
usewind = (wavel - wavelength(negdiffwl(lowint(0)))) / $
(wavelength(posdiffwl(higint(0))) - $
wavelength(negdiffwl(lowint(0)))) + negdiffwl(lowint(0))
endif
endif
; Use SFIT to calculate fourth-order fit coefficients.
tempxres = sfit(xenrad, fitord, kx = xenfit)
; Calculate spectral radiance from xenon lamp.
```

```
xensprad = 0.D0
for j=0, fitord do begin
for i=0, fitord do xensprad = xensprad + $
xenfit(j,i) * useaind^i * usewind^j
endfor
; ======================== Final radiance calculations ====================
; Superpose spectral radiances of the two lamps.
specrad = halsprad + xensprad
; Return fitted value, end program, return control to main.
return, specrad
end
```

6.2 Calculated calibration data

6.2.1 Halogen lamp radiances

Wavelength [nm]	Attenuator Position				
	0	100	170	200	220
300	4.8400E-10	1.6140E-10	-6.1076E-09	3.3874E-09	1.2658E-08
302	7.9900E-11	-5.9950E-11	-6.6331E-12	-3.0456E-10	4.0184E-11
304	6.7400E-10	3.7460E-10	1.6786E-10	1.0483E-09	4.3314E-10
306	-2.6500E-10	-3.5539E-10	1.4270E-12	-4.4398E-11	1.8731E-10
308	5.4600E-10	3.3123E-10	4.8144E-11	-1.7477E-11	4.1372E-11
310	1.5400E-09	9.9988E-10	6.0959E-12	3.8748E-11	1.3541E-10
312	2.1700E-09	1.3158E-09	6.0454E-10	1.4897E-11	1.4034E-10
314	3.7000E-09	2.4693E-09	7.3893E-10	2.0113E-10	5.8345E-11
316	5.9200E-09	3.5798E-09	9.7704E-10	2.2049E-10	-1.5606E-10
318	9.9500E-09	6.0083E-09	1.6294E-09	3.6177E-10	-1.2586E-10
320	1.5400E-08	9.5663E-09	2.2173E-09	4.2855E-10	-8.5353E-11
322	2.4900E-08	1.5682E-08	3.5134E-09	7.2805E-10	3.2146E-11
324	3.5100E-08	2.2100E-08	4.6118E-09	8.7055E-10	-4.6957E-11
326	4.9700E-08	3.1409E-08	6.1931E-09	1.0410E-09	2.6074E-10
328	6.7200E-08	4.2638E-08	8.3825E-09	1.3739E-09	2.6921E-10
330	8.8500E-08	5.6495E-08	1.0509E-08	1.7218E-09	3.9512E-10
332	1.1200E-07	7.1523E-08	1.2908E-08	2.1301E-09	3.7612E-10
334	1.4100E-07	9.0614E-08	1.5946E-08	2.5790E-09	6.6670E-10
336	1.7000E-07	1.0907E-07	1.8712E-08	2.9101E-09	8.0058E-10
338	2.0200E-07	1.3016E-07	2.2046E-08	3.4362E-09	7.0536E-10
340	2.3700E-07	1.5301E-07	2.5672E-08	4.0582E-09	6.8358E-10
342	2.7300E-07	1.7592E-07	2.8993E-08	4.3909E-09	1.0331E-09
344	3.1300E-07	2.0280E-07	3.3056E-08	4.9776E-09	1.0725E-09
346	3.5200E-07	2.2814E-07	3.6981E-08	5.7130E-09	1.2632E-09
348	3.9300E-07	2.5488E-07	4.0958E-08	6.2043E-09	1.2920E-09
350	4.3700E-07	2.8395E-07	4.5570E-08	6.9649E-09	1.4336E-09
352	4.8100E-07	3.1289E-07	5.0106E-08	7.5599E-09	1.6630E-09
354	5.2800E-07	3.4355E-07	5.4849E-08	8.2526E-09	1.8383E-09
356	5.7500E-07	3.7435E-07	5.9656E-08	8.9315E-09	1.8299E-09

358 6.2400E-07 4.0679E-07 6.4771E-08 9.7356E-09 2.0870E-09
360 6.7400E-07 4.3932E-07 7.0008E-08 1.0638E-08 2.3711E-09
362 7.2700E-07 4.7412E-07 7.5659E-08 1.1495E-08 2.5452E-09
364 7.8100E-07 5.0924E-07 8.1232E-08 1.2398E-08 2.6549E-09
366 8.3700E-07 5.4587E-07 8.7249E-08 1.3338E-08 3.0412E-09
368 8.9200E-07 5.8213E-07 9.3294E-08 1.4230E-08 3.2124E-09
370 9.4700E-07 6.1795E-07 9.9426E-08 1.5466E-08 3.3795E-09
372 1.0000E-06 6.5308E-07 1.0525E-07 1.6119E-08 3.7784E-09
374 1.0500E-06 6.8564E-07 1.1087E-07 1.7192E-08 3.9298E-09
376 1.1100E-06 7.2476E-07 1.1765E-07 1.8361E-08 4.2979E-09
378 1.1600E-06 7.5685E-07 1.2351E-07 1.9316E-08 4.4614E-09
380 1.2200E-06 7.9568E-07 1.3031E-07 2.0536E-08 4.8250E-09
382 1.2800E-06 8.3465E-07 1.3704E-07 2.1637E-08 5.1840E-09
384 1.3400E-06 8.7381E-07 1.4377E-07 2.2929E-08 5.5003E-09
386 1.4100E-06 9.1911E-07 1.5166E-07 2.4246E-08 5.8522E-09
388 1.4700E-06 9.5810E-07 1.5845E-07 2.5400E-08 6.1880E-09
390 1.5400E-06 1.0039E-06 1.6638E-07 2.6728E-08 6.4645E-09
392 1.6100E-06 1.0491E-06 1.7443E-07 2.8188E-08 6.8916E-09
394 1.6800E-06 1.0951E-06 1.8265E-07 2.9543E-08 7.2269E-09
396 1.7400E-06 1.1341E-06 1.8968E-07 3.0812E-08 7.6222E-09
398 1.8100E-06 1.1797E-06 1.9776E-07 3.2263E-08 8.1274E-09
400 1.8800E-06 1.2250E-06 2.0605E-07 3.3731E-08 8.4280E-09
402 1.9500E-06 1.2713E-06 2.1444E-07 3.5221E-08 8.8645E-09
404 2.0200E-06 1.3170E-06 2.2283E-07 3.6774E-08 9.2977E-09
406 2.0800E-06 1.3557E-06 2.3009E-07 3.8135E-08 9.7078E-09
408 2.1500E-06 1.4013E-06 2.3869E-07 3.9652E-08 1.0173E-08
410 2.2200E-06 1.4462E-06 2.4711E-07 4.1256E-08 1.0548E-08
412 2.2900E-06 1.4917E-06 2.5566E-07 4.2887E-08 1.1058E-08
414 2.3600E-06 1.5366E-06 2.6425E-07 4.4479E-08 1.1500E-08
416 2.4300E-06 1.5821E-06 2.7282E-07 4.6024E-08 1.2003E-08
418 2.5100E-06 1.6341E-06 2.8268E-07 4.7888E-08 1.2526E-08
420 2.5900E-06 1.6862E-06 2.9251E-07 4.9658E-08 1.3035E-08
422 2.6700E-06 1.7382E-06 3.0240E-07 5.1619E-08 1.3585E-08
424 2.7500E-06 1.7902E-06 3.1237E-07 5.3479E-08 1.4130E-08
426 2.8300E-06 1.8430E-06 3.2245E-07 5.5375E-08 1.4732E-08
428 2.9200E-06 1.9018E-06 3.3381E-07 5.7559E-08 1.5357E-08
430 3.0100E-06 1.9608E-06 3.4510E-07 5.9676E-08 1.6041E-08
432 3.1000E-06 2.0198E-06 3.5656E-07 6.1799E-08 1.6645E-08
434 3.1800E-06 2.0712E-06 3.6659E-07 6.4083E-08 1.7195E-08
436 3.2700E-06 2.1284E-06 3.7778E-07 6.5861E-08 1.7927E-08
438 3.3700E-06 2.1962E-06 3.9082E-07 6.8408E-08 1.8624E-08
440 3.4600E-06 2.2544E-06 4.0212E-07 7.0556E-08 1.9292E-08
442 3.5500E-06 2.3121E-06 4.1336E-07 7.2739E-08 1.9991E-08
444 3.6500E-06 2.3769E-06 4.2603E-07 7.5190E-08 2.0687E-08
446 3.7400E-06 2.4348E-06 4.3736E-07 7.7440E-08 2.1338E-08
448 3.8400E-06 2.4992E-06 4.5005E-07 7.9922E-08 2.2142E-08
450 3.9400E-06 2.5634E-06 4.6267E-07 8.2307E-08 2.2909E-08
452 4.0400E-06 2.6273E-06 4.7539E-07 8.4763E-08 2.3683E-08

454 4.1400E-06 2.6918E-06 4.8815E-07 8.7342E-08 2.4445E-08
456 4.2500E-06 2.7618E-06 5.0205E-07 8.9973E-08 2.5202E-08
458 4.3500E-06 2.8251E-06 5.1482E-07 9.2520E-08 2.5957E-08
460 4.4500E-06 2.8891E-06 5.2777E-07 9.5003E-08 2.6806E-08
462 4.5500E-06 2.9524E-06 5.4063E-07 9.7525E-08 2.7618E-08
464 4.6600E-06 3.0230E-06 5.5477E-07 1.0033E-07 2.8462E-08
466 4.7600E-06 3.0877E-06 5.6768E-07 1.0295E-07 2.9307E-08
468 4.8600E-06 3.1528E-06 5.8082E-07 1.0548E-07 3.0029E-08
470 4.9600E-06 3.2177E-06 5.9391E-07 1.0820E-07 3.0993E-08
472 5.0600E-06 3.2819E-06 6.0680E-07 1.1084E-07 3.1741E-08
474 5.1700E-06 3.3492E-06 6.2112E-07 1.1363E-07 3.2665E-08
476 5.2700E-06 3.4145E-06 6.3435E-07 1.1631E-07 3.3504E-08
478 5.3800E-06 3.4853E-06 6.4888E-07 1.1922E-07 3.4390E-08
480 5.4800E-06 3.5477E-06 6.6171E-07 1.2185E-07 3.5224E-08
482 5.5900E-06 3.6194E-06 6.7633E-07 1.2469E-07 3.6118E-08
484 5.7000E-06 3.6900E-06 6.9061E-07 1.2765E-07 3.7103E-08
486 5.8000E-06 3.7552E-06 7.0412E-07 1.3034E-07 3.7944E-08
488 5.9100E-06 3.8265E-06 7.1860E-07 1.3326E-07 3.8865E-08
490 6.0200E-06 3.8963E-06 7.3306E-07 1.3612E-07 3.9870E-08
492 6.1300E-06 3.9676E-06 7.4786E-07 1.3915E-07 4.0817E-08
494 6.2400E-06 4.0385E-06 7.6247E-07 1.4217E-07 4.1740E-08
496 6.3500E-06 4.1099E-06 7.7711E-07 1.4523E-07 4.2735E-08
498 6.4600E-06 4.1803E-06 7.9161E-07 1.4819E-07 4.3725E-08
500 6.5700E-06 4.2514E-06 8.0660E-07 1.5120E-07 4.4658E-08
502 6.6800E-06 4.3220E-06 8.2111E-07 1.5416E-07 4.5667E-08
504 6.7900E-06 4.3927E-06 8.3598E-07 1.5722E-07 4.6661E-08
506 6.9100E-06 4.4701E-06 8.5193E-07 1.6034E-07 4.7666E-08
508 7.0200E-06 4.5412E-06 8.6676E-07 1.6349E-07 4.8647E-08
510 7.1300E-06 4.6120E-06 8.8141E-07 1.6659E-07 4.9650E-08
512 7.2400E-06 4.6834E-06 8.9638E-07 1.6966E-07 5.0668E-08
514 7.3500E-06 4.7532E-06 9.1111E-07 1.7267E-07 5.1665E-08
516 7.4600E-06 4.8242E-06 9.2586E-07 1.7575E-07 5.2614E-08
518 7.5700E-06 4.8953E-06 9.4118E-07 1.7892E-07 5.3692E-08
520 7.6800E-06 4.9653E-06 9.5593E-07 1.8205E-07 5.4669E-08
522 7.7900E-06 5.0360E-06 9.7079E-07 1.8511E-07 5.5778E-08
524 7.9000E-06 5.1070E-06 9.8568E-07 1.8823E-07 5.6805E-08
526 8.0100E-06 5.1770E-06 1.0008E-06 1.9141E-07 5.7811E-08
528 8.1200E-06 5.2475E-06 1.0156E-06 1.9455E-07 5.8796E-08
530 8.2300E-06 5.3178E-06 1.0306E-06 1.9764E-07 5.9877E-08
532 8.3400E-06 5.3881E-06 1.0459E-06 2.0079E-07 6.0974E-08
534 8.4500E-06 5.4593E-06 1.0612E-06 2.0397E-07 6.1979E-08
536 8.5600E-06 5.5291E-06 1.0762E-06 2.0722E-07 6.3078E-08
538 8.6800E-06 5.6054E-06 1.0926E-06 2.1056E-07 6.4108E-08
540 8.7900E-06 5.6765E-06 1.1078E-06 2.1376E-07 6.5183E-08
542 8.9000E-06 5.7464E-06 1.1230E-06 2.1689E-07 6.6288E-08
544 9.0100E-06 5.8172E-06 1.1382E-06 2.2011E-07 6.7362E-08
546 9.1200E-06 5.8870E-06 1.1535E-06 2.2339E-07 6.8432E-08
548 9.2200E-06 5.9522E-06 1.1674E-06 2.2644E-07 6.9365E-08

550 9.3300E-06 6.0234E-06 1.1829E-06 2.2957E-07 7.0481E-08
552 9.4400E-06 6.0938E-06 1.1980E-06 2.3284E-07 7.1512E-08
554 9.5500E-06 6.1643E-06 1.2134E-06 2.3606E-07 7.2663E-08
556 9.6600E-06 6.2350E-06 1.2286E-06 2.3947E-07 7.3714E-08
558 9.7700E-06 6.3049E-06 1.2438E-06 2.4269E-07 7.4870E-08
560 9.8800E-06 6.3750E-06 1.2592E-06 2.4593E-07 7.5916E-08
562 9.9800E-06 6.4394E-06 1.2737E-06 2.4904E-07 7.6972E-08
564 1.0100E-05 6.5159E-06 1.2904E-06 2.5260E-07 7.8147E-08
566 1.0200E-05 6.5799E-06 1.3047E-06 2.5555E-07 7.9150E-08
568 1.0300E-05 6.6431E-06 1.3186E-06 2.5874E-07 8.0226E-08
570 1.0400E-05 6.7068E-06 1.3329E-06 2.6181E-07 8.1311E-08
572 1.0500E-05 6.7709E-06 1.3471E-06 2.6495E-07 8.2383E-08
574 1.0600E-05 6.8336E-06 1.3614E-06 2.6801E-07 8.3478E-08
576 1.0700E-05 6.8987E-06 1.3758E-06 2.7112E-07 8.4485E-08
578 1.0800E-05 6.9628E-06 1.3905E-06 2.7429E-07 8.5559E-08
580 1.0900E-05 7.0253E-06 1.4049E-06 2.7752E-07 8.6634E-08
582 1.1000E-05 7.0898E-06 1.4194E-06 2.8083E-07 8.7789E-08
584 1.1100E-05 7.1531E-06 1.4337E-06 2.8386E-07 8.8850E-08
586 1.1200E-05 7.2162E-06 1.4478E-06 2.8696E-07 8.9910E-08
588 1.1300E-05 7.2800E-06 1.4624E-06 2.9031E-07 9.1046E-08
590 1.1400E-05 7.3440E-06 1.4766E-06 2.9342E-07 9.2280E-08
592 1.1500E-05 7.4090E-06 1.4912E-06 2.9650E-07 9.3248E-08
594 1.1600E-05 7.4745E-06 1.5058E-06 2.9973E-07 9.4462E-08
596 1.1700E-05 7.5376E-06 1.5201E-06 3.0297E-07 9.5396E-08
598 1.1800E-05 7.6025E-06 1.5349E-06 3.0629E-07 9.6576E-08
600 1.1900E-05 7.6659E-06 1.5494E-06 3.0948E-07 9.7973E-08
602 1.1900E-05 7.6655E-06 1.5508E-06 3.1011E-07 9.8254E-08
604 1.2000E-05 7.7296E-06 1.5654E-06 3.1336E-07 9.9364E-08
606 1.2100E-05 7.7936E-06 1.5800E-06 3.1660E-07 1.0048E-07
608 1.2200E-05 7.8575E-06 1.5947E-06 3.1986E-07 1.0160E-07
610 1.2300E-05 7.9216E-06 1.6093E-06 3.2312E-07 1.0272E-07
612 1.2400E-05 7.9856E-06 1.6239E-06 3.2641E-07 1.0385E-07
614 1.2500E-05 8.0496E-06 1.6386E-06 3.2969E-07 1.0498E-07
616 1.2600E-05 8.1135E-06 1.6532E-06 3.3316E-07 1.0610E-07
618 1.2700E-05 8.1764E-06 1.6680E-06 3.3654E-07 1.0728E-07
620 1.2800E-05 8.2403E-06 1.6831E-06 3.3989E-07 1.0848E-07
622 1.2800E-05 8.2408E-06 1.6852E-06 3.4053E-07 1.0889E-07
624 1.2900E-05 8.3044E-06 1.7001E-06 3.4402E-07 1.1011E-07
626 1.3000E-05 8.3689E-06 1.7152E-06 3.4766E-07 1.1139E-07
628 1.3100E-05 8.4327E-06 1.7301E-06 3.5107E-07 1.1265E-07
630 1.3200E-05 8.4960E-06 1.7452E-06 3.5445E-07 1.1399E-07
632 1.3200E-05 8.4970E-06 1.7468E-06 3.5524E-07 1.1440E-07
634 1.3300E-05 8.5613E-06 1.7621E-06 3.5889E-07 1.1564E-07
636 1.3400E-05 8.6288E-06 1.7776E-06 3.6235E-07 1.1703E-07
638 1.3500E-05 8.6872E-06 1.7921E-06 3.6574E-07 1.1829E-07
640 1.3600E-05 8.7564E-06 1.8080E-06 3.6943E-07 1.1952E-07
642 1.3700E-05 8.8212E-06 1.8229E-06 3.7300E-07 1.2088E-07
644 1.3700E-05 8.8209E-06 1.8246E-06 3.7385E-07 1.2142E-07

646 1.3800E-05 8.8876E-06 1.8401E-06 3.7751E-07 1.2263E-07
648 1.3900E-05 8.9515E-06 1.8547E-06 3.8110E-07 1.2410E-07
650 1.4000E-05 9.0146E-06 1.8703E-06 3.8454E-07 1.2530E-07
652 1.4000E-05 9.0140E-06 1.8719E-06 3.8546E-07 1.2576E-07
654 1.4100E-05 9.0788E-06 1.8874E-06 3.8879E-07 1.2709E-07
656 1.4200E-05 9.1432E-06 1.9025E-06 3.9243E-07 1.2843E-07
658 1.4300E-05 9.2085E-06 1.9178E-06 3.9601E-07 1.2973E-07
660 1.4300E-05 9.2073E-06 1.9195E-06 3.9688E-07 1.3013E-07
662 1.4400E-05 9.2727E-06 1.9351E-06 4.0071E-07 1.3158E-07
664 1.4500E-05 9.3361E-06 1.9502E-06 4.0423E-07 1.3292E-07
666 1.4600E-05 9.3999E-06 1.9655E-06 4.0778E-07 1.3428E-07
668 1.4600E-05 9.3998E-06 1.9671E-06 4.0862E-07 1.3466E-07
670 1.4700E-05 9.4653E-06 1.9824E-06 4.1236E-07 1.3611E-07
672 1.4800E-05 9.5302E-06 1.9980E-06 4.1597E-07 1.3752E-07
674 1.4800E-05 9.5299E-06 1.9995E-06 4.1677E-07 1.3780E-07
676 1.4900E-05 9.5959E-06 2.0154E-06 4.2031E-07 1.3922E-07
678 1.5000E-05 9.6608E-06 2.0305E-06 4.2421E-07 1.4064E-07
680 1.5000E-05 9.6594E-06 2.0325E-06 4.2502E-07 1.4102E-07
682 1.5100E-05 9.7253E-06 2.0477E-06 4.2875E-07 1.4263E-07
684 1.5200E-05 9.7896E-06 2.0632E-06 4.3261E-07 1.4400E-07
686 1.5200E-05 9.7865E-06 2.0649E-06 4.3349E-07 1.4448E-07
688 1.5300E-05 9.8543E-06 2.0811E-06 4.3726E-07 1.4599E-07
690 1.5300E-05 9.8540E-06 2.0831E-06 4.3838E-07 1.4639E-07
692 1.5400E-05 9.9182E-06 2.0987E-06 4.4213E-07 1.4797E-07
694 1.5500E-05 9.9835E-06 2.1140E-06 4.4589E-07 1.4942E-07
696 1.5500E-05 9.9823E-06 2.1159E-06 4.4679E-07 1.4986E-07
698 1.5600E-05 1.0047E-05 2.1316E-06 4.5053E-07 1.5145E-07
700 1.5600E-05 1.0048E-05 2.1339E-06 4.5137E-07 1.5189E-07
702 1.5700E-05 1.0112E-05 2.1492E-06 4.5536E-07 1.5341E-07
704 1.5700E-05 1.0113E-05 2.1511E-06 4.5645E-07 1.5382E-07
706 1.5800E-05 1.0179E-05 2.1670E-06 4.5995E-07 1.5530E-07
708 1.5800E-05 1.0179E-05 2.1686E-06 4.6100E-07 1.5574E-07
710 1.5900E-05 1.0243E-05 2.1843E-06 4.6474E-07 1.5722E-07
712 1.5900E-05 1.0244E-05 2.1859E-06 4.6552E-07 1.5777E-07
714 1.6000E-05 1.0308E-05 2.2019E-06 4.6958E-07 1.5920E-07
716 1.6000E-05 1.0310E-05 2.2032E-06 4.7014E-07 1.5974E-07
718 1.6000E-05 1.0311E-05 2.2048E-06 4.7126E-07 1.6024E-07
720 1.6100E-05 1.0376E-05 2.2207E-06 4.7503E-07 1.6160E-07
722 1.6100E-05 1.0376E-05 2.2221E-06 4.7579E-07 1.6203E-07
724 1.6200E-05 1.0441E-05 2.2377E-06 4.7965E-07 1.6352E-07
726 1.6200E-05 1.0442E-05 2.2395E-06 4.8039E-07 1.6388E-07
728 1.6300E-05 1.0505E-05 2.2545E-06 4.8426E-07 1.6540E-07
730 1.6300E-05 1.0505E-05 2.2567E-06 4.8501E-07 1.6577E-07
732 1.6300E-05 1.0507E-05 2.2584E-06 4.8572E-07 1.6616E-07
734 1.6400E-05 1.0571E-05 2.2737E-06 4.8954E-07 1.6764E-07
736 1.6400E-05 1.0571E-05 2.2753E-06 4.9018E-07 1.6800E-07
738 1.6500E-05 1.0634E-05 2.2909E-06 4.9373E-07 1.6942E-07
740 1.6500E-05 1.0635E-05 2.2927E-06 4.9457E-07 1.6980E-07

742 1.6500E-05 1.0631E-05 2.2933E-06 4.9520E-07 1.7020E-07
744 1.6600E-05 1.0697E-05 2.3089E-06 4.9876E-07 1.7159E-07
746 1.6600E-05 1.0695E-05 2.3102E-06 4.9964E-07 1.7194E-07
748 1.6600E-05 1.0695E-05 2.3119E-06 5.0021E-07 1.7257E-07
750 1.6700E-05 1.0758E-05 2.3270E-06 5.0377E-07 1.7388E-07
752 1.6700E-05 1.0758E-05 2.3285E-06 5.0456E-07 1.7408E-07
754 1.6700E-05 1.0758E-05 2.3300E-06 5.0507E-07 1.7425E-07
756 1.6800E-05 1.0823E-05 2.3453E-06 5.0867E-07 1.7566E-07
758 1.6800E-05 1.0823E-05 2.3463E-06 5.0944E-07 1.7600E-07
760 1.6700E-05 1.0759E-05 2.3342E-06 5.0720E-07 1.7540E-07
762 1.6800E-05 1.0823E-05 2.3498E-06 5.1069E-07 1.7660E-07
764 1.6800E-05 1.0826E-05 2.3503E-06 5.1127E-07 1.7682E-07
766 1.6900E-05 1.0888E-05 2.3658E-06 5.1499E-07 1.7835E-07
768 1.6900E-05 1.0888E-05 2.3670E-06 5.1525E-07 1.7863E-07
770 1.6900E-05 1.0889E-05 2.3682E-06 5.1592E-07 1.7899E-07
772 1.7000E-05 1.0954E-05 2.3832E-06 5.1959E-07 1.8008E-07
774 1.7000E-05 1.0950E-05 2.3854E-06 5.2018E-07 1.8054E-07
776 1.7000E-05 1.0953E-05 2.3865E-06 5.2076E-07 1.8100E-07
778 1.7000E-05 1.0952E-05 2.3880E-06 5.2127E-07 1.8120E-07
780 1.7100E-05 1.1014E-05 2.4034E-06 5.2497E-07 1.8242E-07
782 1.7100E-05 1.1016E-05 2.4039E-06 5.2523E-07 1.8266E-07
784 1.7100E-05 1.1014E-05 2.4055E-06 5.2591E-07 1.8309E-07
786 1.7100E-05 1.1013E-05 2.4068E-06 5.2630E-07 1.8314E-07
788 1.7100E-05 1.1012E-05 2.4077E-06 5.2680E-07 1.8357E-07
790 1.7100E-05 1.1013E-05 2.4089E-06 5.2735E-07 1.8386E-07
792 1.7200E-05 1.1079E-05 2.4243E-06 5.3112E-07 1.8502E-07
794 1.7200E-05 1.1078E-05 2.4252E-06 5.3162E-07 1.8504E-07
796 1.7200E-05 1.1074E-05 2.4264E-06 5.3162E-07 1.8536E-07
798 1.7200E-05 1.1074E-05 2.4274E-06 5.3248E-07 1.8602E-07
800 1.7200E-05 1.1073E-05 2.4290E-06 5.3279E-07 1.8610E-07
802 1.7200E-05 1.1074E-05 2.4298E-06 5.3329E-07 1.8636E-07
804 1.7200E-05 1.1075E-05 2.4309E-06 5.3370E-07 1.8657E-07
806 1.7300E-05 1.1139E-05 2.4462E-06 5.3737E-07 1.8772E-07
808 1.7300E-05 1.1140E-05 2.4476E-06 5.3806E-07 1.8796E-07
810 1.7300E-05 1.1140E-05 2.4485E-06 5.3834E-07 1.8821E-07
812 1.7300E-05 1.1140E-05 2.4495E-06 5.3910E-07 1.8869E-07
814 1.7300E-05 1.1137E-05 2.4502E-06 5.3936E-07 1.8881E-07
816 1.7300E-05 1.1138E-05 2.4518E-06 5.4014E-07 1.8926E-07
818 1.7300E-05 1.1141E-05 2.4531E-06 5.4042E-07 1.8931E-07
820 1.7300E-05 1.1137E-05 2.4538E-06 5.4085E-07 1.8959E-07
822 1.7300E-05 1.1137E-05 2.4545E-06 5.4101E-07 1.8985E-07
824 1.7300E-05 1.1138E-05 2.4556E-06 5.4128E-07 1.8994E-07
826 1.7300E-05 1.1137E-05 2.4566E-06 5.4184E-07 1.9039E-07
828 1.7300E-05 1.1138E-05 2.4576E-06 5.4213E-07 1.9063E-07
830 1.7200E-05 1.1073E-05 2.4439E-06 5.3968E-07 1.8958E-07
832 1.7200E-05 1.1073E-05 2.4455E-06 5.4025E-07 1.8992E-07
834 1.7200E-05 1.1072E-05 2.4460E-06 5.4061E-07 1.9006E-07
836 1.7200E-05 1.1072E-05 2.4465E-06 5.4091E-07 1.9004E-07

838 1.7200E-05 1.1071E-05 2.4482E-06 5.4116E-07 1.9037E-07
840 1.7200E-05 1.1073E-05 2.4489E-06 5.4192E-07 1.9078E-07
842 1.7200E-05 1.1074E-05 2.4496E-06 5.4208E-07 1.9083E-07
844 1.7100E-05 1.1008E-05 2.4369E-06 5.3944E-07 1.9008E-07
846 1.7100E-05 1.1007E-05 2.4374E-06 5.3986E-07 1.9044E-07
848 1.7100E-05 1.1007E-05 2.4393E-06 5.4039E-07 1.9037E-07
850 1.7100E-05 1.1006E-05 2.4403E-06 5.4079E-07 1.9080E-07
852 1.7100E-05 1.1007E-05 2.4414E-06 5.4101E-07 1.9102E-07
854 1.7000E-05 1.0944E-05 2.4286E-06 5.3851E-07 1.9025E-07
856 1.7000E-05 1.0940E-05 2.4290E-06 5.3915E-07 1.9057E-07
858 1.7000E-05 1.0940E-05 2.4303E-06 5.3958E-07 1.9060E-07
860 1.6900E-05 1.0878E-05 2.4164E-06 5.3683E-07 1.8980E-07
862 1.6900E-05 1.0877E-05 2.4181E-06 5.3749E-07 1.9004E-07
864 1.6900E-05 1.0873E-05 2.4186E-06 5.3813E-07 1.9043E-07
866 1.6900E-05 1.0875E-05 2.4191E-06 5.3859E-07 1.9073E-07
868 1.6800E-05 1.0811E-05 2.4066E-06 5.3579E-07 1.8974E-07
870 1.6800E-05 1.0811E-05 2.4074E-06 5.3622E-07 1.9008E-07
872 1.6800E-05 1.0810E-05 2.4086E-06 5.3679E-07 1.9043E-07
874 1.6700E-05 1.0746E-05 2.3951E-06 5.3410E-07 1.8956E-07
876 1.6700E-05 1.0747E-05 2.3963E-06 5.3475E-07 1.9001E-07
878 1.6700E-05 1.0746E-05 2.3973E-06 5.3508E-07 1.9018E-07
880 1.6600E-05 1.0682E-05 2.3844E-06 5.3231E-07 1.8919E-07
882 1.6600E-05 1.0681E-05 2.3851E-06 5.3301E-07 1.8949E-07
884 1.6600E-05 1.0681E-05 2.3858E-06 5.3362E-07 1.8980E-07
886 1.6500E-05 1.0617E-05 2.3729E-06 5.3077E-07 1.8922E-07
888 1.6500E-05 1.0619E-05 2.3742E-06 5.3125E-07 1.8944E-07
890 1.6500E-05 1.0617E-05 2.3755E-06 5.3186E-07 1.8988E-07
892 1.6400E-05 1.0553E-05 2.3621E-06 5.2898E-07 1.8876E-07
894 1.6400E-05 1.0553E-05 2.3632E-06 5.2964E-07 1.8906E-07
896 1.6300E-05 1.0489E-05 2.3500E-06 5.2704E-07 1.8825E-07
898 1.6300E-05 1.0487E-05 2.3508E-06 5.2744E-07 1.8882E-07
900 1.6300E-05 1.0489E-05 2.3518E-06 5.2812E-07 1.8887E-07
902 1.6200E-05 1.0425E-05 2.3388E-06 5.2538E-07 1.8816E-07
904 1.6200E-05 1.0427E-05 2.3401E-06 5.2601E-07 1.8824E-07
906 1.6200E-05 1.0427E-05 2.3404E-06 5.2635E-07 1.8873E-07
908 1.6200E-05 1.0427E-05 2.3424E-06 5.2720E-07 1.8891E-07
910 1.6100E-05 1.0364E-05 2.3287E-06 5.2443E-07 1.8811E-07
912 1.6100E-05 1.0364E-05 2.3300E-06 5.2494E-07 1.8831E-07
914 1.6100E-05 1.0364E-05 2.3313E-06 5.2541E-07 1.8861E-07
916 1.6000E-05 1.0301E-05 2.3178E-06 5.2291E-07 1.8803E-07
918 1.6000E-05 1.0301E-05 2.3189E-06 5.2358E-07 1.8813E-07
920 1.6000E-05 1.0302E-05 2.3205E-06 5.2398E-07 1.8837E-07
922 1.6000E-05 1.0303E-05 2.3216E-06 5.2469E-07 1.8866E-07
924 1.5900E-05 1.0238E-05 2.3082E-06 5.2206E-07 1.8792E-07
926 1.5900E-05 1.0237E-05 2.3098E-06 5.2246E-07 1.8835E-07
928 1.5904E-05 1.0239E-05 2.3107E-06 5.2323E-07 1.8892E-07
930 1.5827E-05 1.0187E-05 2.2995E-06 5.2145E-07 1.8858E-07
932 1.5774E-05 1.0148E-05 2.2913E-06 5.2051E-07 1.8844E-07

934 1.5721E-05 1.0112E-05 2.2835E-06 5.1958E-07 1.8843E-07
936 1.5683E-05 1.0088E-05 2.2798E-06 5.1890E-07 1.8812E-07
938 1.5782E-05 1.0156E-05 2.2968E-06 5.2240E-07 1.8935E-07
940 1.5700E-05 1.0105E-05 2.2870E-06 5.2008E-07 1.8842E-07
942 1.5625E-05 1.0056E-05 2.2759E-06 5.1834E-07 1.8820E-07
944 1.5664E-05 1.0079E-05 2.2821E-06 5.2034E-07 1.8900E-07
946 1.5636E-05 1.0063E-05 2.2800E-06 5.2002E-07 1.8882E-07
948 1.5522E-05 9.9904E-06 2.2645E-06 5.1670E-07 1.8774E-07
950 1.5540E-05 1.0003E-05 2.2688E-06 5.1790E-07 1.8836E-07
952 1.5515E-05 9.9882E-06 2.2666E-06 5.1769E-07 1.8835E-07
954 1.5500E-05 9.9787E-06 2.2656E-06 5.1753E-07 1.8845E-07
956 1.5400E-05 9.9165E-06 2.2521E-06 5.1488E-07 1.8766E-07
958 1.5400E-05 9.9164E-06 2.2536E-06 5.1530E-07 1.8788E-07
960 1.5400E-05 9.9184E-06 2.2550E-06 5.1593E-07 1.8831E-07
962 1.5400E-05 9.9178E-06 2.2563E-06 5.1644E-07 1.8833E-07
964 1.5300E-05 9.8538E-06 2.2431E-06 5.1353E-07 1.8746E-07
966 1.5300E-05 9.8543E-06 2.2441E-06 5.1403E-07 1.8753E-07
968 1.5300E-05 9.8572E-06 2.2460E-06 5.1455E-07 1.8779E-07
970 1.5300E-05 9.8582E-06 2.2471E-06 5.1517E-07 1.8817E-07
972 1.5300E-05 9.8578E-06 2.2482E-06 5.1572E-07 1.8837E-07
974 1.5200E-05 9.7941E-06 2.2347E-06 5.1279E-07 1.8752E-07
976 1.5200E-05 9.7950E-06 2.2356E-06 5.1336E-07 1.8783E-07
978 1.5200E-05 9.7944E-06 2.2370E-06 5.1390E-07 1.8801E-07
980 1.5200E-05 9.7961E-06 2.2384E-06 5.1446E-07 1.8833E-07
982 1.5200E-05 9.7964E-06 2.2396E-06 5.1484E-07 1.8857E-07
984 1.5200E-05 9.7969E-06 2.2408E-06 5.1531E-07 1.8904E-07
986 1.5100E-05 9.7347E-06 2.2274E-06 5.1287E-07 1.8806E-07
988 1.5100E-05 9.7336E-06 2.2283E-06 5.1320E-07 1.8831E-07
990 1.5100E-05 9.7339E-06 2.2297E-06 5.1372E-07 1.8869E-07
992 1.5100E-05 9.7341E-06 2.2306E-06 5.1420E-07 1.8884E-07
994 1.5100E-05 9.7350E-06 2.2319E-06 5.1483E-07 1.8920E-07
996 1.5100E-05 9.7359E-06 2.2331E-06 5.1538E-07 1.8938E-07
998 1.5000E-05 9.6726E-06 2.2192E-06 5.1231E-07 1.8845E-07

6.2.2 Xenon lamp radiances

____Wavelength_____Attenuator Position_____
[nm]
_____0_____ 100_____170_____200_____ 220_____
==========
350 6.2153E-08 2.6084E-08 7.5715E-09 5.1108E-09 3.1509E-09
351 8.2904E-08 3.4382E-08 9.2687E-09 5.3635E-09 4.4669E-09
352 1.0669E-07 3.9982E-08 9.6075E-09 4.7710E-09 3.2052E-09
353 1.3100E-07 4.5059E-08 1.0531E-08 5.6989E-09 4.7803E-09
354 1.5266E-07 4.7769E-08 1.0696E-08 5.4548E-09 3.7464E-09
355 1.6604E-07 4.7426E-08 1.0053E-08 5.3201E-09 3.9805E-09
356 1.6793E-07 4.3148E-08 1.0465E-08 4.0409E-09 3.4768E-09
357 1.5635E-07 3.8892E-08 9.0079E-09 5.9164E-09 3.9813E-09

358 1.3694E-07 3.4245E-08 8.3992E-09 4.6817E-09 2.5799E-09
359 1.1357E-07 3.0591E-08 8.5601E-09 3.4714E-09 4.8146E-09
360 9.1787E-08 2.6798E-08 7.3413E-09 3.3720E-09 3.9026E-09
361 7.6255E-08 2.4428E-08 7.1425E-09 2.9293E-09 2.0075E-09
362 6.4834E-08 2.1992E-08 7.5460E-09 3.0603E-09 2.1802E-09
363 5.7930E-08 2.0347E-08 6.2906E-09 3.5079E-09 3.3362E-09
364 5.2130E-08 1.8176E-08 5.3162E-09 3.0317E-09 3.2718E-09
365 4.6948E-08 1.6381E-08 6.2455E-09 4.0426E-09 2.5544E-09
366 4.2597E-08 1.6219E-08 5.4729E-09 3.7594E-09 2.0787E-09
367 3.9119E-08 1.6022E-08 5.9007E-09 4.6540E-09 2.7216E-09
368 3.7552E-08 1.7414E-08 7.5573E-09 3.9636E-09 3.4990E-09
369 3.8361E-08 2.0518E-08 7.6204E-09 5.1477E-09 2.6008E-09
370 4.2698E-08 2.5195E-08 9.8756E-09 5.4560E-09 3.9117E-09
371 5.1314E-08 3.2854E-08 1.3918E-08 6.6041E-09 4.0221E-09
372 6.4805E-08 4.5472E-08 1.7830E-08 9.0986E-09 5.4209E-09
373 8.6335E-08 6.0836E-08 2.3792E-08 1.1624E-08 6.4999E-09
374 1.1653E-07 8.1214E-08 3.0213E-08 1.4388E-08 8.4393E-09
375 1.5769E-07 1.0886E-07 3.9881E-08 1.7986E-08 1.0776E-08
376 2.1253E-07 1.4605E-07 5.4267E-08 2.4358E-08 1.4634E-08
377 2.9016E-07 2.0092E-07 7.7580E-08 3.3795E-08 1.9391E-08
378 4.0174E-07 2.8372E-07 1.1111E-07 4.8627E-08 2.8100E-08
379 5.6409E-07 4.0799E-07 1.6019E-07 7.0664E-08 3.9887E-08
380 7.9255E-07 5.8512E-07 2.2206E-07 9.6231E-08 5.3767E-08
381 1.1189E-06 8.2821E-07 2.9531E-07 1.2534E-07 6.6222E-08
382 1.5634E-06 1.1364E-06 3.7497E-07 1.5379E-07 7.7635E-08
383 2.1270E-06 1.4847E-06 4.5616E-07 1.7942E-07 8.7484E-08
384 2.8251E-06 1.8623E-06 5.3516E-07 2.0390E-07 9.8449E-08
385 3.6257E-06 2.2434E-06 6.0727E-07 2.2636E-07 1.0897E-07
386 4.5552E-06 2.6317E-06 6.6775E-07 2.4674E-07 1.1691E-07
387 5.5333E-06 2.9865E-06 7.1225E-07 2.5869E-07 1.1866E-07
388 6.5091E-06 3.2542E-06 7.3188E-07 2.5898E-07 1.1578E-07
389 7.4193E-06 3.4499E-06 7.3421E-07 2.5363E-07 1.1184E-07
390 8.1939E-06 3.5373E-06 7.2354E-07 2.4901E-07 1.1122E-07
391 8.8001E-06 3.5422E-06 7.1503E-07 2.4756E-07 1.1285E-07
392 9.1757E-06 3.4924E-06 7.1616E-07 2.5463E-07 1.1830E-07
393 9.3617E-06 3.4437E-06 7.3992E-07 2.6702E-07 1.2586E-07
394 9.3989E-06 3.4548E-06 7.8050E-07 2.8677E-07 1.3602E-07
395 9.4041E-06 3.5524E-06 8.3974E-07 3.1011E-07 1.4782E-07
396 9.4684E-06 3.7368E-06 9.0655E-07 3.3659E-07 1.5897E-07
397 9.6011E-06 3.9662E-06 9.6664E-07 3.5735E-07 1.6783E-07
398 9.7977E-06 4.2014E-06 1.0080E-06 3.6868E-07 1.7015E-07
399 1.0039E-05 4.3902E-06 1.0271E-06 3.6989E-07 1.6846E-07
400 1.0314E-05 4.5218E-06 1.0299E-06 3.6557E-07 1.6580E-07
401 1.0641E-05 4.6166E-06 1.0216E-06 3.5946E-07 1.6442E-07
402 1.0996E-05 4.6943E-06 1.0245E-06 3.6017E-07 1.6508E-07
403 1.1351E-05 4.7434E-06 1.0289E-06 3.6277E-07 1.6710E-07
404 1.1669E-05 4.7895E-06 1.0386E-06 3.6760E-07 1.6883E-07
405 1.1950E-05 4.8507E-06 1.0494E-06 3.7197E-07 1.7007E-07

406 1.2168E-05 4.8817E-06 1.0568E-06 3.7278E-07 1.6995E-07
407 1.2322E-05 4.9193E-06 1.0531E-06 3.6897E-07 1.6519E-07
408 1.2429E-05 4.9278E-06 1.0382E-06 3.6030E-07 1.5879E-07
409 1.2494E-05 4.9081E-06 1.0148E-06 3.4756E-07 1.5183E-07
410 1.2486E-05 4.8411E-06 9.7920E-07 3.3363E-07 1.4433E-07
411 1.2422E-05 4.7395E-06 9.4395E-07 3.2070E-07 1.3862E-07
412 1.2317E-05 4.6157E-06 9.1397E-07 3.0942E-07 1.3557E-07
413 1.2129E-05 4.4743E-06 8.9027E-07 3.0313E-07 1.3358E-07
414 1.1841E-05 4.3356E-06 8.6792E-07 2.9777E-07 1.3368E-07
415 1.1539E-05 4.2222E-06 8.5916E-07 2.9797E-07 1.3495E-07
416 1.1307E-05 4.1699E-06 8.6506E-07 3.0395E-07 1.3767E-07
417 1.1156E-05 4.1794E-06 8.8600E-07 3.1441E-07 1.4385E-07
418 1.1180E-05 4.2769E-06 9.2563E-07 3.3031E-07 1.5280E-07
419 1.1462E-05 4.4853E-06 9.8846E-07 3.5470E-07 1.6361E-07
420 1.1759E-05 4.6931E-06 1.0412E-06 3.7273E-07 1.7083E-07
421 1.1849E-05 4.7903E-06 1.0582E-06 3.7702E-07 1.7108E-07
422 1.1935E-05 4.8658E-06 1.0621E-06 3.7490E-07 1.6910E-07
423 1.2174E-05 4.9694E-06 1.0693E-06 3.7452E-07 1.6677E-07
424 1.2513E-05 5.0714E-06 1.0732E-06 3.7159E-07 1.6461E-07
425 1.2860E-05 5.1565E-06 1.0708E-06 3.6868E-07 1.6192E-07
426 1.3175E-05 5.1986E-06 1.0628E-06 3.6441E-07 1.5973E-07
427 1.3443E-05 5.2119E-06 1.0518E-06 3.5894E-07 1.5810E-07
428 1.3640E-05 5.1852E-06 1.0430E-06 3.5591E-07 1.5866E-07
429 1.3760E-05 5.1544E-06 1.0367E-06 3.5596E-07 1.6004E-07
430 1.3821E-05 5.1150E-06 1.0364E-06 3.5958E-07 1.6283E-07
431 1.3833E-05 5.0744E-06 1.0456E-06 3.6576E-07 1.6746E-07
432 1.3810E-05 5.0743E-06 1.0650E-06 3.7583E-07 1.7348E-07
433 1.3774E-05 5.0928E-06 1.0917E-06 3.8971E-07 1.8081E-07
434 1.3763E-05 5.1490E-06 1.1286E-06 4.0514E-07 1.8912E-07
435 1.3790E-05 5.2410E-06 1.1729E-06 4.2339E-07 1.9826E-07
436 1.3905E-05 5.3899E-06 1.2252E-06 4.4538E-07 2.0814E-07
437 1.4161E-05 5.6021E-06 1.2892E-06 4.6870E-07 2.1959E-07
438 1.4557E-05 5.8620E-06 1.3586E-06 4.9396E-07 2.2987E-07
439 1.4847E-05 6.0810E-06 1.4050E-06 5.0815E-07 2.3394E-07
440 1.4926E-05 6.1770E-06 1.4104E-06 5.0784E-07 2.3222E-07
441 1.5055E-05 6.2818E-06 1.4179E-06 5.0665E-07 2.2971E-07
442 1.5335E-05 6.4113E-06 1.4320E-06 5.0857E-07 2.2897E-07
443 1.5605E-05 6.5093E-06 1.4356E-06 5.0463E-07 2.2724E-07
444 1.5859E-05 6.5788E-06 1.4296E-06 5.0187E-07 2.2599E-07
445 1.6107E-05 6.6176E-06 1.4260E-06 4.9993E-07 2.2556E-07
446 1.6296E-05 6.6271E-06 1.4217E-06 4.9735E-07 2.2559E-07
447 1.6458E-05 6.6204E-06 1.4160E-06 4.9804E-07 2.2664E-07
448 1.6714E-05 6.6612E-06 1.4308E-06 5.0490E-07 2.2985E-07
449 1.7816E-05 7.0665E-06 1.5427E-06 5.4610E-07 2.5124E-07
450 1.9643E-05 7.7812E-06 1.7273E-06 6.1756E-07 2.8418E-07
451 1.9879E-05 7.8741E-06 1.7452E-06 6.2506E-07 2.8695E-07
452 1.9224E-05 7.6417E-06 1.6901E-06 6.0590E-07 2.7744E-07
453 1.8865E-05 7.5196E-06 1.6748E-06 5.9964E-07 2.7483E-07

454 1.8175E-05 7.2820E-06 1.6177E-06 5.7604E-07 2.6370E-07
455 1.7998E-05 7.2480E-06 1.6061E-06 5.7131E-07 2.6074E-07
456 1.8371E-05 7.4403E-06 1.6498E-06 5.8581E-07 2.6638E-07
457 1.8990E-05 7.7312E-06 1.7158E-06 6.1155E-07 2.7648E-07
458 1.9701E-05 8.0532E-06 1.7846E-06 6.3508E-07 2.8801E-07
459 1.9961E-05 8.1545E-06 1.7939E-06 6.3660E-07 2.8838E-07
460 1.9935E-05 8.1223E-06 1.7741E-06 6.2584E-07 2.8473E-07
461 2.0403E-05 8.2932E-06 1.8261E-06 6.4675E-07 2.9411E-07
462 2.1640E-05 8.7919E-06 1.9722E-06 7.0622E-07 3.2339E-07
463 2.2808E-05 9.2459E-06 2.0984E-06 7.5574E-07 3.4611E-07
464 2.2882E-05 9.2427E-06 2.0730E-06 7.4344E-07 3.3879E-07
465 2.2340E-05 8.9673E-06 1.9793E-06 7.0346E-07 3.2074E-07
466 2.2897E-05 9.1737E-06 2.0493E-06 7.3227E-07 3.3590E-07
467 2.5482E-05 1.0269E-05 2.3838E-06 8.6896E-07 3.9928E-07
468 2.7866E-05 1.1274E-05 2.6445E-06 9.6684E-07 4.4329E-07
469 2.7341E-05 1.1030E-05 2.5215E-06 9.0250E-07 4.1301E-07
470 2.5351E-05 1.0194E-05 2.2646E-06 8.0401E-07 3.6379E-07
471 2.3588E-05 9.4673E-06 2.0705E-06 7.3059E-07 3.3021E-07
472 2.3028E-05 9.2370E-06 2.0093E-06 7.0786E-07 3.1921E-07
473 2.4480E-05 9.8282E-06 2.1617E-06 7.6444E-07 3.4480E-07
474 2.4402E-05 9.8106E-06 2.1441E-06 7.6020E-07 3.4204E-07
475 2.1764E-05 8.7226E-06 1.8806E-06 6.6243E-07 2.9714E-07
476 2.0164E-05 8.0626E-06 1.7328E-06 6.0891E-07 2.7486E-07
477 1.9630E-05 7.8451E-06 1.6874E-06 5.9347E-07 2.6830E-07
478 1.9454E-05 7.7536E-06 1.6716E-06 5.8924E-07 2.6724E-07
479 1.9661E-05 7.8406E-06 1.7007E-06 6.0102E-07 2.7209E-07
480 2.0627E-05 8.2296E-06 1.8118E-06 6.4560E-07 2.9396E-07
481 2.1939E-05 8.7510E-06 1.9565E-06 7.0014E-07 3.1792E-07
482 2.2443E-05 8.9615E-06 1.9980E-06 7.1351E-07 3.2401E-07
483 2.2174E-05 8.8496E-06 1.9648E-06 7.0116E-07 3.1744E-07
484 2.1616E-05 8.6187E-06 1.9083E-06 6.8114E-07 3.0710E-07
485 2.0774E-05 8.2776E-06 1.8270E-06 6.4809E-07 2.9196E-07
486 2.0062E-05 7.9991E-06 1.7539E-06 6.1907E-07 2.7984E-07
487 1.9617E-05 7.8221E-06 1.7037E-06 6.0185E-07 2.6997E-07
488 1.9483E-05 7.7661E-06 1.6903E-06 5.9484E-07 2.6618E-07
489 1.9494E-05 7.7715E-06 1.6840E-06 5.9186E-07 2.6656E-07
490 1.9674E-05 7.8401E-06 1.7023E-06 5.9724E-07 2.6859E-07
491 2.0617E-05 8.2233E-06 1.8017E-06 6.3779E-07 2.8757E-07
492 2.2040E-05 8.8134E-06 1.9552E-06 6.9567E-07 3.1409E-07
493 2.2253E-05 8.8921E-06 1.9639E-06 6.9825E-07 3.1519E-07
494 2.1268E-05 8.4666E-06 1.8452E-06 6.5110E-07 2.9501E-07
495 2.0329E-05 8.1040E-06 1.7521E-06 6.1784E-07 2.7979E-07
496 1.9742E-05 7.8538E-06 1.7006E-06 6.0095E-07 2.7270E-07
497 1.9451E-05 7.7471E-06 1.6843E-06 5.9697E-07 2.7167E-07
498 1.9300E-05 7.6947E-06 1.6829E-06 5.9923E-07 2.7227E-07
499 1.9240E-05 7.6827E-06 1.6910E-06 6.0185E-07 2.7480E-07
500 1.9227E-05 7.6931E-06 1.7001E-06 6.0577E-07 2.7693E-07
501 1.9252E-05 7.7218E-06 1.7104E-06 6.0967E-07 2.7871E-07

502 1.9366E-05 7.7861E-06 1.7288E-06 6.1640E-07 2.8181E-07
503 1.9539E-05 7.8746E-06 1.7525E-06 6.2507E-07 2.8578E-07
504 1.9625E-05 7.9283E-06 1.7685E-06 6.3098E-07 2.8851E-07
505 1.9601E-05 7.9376E-06 1.7747E-06 6.3339E-07 2.8960E-07
506 1.9603E-05 7.9574E-06 1.7832E-06 6.3663E-07 2.9110E-07
507 1.9643E-05 7.9927E-06 1.7951E-06 6.4109E-07 2.9315E-07
508 1.9705E-05 8.0264E-06 1.7987E-06 6.4337E-07 2.9288E-07
509 1.9769E-05 8.0478E-06 1.8034E-06 6.4481E-07 2.9456E-07
510 1.9844E-05 8.0694E-06 1.8074E-06 6.4503E-07 2.9425E-07
511 1.9931E-05 8.0934E-06 1.8123E-06 6.4608E-07 2.9464E-07
512 2.0031E-05 8.1418E-06 1.8176E-06 6.4872E-07 2.9504E-07
513 2.0157E-05 8.1934E-06 1.8317E-06 6.5103E-07 2.9711E-07
514 2.0207E-05 8.2081E-06 1.8311E-06 6.5281E-07 2.9688E-07
515 2.0187E-05 8.1784E-06 1.8288E-06 6.5158E-07 2.9683E-07
516 2.0153E-05 8.1634E-06 1.8222E-06 6.5092E-07 2.9546E-07
517 2.0141E-05 8.1553E-06 1.8219E-06 6.5015E-07 2.9444E-07
518 2.0144E-05 8.1628E-06 1.8243E-06 6.4936E-07 2.9628E-07
519 2.0147E-05 8.1722E-06 1.8253E-06 6.4962E-07 2.9598E-07
520 2.0146E-05 8.1662E-06 1.8248E-06 6.5116E-07 2.9629E-07
521 2.0115E-05 8.1554E-06 1.8221E-06 6.4859E-07 2.9525E-07
522 2.0088E-05 8.1457E-06 1.8201E-06 6.4802E-07 2.9377E-07
523 2.0075E-05 8.1478E-06 1.8172E-06 6.4714E-07 2.9380E-07
524 2.0060E-05 8.1496E-06 1.8154E-06 6.4539E-07 2.9211E-07
525 2.0045E-05 8.1391E-06 1.8100E-06 6.4240E-07 2.9097E-07
526 2.0037E-05 8.1392E-06 1.8054E-06 6.4054E-07 2.9002E-07
527 2.0035E-05 8.1302E-06 1.7994E-06 6.3850E-07 2.8874E-07
528 2.0038E-05 8.1096E-06 1.7925E-06 6.3679E-07 2.8793E-07
529 2.0046E-05 8.1096E-06 1.7883E-06 6.3383E-07 2.8584E-07
530 2.0002E-05 8.0780E-06 1.7797E-06 6.3078E-07 2.8535E-07
531 1.9951E-05 8.0385E-06 1.7700E-06 6.2880E-07 2.8364E-07
532 1.9923E-05 8.0027E-06 1.7666E-06 6.2445E-07 2.8303E-07
533 1.9902E-05 7.9721E-06 1.7556E-06 6.2405E-07 2.8327E-07
534 1.9873E-05 7.9436E-06 1.7541E-06 6.2262E-07 2.8236E-07
535 1.9810E-05 7.8830E-06 1.7443E-06 6.2184E-07 2.8180E-07
536 1.9747E-05 7.8585E-06 1.7404E-06 6.2189E-07 2.8264E-07
537 1.9663E-05 7.8196E-06 1.7367E-06 6.1874E-07 2.8220E-07
538 1.9545E-05 7.7703E-06 1.7311E-06 6.1815E-07 2.8243E-07
539 1.9463E-05 7.7317E-06 1.7298E-06 6.1999E-07 2.8307E-07
540 1.9435E-05 7.7347E-06 1.7346E-06 6.2371E-07 2.8501E-07
541 1.9416E-05 7.7355E-06 1.7420E-06 6.2712E-07 2.8757E-07
542 1.9390E-05 7.7335E-06 1.7459E-06 6.3019E-07 2.8916E-07
543 1.9316E-05 7.7183E-06 1.7505E-06 6.3262E-07 2.9793E-07
544 1.9232E-05 7.7076E-06 1.7553E-06 6.3519E-07 2.9135E-07
545 1.9158E-05 7.7017E-06 1.7611E-06 6.3637E-07 2.9250E-07
546 1.9086E-05 7.7073E-06 1.7650E-06 6.3898E-07 2.9427E-07
547 1.9030E-05 7.7195E-06 1.7745E-06 6.4297E-07 2.9559E-07
548 1.8943E-05 7.7128E-06 1.7760E-06 6.4372E-07 2.9606E-07
549 1.8926E-05 7.7434E-06 1.7867E-06 6.4869E-07 2.9799E-07

550 1.8912E-05 7.7808E-06 1.7963E-06 6.5186E-07 2.9947E-07
551 1.8913E-05 7.8010E-06 1.8054E-06 6.5486E-07 3.0053E-07
552 1.8942E-05 7.8382E-06 1.8156E-06 6.5986E-07 3.0254E-07
553 1.8982E-05 7.8785E-06 1.8273E-06 6.6213E-07 3.0364E-07
554 1.9004E-05 7.9199E-06 1.8356E-06 6.6600E-07 3.0602E-07
555 1.9033E-05 7.9617E-06 1.8437E-06 6.6878E-07 3.0660E-07
556 1.9076E-05 8.0020E-06 1.8477E-06 6.7174E-07 3.0762E-07
557 1.9135E-05 8.0289E-06 1.8576E-06 6.7346E-07 3.0886E-07
558 1.9203E-05 8.0724E-06 1.8664E-06 6.7716E-07 3.0990E-07
559 1.9279E-05 8.1292E-06 1.8739E-06 6.7982E-07 3.1199E-07
560 1.9364E-05 8.1799E-06 1.8833E-06 6.8072E-07 3.1153E-07
561 1.9446E-05 8.2021E-06 1.8882E-06 6.8287E-07 3.1294E-07
562 1.9536E-05 8.2315E-06 1.8912E-06 6.8366E-07 3.1236E-07
563 1.9625E-05 8.2641E-06 1.8989E-06 6.8599E-07 3.1270E-07
564 1.9706E-05 8.2840E-06 1.9008E-06 6.8532E-07 3.1258E-07
565 1.9793E-05 8.3010E-06 1.8990E-06 6.8563E-07 3.1227E-07
566 1.9899E-05 8.3413E-06 1.9059E-06 6.8419E-07 3.1166E-07
567 2.0010E-05 8.3598E-06 1.9079E-06 6.8500E-07 3.1222E-07
568 2.0114E-05 8.3954E-06 1.9117E-06 6.8593E-07 3.1084E-07
569 2.0225E-05 8.4041E-06 1.9123E-06 6.8636E-07 3.1124E-07
570 2.0314E-05 8.4338E-06 1.9122E-06 6.8466E-07 3.1113E-07
571 2.0367E-05 8.4295E-06 1.9061E-06 6.8319E-07 3.0882E-07
572 2.0394E-05 8.4162E-06 1.9004E-06 6.7837E-07 3.0717E-07
573 2.0396E-05 8.3985E-06 1.8892E-06 6.7480E-07 3.0653E-07
574 2.0409E-05 8.3803E-06 1.8834E-06 6.7191E-07 3.0424E-07
575 2.0437E-05 8.3600E-06 1.8769E-06 6.7718E-07 3.0314E-07
576 2.0430E-05 8.3477E-06 1.8717E-06 6.7115E-07 3.0328E-07
577 2.0425E-05 8.3230E-06 1.8688E-06 6.6739E-07 3.0280E-07
578 2.0404E-05 8.2979E-06 1.8634E-06 6.6668E-07 3.0347E-07
579 2.0377E-05 8.2814E-06 1.8596E-06 6.6777E-07 3.0360E-07
580 2.0330E-05 8.2343E-06 1.8546E-06 6.6709E-07 3.0326E-07
581 2.0287E-05 8.2201E-06 1.8563E-06 6.6771E-07 3.0491E-07
582 2.0251E-05 8.2021E-06 1.8608E-06 6.7088E-07 3.0739E-07
583 2.0227E-05 8.1901E-06 1.8657E-06 6.7423E-07 3.0818E-07
584 2.0199E-05 8.1945E-06 1.8716E-06 6.7790E-07 3.1216E-07
585 2.0159E-05 8.1894E-06 1.8791E-06 6.8246E-07 3.1321E-07
586 2.0105E-05 8.1773E-06 1.8830E-06 6.8323E-07 3.1521E-07
587 2.0048E-05 8.1742E-06 1.8868E-06 6.8678E-07 3.1702E-07
588 1.9975E-05 8.2730E-06 1.8943E-06 6.9024E-07 3.1912E-07
589 1.9921E-05 8.2001E-06 1.8942E-06 6.9273E-07 3.1999E-07
590 1.9856E-05 8.1803E-06 1.8983E-06 6.9216E-07 3.1944E-07
591 1.9794E-05 8.1619E-06 1.9013E-06 6.9594E-07 3.2118E-07
592 1.9713E-05 8.1466E-06 1.9009E-06 6.9461E-07 3.2063E-07
593 1.9654E-05 8.1295E-06 1.9005E-06 6.9394E-07 3.1979E-07
594 1.9592E-05 8.1356E-06 1.8999E-06 6.9320E-07 3.1923E-07
595 1.9531E-05 8.1204E-06 1.8943E-06 6.9042E-07 3.1878E-07
596 1.9476E-05 8.1153E-06 1.8879E-06 6.8816E-07 3.1650E-07
597 1.9450E-05 8.1159E-06 1.8865E-06 6.8717E-07 3.1503E-07

598 1.9399E-05 8.1001E-06 1.8815E-06 6.8335E-07 3.1308E-07
599 1.9367E-05 8.0956E-06 1.8777E-06 6.8120E-07 3.1136E-07
600 1.9354E-05 8.0966E-06 1.8750E-06 6.7828E-07 3.1094E-07
601 1.9344E-05 8.0883E-06 1.8684E-06 6.7619E-07 3.0846E-07
602 1.9488E-05 8.1109E-06 1.8722E-06 6.7561E-07 3.0809E-07
603 1.9508E-05 8.1184E-06 1.8679E-06 6.7502E-07 3.0885E-07
604 1.9544E-05 8.1354E-06 1.8681E-06 6.7401E-07 3.0889E-07
605 1.9562E-05 8.1292E-06 1.8631E-06 6.7350E-07 3.0632E-07
606 1.9585E-05 8.1282E-06 1.8632E-06 6.7114E-07 3.0666E-07
607 1.9614E-05 8.1433E-06 1.8650E-06 6.7247E-07 3.0706E-07
608 1.9644E-05 8.1638E-06 1.8649E-06 6.7249E-07 3.0733E-07
609 1.9706E-05 8.1695E-06 1.8692E-06 6.7373E-07 3.0812E-07
610 1.9763E-05 8.1963E-06 1.8744E-06 6.7710E-07 3.0905E-07
611 1.9826E-05 8.2022E-06 1.8820E-06 6.7906E-07 3.1075E-07
612 1.9887E-05 8.2213E-06 1.8913E-06 6.8238E-07 3.1250E-07
613 1.9956E-05 8.2456E-06 1.9013E-06 6.8691E-07 3.1461E-07
614 2.0016E-05 8.2570E-06 1.9092E-06 6.9085E-07 3.1703E-07
615 2.0071E-05 8.2863E-06 1.9164E-06 6.9574E-07 3.1825E-07
616 2.0106E-05 8.2973E-06 1.9255E-06 6.9937E-07 3.2145E-07
617 2.0136E-05 8.2989E-06 1.9311E-06 7.0289E-07 3.2246E-07
618 2.0174E-05 8.3206E-06 1.9424E-06 7.0678E-07 3.2482E-07
619 2.0221E-05 8.3424E-06 1.9509E-06 7.1299E-07 3.2778E-07
620 2.0247E-05 8.3640E-06 1.9577E-06 7.1514E-07 3.2750E-07
621 2.0227E-05 8.3479E-06 1.9574E-06 7.1456E-07 3.2812E-07
622 2.0184E-05 8.3316E-06 1.9559E-06 7.1169E-07 3.2625E-07
623 2.0098E-05 8.2948E-06 1.9387E-06 7.0448E-07 3.2402E-07
624 1.9987E-05 8.2284E-06 1.9158E-06 6.9557E-07 3.1813E-07
625 1.9870E-05 8.1946E-06 1.9023E-06 6.8832E-07 3.1428E-07
626 1.9751E-05 8.1331E-06 1.8813E-06 6.7894E-07 3.0962E-07
627 1.9617E-05 8.0732E-06 1.8627E-06 6.7004E-07 3.0508E-07
628 1.9526E-05 8.0189E-06 1.8454E-06 6.6299E-07 3.0256E-07
629 1.9420E-05 7.9717E-06 1.8288E-06 6.5624E-07 2.9660E-07
630 1.9351E-05 7.9424E-06 1.8175E-06 6.5029E-07 2.9481E-07
631 1.9277E-05 7.8999E-06 1.8035E-06 6.4557E-07 2.9205E-07
632 1.9159E-05 7.8433E-06 1.7856E-06 6.3819E-07 2.8740E-07
633 1.9013E-05 7.7660E-06 1.7602E-06 6.2707E-07 2.8348E-07
634 1.8865E-05 7.6899E-06 1.7341E-06 6.1592E-07 2.7690E-07
635 1.8676E-05 7.5972E-06 1.7074E-06 6.0417E-07 2.7153E-07
636 1.8480E-05 7.4912E-06 1.6714E-06 5.8997E-07 2.6517E-07
637 1.8294E-05 7.4049E-06 1.6398E-06 5.7708E-07 2.5844E-07
638 1.8124E-05 7.3119E-06 1.6132E-06 5.6507E-07 2.5209E-07
639 1.7956E-05 7.2138E-06 1.5808E-06 5.5518E-07 2.4716E-07
640 1.7843E-05 7.1392E-06 1.5590E-06 5.4462E-07 2.4334E-07
641 1.7704E-05 7.0497E-06 1.5370E-06 5.3491E-07 2.3909E-07
642 1.7584E-05 6.9805E-06 1.5154E-06 5.2812E-07 2.3552E-07
643 1.7483E-05 6.9126E-06 1.4975E-06 5.2176E-07 2.3329E-07
644 1.7413E-05 6.8616E-06 1.4866E-06 5.1899E-07 2.3225E-07
645 1.7386E-05 6.8287E-06 1.4800E-06 5.1836E-07 2.3250E-07

646 1.7402E-05 6.8061E-06 1.4824E-06 5.1961E-07 2.3347E-07
647 1.7469E-05 6.8204E-06 1.4945E-06 5.2666E-07 2.3791E-07
648 1.7517E-05 6.8234E-06 1.5041E-06 5.3234E-07 2.4109E-07
649 1.7472E-05 6.7844E-06 1.4965E-06 5.3059E-07 2.4096E-07
650 1.7299E-05 6.6968E-06 1.4731E-06 5.2338E-07 2.3708E-07
651 1.6921E-05 6.5324E-06 1.4320E-06 5.0729E-07 2.2906E-07
652 1.6491E-05 6.3449E-06 1.3881E-06 4.9153E-07 2.2070E-07
653 1.6151E-05 6.2044E-06 1.3519E-06 4.7796E-07 2.1605E-07
654 1.5877E-05 6.0877E-06 1.3278E-06 4.6897E-07 2.1115E-07
655 1.5647E-05 5.9809E-06 1.3056E-06 4.6267E-07 2.0854E-07
656 1.5453E-05 5.9038E-06 1.2900E-06 4.5747E-07 2.0483E-07
657 1.5270E-05 5.8321E-06 1.2736E-06 4.5034E-07 2.0216E-07
658 1.5104E-05 5.7678E-06 1.2595E-06 4.4502E-07 1.9939E-07
659 1.4953E-05 5.7116E-06 1.2514E-06 4.4011E-07 1.9611E-07
660 1.4817E-05 5.6531E-06 1.2346E-06 4.3372E-07 1.9351E-07
661 1.4689E-05 5.5943E-06 1.2220E-06 4.2959E-07 1.9134E-07
662 1.4574E-05 5.5377E-06 1.2084E-06 4.2482E-07 1.8831E-07
663 1.4464E-05 5.4769E-06 1.1941E-06 4.1872E-07 1.8570E-07
664 1.4361E-05 5.4372E-06 1.1841E-06 4.1556E-07 1.8388E-07
665 1.4274E-05 5.4051E-06 1.1742E-06 4.1142E-07 1.8242E-07
666 1.4176E-05 5.3568E-06 1.1633E-06 4.0685E-07 1.7981E-07
667 1.4063E-05 5.2954E-06 1.1503E-06 4.0193E-07 1.7815E-07
668 1.3919E-05 5.2292E-06 1.1321E-06 3.9462E-07 1.7442E-07
669 1.3740E-05 5.1470E-06 1.1102E-06 3.8607E-07 1.7061E-07
670 1.3550E-05 5.0634E-06 1.0852E-06 3.7715E-07 1.6622E-07
671 1.3362E-05 4.9712E-06 1.0630E-06 3.6926E-07 1.6286E-07
672 1.3183E-05 4.8844E-06 1.0447E-06 3.6208E-07 1.5999E-07
673 1.3006E-05 4.7991E-06 1.0246E-06 3.5461E-07 1.5666E-07
674 1.2812E-05 4.7116E-06 1.0058E-06 3.4828E-07 1.5423E-07
675 1.2606E-05 4.6159E-06 9.8405E-07 3.3996E-07 1.5094E-07
676 1.2369E-05 4.5130E-06 9.5614E-07 3.3024E-07 1.4597E-07
677 1.2114E-05 4.4060E-06 9.2946E-07 3.2012E-07 1.4056E-07
678 1.1840E-05 4.2831E-06 8.9791E-07 3.0821E-07 1.3588E-07
679 1.1600E-05 4.1777E-06 8.6951E-07 2.9916E-07 1.3033E-07
680 1.1407E-05 4.0923E-06 8.4838E-07 2.9019E-07 1.2642E-07
681 1.1329E-05 4.0437E-06 8.3648E-07 2.8504E-07 1.2417E-07
682 1.1522E-05 4.1022E-06 8.5554E-07 2.9260E-07 1.2657E-07
683 1.1822E-05 4.1937E-06 8.8127E-07 3.0213E-07 1.3096E-07
684 1.1655E-05 4.1100E-06 8.5696E-07 2.9279E-07 1.2614E-07
685 1.1138E-05 3.8996E-06 8.0341E-07 2.7171E-07 1.1745E-07
686 1.0680E-05 3.7065E-06 7.5869E-07 2.5643E-07 1.0875E-07
687 1.0381E-05 3.5762E-06 7.3426E-07 2.4703E-07 1.0519E-07
688 1.0164E-05 3.4695E-06 7.1217E-07 2.4024E-07 1.0151E-07
689 9.9126E-06 3.3572E-06 6.8675E-07 2.3102E-07 9.8166E-08
690 9.5392E-06 3.1941E-06 6.4473E-07 2.1519E-07 9.0438E-08
691 9.0491E-06 2.9887E-06 5.9057E-07 1.9358E-07 8.1096E-08
692 8.4981E-06 2.7646E-06 5.3441E-07 1.7322E-07 7.1764E-08
693 7.9742E-06 2.5554E-06 4.8310E-07 1.5476E-07 6.4395E-08

694 7.5001E-06 2.3644E-06 4.3910E-07 1.3988E-07 5.8684E-08
695 7.0357E-06 2.1836E-06 3.9914E-07 1.2640E-07 5.3390E-08
696 6.6058E-06 2.0181E-06 3.6500E-07 1.1587E-07 4.7482E-08
697 6.2283E-06 1.8722E-06 3.3711E-07 1.0632E-07 4.5151E-08
698 5.8921E-06 1.7425E-06 3.1354E-07 9.9506E-08 4.2097E-08
699 5.5714E-06 1.6244E-06 2.9098E-07 9.3015E-08 3.8871E-08
700 5.2297E-06 1.5025E-06 2.6944E-07 8.5532E-08 3.5712E-08
701 4.9043E-06 1.3890E-06 2.4987E-07 7.9695E-08 3.3625E-08
702 4.5833E-06 1.2853E-06 2.2932E-07 7.4639E-08 3.1463E-08
703 4.2838E-06 1.1893E-06 2.1379E-07 6.9115E-08 2.9407E-08
704 4.0046E-06 1.1048E-06 1.9924E-07 6.4730E-08 2.7931E-08
705 3.7592E-06 1.0340E-06 1.8840E-07 6.2572E-08 2.6505E-08
706 3.5319E-06 9.6926E-07 1.7847E-07 5.9170E-08 2.6544E-08
707 3.3381E-06 9.1644E-07 1.7274E-07 5.7672E-08 2.4933E-08
708 3.1750E-06 8.7532E-07 1.6710E-07 5.6344E-08 2.4559E-08
709 3.0316E-06 8.4336E-07 1.6612E-07 5.6876E-08 2.5415E-08
710 2.9119E-06 8.1830E-07 1.6629E-07 5.6750E-08 2.4975E-08
711 2.8002E-06 7.9486E-07 1.6556E-07 5.7886E-08 2.7111E-08
712 2.6871E-06 7.7429E-07 1.6595E-07 5.8678E-08 2.7674E-08
713 2.5449E-06 7.4278E-07 1.6255E-07 5.8367E-08 2.7701E-08
714 2.3680E-06 7.0472E-07 1.5645E-07 5.7417E-08 2.6330E-08
715 2.1866E-06 6.6145E-07 1.4762E-07 5.2835E-08 2.5196E-08
716 2.0082E-06 6.1845E-07 1.3782E-07 4.9729E-08 2.4538E-08
717 1.8495E-06 5.8104E-07 1.3204E-07 4.7684E-08 2.2281E-08
718 1.7171E-06 5.5095E-07 1.2498E-07 4.5951E-08 2.3009E-08
719 1.5964E-06 5.2324E-07 1.2031E-07 4.4769E-08 2.1377E-08
720 1.4838E-06 4.9740E-07 1.1629E-07 4.2793E-08 2.0356E-08
721 1.3855E-06 4.7485E-07 1.1222E-07 4.1620E-08 2.0022E-08
722 1.3052E-06 4.5777E-07 1.0999E-07 4.1145E-08 2.0151E-08
723 1.2432E-06 4.4684E-07 1.0891E-07 4.0700E-08 1.9472E-08
724 1.1958E-06 4.4029E-07 1.0790E-07 4.0890E-08 1.9952E-08
725 1.1624E-06 4.3856E-07 1.0941E-07 4.0768E-08 2.0998E-08
726 1.1428E-06 4.3925E-07 1.1113E-07 4.2185E-08 2.1044E-08
727 1.1387E-06 4.4856E-07 1.1623E-07 4.5535E-08 2.1766E-08
728 1.1486E-06 4.6320E-07 1.2189E-07 4.7314E-08 2.3575E-08
729 1.1566E-06 4.7454E-07 1.2622E-07 5.0193E-08 2.5055E-08
730 1.1544E-06 4.8212E-07 1.3009E-07 5.0728E-08 2.5065E-08
731 1.1769E-06 5.0038E-07 1.3629E-07 5.2923E-08 2.6120E-08
732 1.2285E-06 5.3216E-07 1.4538E-07 5.7737E-08 2.7558E-08
733 1.2607E-06 5.5453E-07 1.5304E-07 5.9969E-08 2.9848E-08
734 1.2406E-06 5.5094E-07 1.4984E-07 5.7548E-08 2.9029E-08
735 1.1734E-06 5.2743E-07 1.4170E-07 5.3985E-08 2.6642E-08
736 1.1087E-06 5.0090E-07 1.3317E-07 5.1922E-08 2.6025E-08
737 1.0824E-06 4.9352E-07 1.3238E-07 5.0123E-08 2.3790E-08
738 1.0832E-06 4.9639E-07 1.3278E-07 5.0331E-08 2.5562E-08
739 1.1032E-06 5.0979E-07 1.3858E-07 5.3764E-08 2.5598E-08
740 1.1332E-06 5.2656E-07 1.4396E-07 5.6149E-08 2.6662E-08
741 1.1553E-06 5.4081E-07 1.4706E-07 5.6215E-08 2.8454E-08

742 1.1623E-06 5.4283E-07 1.4796E-07 5.6175E-08 2.7609E-08
743 1.1557E-06 5.3895E-07 1.4407E-07 5.4670E-08 2.8116E-08
744 1.1435E-06 5.3124E-07 1.3904E-07 5.3161E-08 2.5390E-08
745 1.1306E-06 5.2340E-07 1.3538E-07 5.0490E-08 2.4670E-08
746 1.1239E-06 5.1851E-07 1.3136E-07 4.9373E-08 2.3748E-08
747 1.1256E-06 5.1358E-07 1.2941E-07 4.7564E-08 2.2677E-08
748 1.1400E-06 5.1610E-07 1.3219E-07 4.6628E-08 2.2553E-08
749 1.1674E-06 5.2546E-07 1.3050E-07 4.7744E-08 2.2292E-08
750 1.1860E-06 5.2758E-07 1.3120E-07 4.7397E-08 2.2074E-08
751 1.1850E-06 5.2339E-07 1.2851E-07 4.5682E-08 2.2930E-08
752 1.1796E-06 5.1453E-07 1.2512E-07 4.5824E-08 2.1931E-08
753 1.1809E-06 5.0859E-07 1.1993E-07 4.3184E-08 2.0218E-08
754 1.1643E-06 4.9296E-07 1.1694E-07 4.2982E-08 1.9719E-08
755 1.1386E-06 4.7404E-07 1.1050E-07 4.0115E-08 1.8190E-08
756 1.1235E-06 4.5970E-07 1.0561E-07 3.7623E-08 1.8509E-08
757 1.1153E-06 4.4848E-07 1.0194E-07 3.7157E-08 1.7679E-08
758 1.1130E-06 4.4044E-07 1.0065E-07 3.5751E-08 1.5876E-08
759 1.1187E-06 4.3545E-07 9.8133E-08 3.4388E-08 1.5746E-08
760 1.1361E-06 4.3544E-07 9.7146E-08 3.4417E-08 1.7320E-08
761 1.1521E-06 4.3357E-07 9.7221E-08 3.4615E-08 1.7832E-08
762 1.1797E-06 4.3753E-07 9.6562E-08 3.5194E-08 1.5145E-08
763 1.4047E-06 5.1245E-07 1.1422E-07 4.1132E-08 1.9174E-08
764 1.9212E-06 6.9497E-07 1.5947E-07 5.6681E-08 2.7581E-08
765 2.0229E-06 7.1991E-07 1.6377E-07 5.7683E-08 2.7659E-08
766 1.5250E-06 5.3187E-07 1.1594E-07 4.0536E-08 1.9278E-08
767 1.1434E-06 3.9057E-07 8.3371E-08 3.0807E-08 1.5219E-08
768 9.5329E-07 3.2227E-07 7.0159E-08 2.5949E-08 1.2428E-08
769 8.4417E-07 2.8256E-07 6.3692E-08 2.3133E-08 1.0463E-08
770 7.7448E-07 2.5556E-07 5.7093E-08 2.1866E-08 9.7399E-09
771 7.1933E-07 2.3754E-07 5.5500E-08 1.9631E-08 8.3205E-09
772 6.7502E-07 2.2431E-07 5.1432E-08 1.9451E-08 8.8218E-09
773 6.3648E-07 2.1013E-07 4.9647E-08 1.6962E-08 8.6421E-09
774 5.9376E-07 1.9531E-07 4.7266E-08 1.7625E-08 9.0649E-09
775 5.5136E-07 1.8204E-07 4.4378E-08 1.6544E-08 8.5764E-09
776 5.1762E-07 1.7261E-07 4.3275E-08 1.5357E-08 1.1389E-08
777 4.8897E-07 1.6355E-07 3.9828E-08 1.5159E-08 9.4811E-09
778 4.6254E-07 1.5863E-07 4.0867E-08 1.5323E-08 8.6282E-09
779 4.4193E-07 1.5250E-07 3.9898E-08 1.4947E-08 7.3758E-09
780 4.2301E-07 1.5042E-07 3.9666E-08 1.4933E-08 9.0359E-09
781 4.0952E-07 1.4671E-07 3.8789E-08 1.4794E-08 7.8775E-09
782 3.9731E-07 1.4592E-07 3.8806E-08 1.5527E-08 8.5096E-09
783 3.8538E-07 1.4286E-07 3.9713E-08 1.4380E-08 8.9204E-09
784 3.7094E-07 1.4027E-07 3.9104E-08 1.6018E-08 8.9786E-09
785 3.5708E-07 1.3835E-07 3.9957E-08 1.6084E-08 5.1894E-09
786 3.4757E-07 1.3609E-07 4.0614E-08 1.4768E-08 8.0198E-09
787 3.4609E-07 1.3965E-07 4.0711E-08 1.6155E-08 9.2891E-09
788 3.6606E-07 1.5058E-07 4.4758E-08 1.8056E-08 1.0724E-08
789 4.1250E-07 1.7334E-07 5.2420E-08 2.0605E-08 1.1346E-08

790 4.2797E-07 1.8116E-07 5.6454E-08 2.2034E-08 1.2599E-08
791 3.9705E-07 1.7168E-07 5.0640E-08 2.0208E-08 1.2572E-08
792 3.5927E-07 1.5647E-07 4.6202E-08 1.7612E-08 9.9191E-09
793 3.3729E-07 1.5004E-07 4.5558E-08 1.5700E-08 7.6727E-09
794 3.2592E-07 1.4754E-07 4.5482E-08 1.9073E-08 1.1359E-08
795 3.2719E-07 1.5217E-07 4.5862E-08 1.8165E-08 1.1367E-08
796 3.4425E-07 1.6046E-07 4.9964E-08 2.1181E-08 1.0200E-08
797 3.6854E-07 1.7592E-07 5.4935E-08 2.3272E-08 1.3559E-08
798 3.7966E-07 1.8050E-07 5.6391E-08 2.3649E-08 1.2802E-08
799 3.7646E-07 1.8261E-07 5.7290E-08 2.3458E-08 1.2710E-08
800 3.6826E-07 1.8008E-07 5.6020E-08 2.2876E-08 1.2396E-08
801 3.6042E-07 1.7783E-07 5.5119E-08 2.1948E-08 1.3846E-08
802 3.5338E-07 1.7468E-07 5.5739E-08 2.2983E-08 1.2554E-08
803 3.4939E-07 1.7199E-07 5.6573E-08 2.3951E-08 1.2490E-08
804 3.4869E-07 1.7656E-07 5.6624E-08 2.3719E-08 1.3646E-08
805 3.5268E-07 1.7861E-07 5.8499E-08 2.5428E-08 1.5673E-08
806 3.6223E-07 1.8437E-07 6.1608E-08 2.5585E-08 1.3853E-08
807 3.7673E-07 1.9486E-07 6.4911E-08 2.8442E-08 1.6467E-08
808 3.9225E-07 2.0422E-07 6.8969E-08 3.0300E-08 1.8597E-08
809 4.0833E-07 2.1480E-07 7.2626E-08 3.1284E-08 1.5831E-08
810 4.2186E-07 2.2221E-07 7.5412E-08 3.0088E-08 1.9012E-08
811 4.3524E-07 2.3117E-07 7.7307E-08 3.1881E-08 1.8029E-08
812 4.5042E-07 2.3808E-07 7.7432E-08 3.3408E-08 1.6623E-08
813 4.6796E-07 2.5112E-07 8.0756E-08 3.4756E-08 1.7435E-08
814 4.8998E-07 2.6385E-07 8.5257E-08 3.5888E-08 1.9645E-08
815 5.1834E-07 2.7865E-07 8.8983E-08 3.5779E-08 1.6629E-08
816 5.5836E-07 2.9952E-07 9.4949E-08 3.9210E-08 2.1896E-08
817 6.2225E-07 3.3513E-07 1.0228E-07 4.2777E-08 2.0325E-08
818 7.0853E-07 3.7873E-07 1.1324E-07 4.5268E-08 2.3917E-08
819 8.4285E-07 4.4981E-07 1.3041E-07 5.0039E-08 2.4685E-08
820 1.1037E-06 5.8648E-07 1.6966E-07 6.7829E-08 3.2470E-08
821 1.6390E-06 8.6652E-07 2.5250E-07 9.6760E-08 4.4173E-08
822 3.0350E-06 1.6178E-06 4.9807E-07 1.9752E-07 9.2391E-08
823 5.4443E-06 2.9458E-06 9.5030E-07 3.8355E-07 1.7904E-07
824 6.0161E-06 3.1998E-06 9.8544E-07 3.8981E-07 1.7524E-07
825 4.4288E-06 2.2580E-06 6.2313E-07 2.3438E-07 9.9905E-08
826 3.1828E-06 1.5692E-06 3.9705E-07 1.3995E-07 5.9681E-08
827 3.3132E-06 1.6062E-06 4.1806E-07 1.4921E-07 6.6903E-08
828 4.0454E-06 1.9437E-06 5.0875E-07 1.8418E-07 7.8804E-08
829 3.3420E-06 1.5479E-06 3.7738E-07 1.3331E-07 5.9768E-08
830 2.0096E-06 8.8475E-07 1.9529E-07 6.4677E-08 2.9993E-08
831 1.3854E-06 5.8273E-07 1.2559E-07 4.4165E-08 1.8786E-08
832 1.2250E-06 4.9800E-07 1.0506E-07 3.8068E-08 1.1495E-08
833 1.4274E-06 5.6739E-07 1.2226E-07 4.0745E-08 1.5093E-08
834 2.1775E-06 8.5018E-07 1.9492E-07 6.7984E-08 2.8612E-08
835 2.5319E-06 9.6270E-07 2.1917E-07 7.8646E-08 3.3213E-08
836 1.7964E-06 6.5190E-07 1.3780E-07 4.8664E-08 2.1334E-08
837 1.1476E-06 3.9566E-07 8.1421E-08 2.6362E-08 1.0895E-08

838 8.3610E-07 2.7840E-07 5.8310E-08 1.9943E-08 1.1001E-08
839 7.0677E-07 2.3024E-07 5.0041E-08 1.4560E-08 8.7809E-09
840 8.3639E-07 2.6952E-07 6.1371E-08 2.2176E-08 9.7824E-09
841 1.0874E-06 3.4318E-07 8.0109E-08 3.0188E-08 1.4726E-08
842 8.6804E-07 2.7171E-07 6.1635E-08 2.3188E-08 1.1835E-08
843 5.3577E-07 1.5975E-07 3.6544E-08 1.2942E-08 1.0013E-08
844 3.9638E-07 1.1953E-07 2.9127E-08 9.4180E-09 5.5783E-09
845 3.2664E-07 9.8048E-08 2.5386E-08 1.0468E-08 3.5062E-09
846 2.8168E-07 8.5690E-08 2.4225E-08 9.5551E-09 2.0583E-09
847 2.4953E-07 7.5977E-08 2.0671E-08 8.0314E-09 3.7095E-09
848 2.2360E-07 6.4672E-08 2.1597E-08 7.0716E-09 4.5968E-09
849 2.0256E-07 6.1886E-08 2.0345E-08 7.7366E-09 3.0751E-09
850 1.8528E-07 5.8482E-08 1.8600E-08 7.0747E-09 1.9467E-09
851 1.7217E-07 5.5704E-08 1.7513E-08 5.3906E-09 2.5850E-09
852 1.5985E-07 5.2225E-08 1.6719E-08 6.0092E-09 4.3321E-09
853 1.5012E-07 4.8852E-08 1.7837E-08 7.8125E-09 2.9584E-09
854 1.4249E-07 3.8606E-08 1.4026E-08 6.1378E-09 1.7706E-09
855 1.3493E-07 4.6717E-08 1.5023E-08 6.7335E-09 2.3371E-09
856 1.2805E-07 4.1757E-08 1.6886E-08 5.9402E-09 3.9553E-09
857 1.2323E-07 4.2608E-08 1.6110E-08 5.8129E-09 2.0313E-09
858 1.2001E-07 4.4374E-08 1.6210E-08 5.8627E-09 4.2841E-09
859 1.1621E-07 4.1710E-08 1.5750E-08 6.2363E-09 4.2492E-09
860 1.1127E-07 4.0028E-08 1.7735E-08 7.3321E-09 1.9116E-09
861 1.0560E-07 4.0988E-08 1.5254E-08 5.6041E-09 2.5948E-09
862 1.0304E-07 3.8116E-08 1.5031E-08 6.6546E-09 3.4682E-09
863 1.0073E-07 4.0047E-08 1.5007E-08 6.0132E-09 3.2148E-09
864 1.0229E-07 4.0307E-08 1.6635E-08 6.8168E-09 3.2198E-09
865 1.0519E-07 4.3479E-08 1.5592E-08 6.0442E-09 2.9347E-09
866 1.0937E-07 4.4690E-08 1.5695E-08 4.2070E-09 2.2581E-09
867 1.0785E-07 4.4120E-08 1.6721E-08 6.9604E-09 2.9080E-09
868 1.0801E-07 4.4605E-08 2.0268E-08 6.9162E-09 3.1810E-09
869 1.0952E-07 4.7124E-08 1.9452E-08 7.0565E-09 1.4291E-09
870 1.1153E-07 4.7506E-08 1.9634E-08 6.7724E-09 2.9124E-09
871 1.1425E-07 5.0263E-08 2.1180E-08 7.9553E-09 2.5656E-09
872 1.2055E-07 5.2729E-08 2.1716E-08 8.4696E-09 4.7052E-09
873 1.2078E-07 5.1040E-08 2.2920E-08 8.5678E-09 4.6493E-09
874 1.2586E-07 5.5105E-08 2.2102E-08 8.5200E-09 2.8779E-09
875 1.3110E-07 5.8686E-08 2.3601E-08 9.8502E-09 5.4268E-09
876 1.3811E-07 6.2335E-08 2.5746E-08 9.3732E-09 6.3453E-09
877 1.4876E-07 6.7751E-08 2.5637E-08 9.7975E-09 4.3243E-09
878 1.6981E-07 7.5908E-08 3.0140E-08 1.1168E-08 5.9321E-09
879 2.1656E-07 9.6270E-08 3.6339E-08 1.5509E-08 7.3903E-09
880 3.3110E-07 1.5109E-07 5.3661E-08 2.3564E-08 1.3266E-08
881 5.7035E-07 2.7239E-07 1.0262E-07 4.6829E-08 2.6985E-08
882 7.6319E-07 3.7388E-07 1.4558E-07 6.8123E-08 3.6804E-08
883 7.3475E-07 3.5655E-07 1.3675E-07 6.0835E-08 3.3061E-08
884 5.6266E-07 2.6690E-07 1.0016E-07 4.3657E-08 2.3583E-08
885 3.9832E-07 1.8725E-07 6.9463E-08 3.0352E-08 1.6425E-08

886 2.9292E-07 1.3864E-07 5.2110E-08 2.1017E-08 1.2492E-08
887 2.3203E-07 1.1065E-07 4.2891E-08 1.8169E-08 9.7165E-09
888 1.9680E-07 9.4669E-08 3.6050E-08 1.4768E-08 9.3468E-09
889 1.7359E-07 8.5748E-08 3.3024E-08 1.3671E-08 8.4491E-09
890 1.6137E-07 7.7863E-08 3.0639E-08 1.2820E-08 7.3786E-09
891 1.6026E-07 7.9809E-08 3.1251E-08 1.3812E-08 7.7811E-09
892 1.6692E-07 8.3303E-08 3.4402E-08 1.3503E-08 8.6516E-09
893 1.9590E-07 9.8620E-08 4.0142E-08 1.5747E-08 9.6120E-09
894 2.8738E-07 1.4811E-07 6.0399E-08 2.9508E-08 1.7857E-08
895 4.2944E-07 2.2070E-07 8.9646E-08 4.4095E-08 2.4119E-08
896 4.1505E-07 2.1415E-07 8.4023E-08 3.9273E-08 2.2815E-08
897 2.8870E-07 1.5007E-07 5.7769E-08 2.7150E-08 1.3048E-08
898 2.1617E-07 1.1191E-07 4.4479E-08 2.0597E-08 1.1821E-08
899 1.8270E-07 9.6250E-08 3.9586E-08 1.8935E-08 1.0102E-08
900 1.6157E-07 8.6285E-08 3.5555E-08 1.5184E-08 9.3909E-09
901 1.4929E-07 7.9819E-08 3.3325E-08 1.4717E-08 9.4296E-09
902 1.5359E-07 8.2767E-08 3.3943E-08 1.4597E-08 9.4260E-09
903 2.1468E-07 1.1739E-07 4.7983E-08 2.1539E-08 1.1205E-08
904 4.3109E-07 2.4270E-07 1.0321E-07 4.8243E-08 2.8411E-08
905 5.3503E-07 2.9818E-07 1.2538E-07 6.1309E-08 3.3429E-08
906 3.5933E-07 1.9703E-07 7.9836E-08 3.6939E-08 2.2058E-08
907 2.1383E-07 1.1717E-07 4.7855E-08 2.1215E-08 1.2576E-08
908 1.5520E-07 8.5476E-08 3.4482E-08 1.7300E-08 1.0906E-08
909 1.3327E-07 7.3688E-08 3.1104E-08 1.4033E-08 9.1201E-09
910 1.2692E-07 7.2908E-08 3.0726E-08 1.3184E-08 7.4829E-09
911 1.3032E-07 7.5010E-08 3.2098E-08 1.3981E-08 9.2407E-09
912 1.4573E-07 8.3490E-08 3.4413E-08 1.7281E-08 7.8551E-09
913 1.7926E-07 1.0518E-07 4.3696E-08 2.0952E-08 1.1088E-08
914 2.6283E-07 1.5611E-07 6.8013E-08 3.2814E-08 1.8276E-08
915 4.6546E-07 2.8102E-07 1.2509E-07 6.1152E-08 3.6140E-08
916 7.3494E-07 4.4986E-07 2.0392E-07 1.0387E-07 5.9351E-08
917 7.4202E-07 4.5248E-07 2.0245E-07 1.0135E-07 5.8070E-08
918 5.3865E-07 3.2534E-07 1.4172E-07 6.7687E-08 3.9439E-08
919 3.8406E-07 2.3329E-07 1.0009E-07 4.8488E-08 2.8268E-08
920 3.0492E-07 1.8691E-07 8.0075E-08 3.7929E-08 2.2151E-08
921 2.6555E-07 1.6564E-07 7.1507E-08 3.3170E-08 1.9467E-08
922 2.4104E-07 1.5059E-07 6.5676E-08 3.0046E-08 1.7368E-08
923 2.1729E-07 1.3710E-07 5.8581E-08 2.7246E-08 1.7245E-08
924 1.9762E-07 1.2513E-07 5.5025E-08 2.4594E-08 1.5920E-08
925 1.8167E-07 1.1627E-07 5.2161E-08 2.2318E-08 1.4465E-08
926 1.7033E-07 1.1127E-07 4.8658E-08 2.3006E-08 1.3099E-08
927 1.6455E-07 1.0718E-07 4.6666E-08 2.0697E-08 1.2466E-08
928 1.6401E-07 1.0666E-07 4.5936E-08 2.1118E-08 1.3028E-08
929 1.7052E-07 1.1484E-07 4.8150E-08 2.2536E-08 1.2086E-08
930 1.8537E-07 1.2206E-07 5.3707E-08 2.4445E-08 1.4634E-08
931 2.0175E-07 1.3573E-07 6.0117E-08 2.7872E-08 1.5765E-08
932 2.1219E-07 1.4364E-07 6.2441E-08 2.9342E-08 1.5792E-08
933 2.2145E-07 1.4959E-07 6.4207E-08 2.9127E-08 1.5347E-08

934 2.3577E-07 1.6080E-07 6.7668E-08 3.0603E-08 1.7400E-08
935 2.6387E-07 1.8014E-07 7.5129E-08 3.3802E-08 1.9635E-08
936 3.2364E-07 2.2329E-07 9.6380E-08 4.5290E-08 2.4033E-08
937 4.3298E-07 3.0133E-07 1.3213E-07 6.5484E-08 3.5951E-08
938 5.5505E-07 3.9081E-07 1.7543E-07 8.4057E-08 4.6866E-08
939 6.0334E-07 4.2460E-07 1.8555E-07 9.0217E-08 4.8590E-08
940 5.9738E-07 4.1968E-07 1.7795E-07 8.4655E-08 4.5661E-08
941 5.8329E-07 4.0831E-07 1.6932E-07 7.8820E-08 4.2798E-08
942 5.6656E-07 3.9637E-07 1.5944E-07 7.3460E-08 3.9859E-08
943 5.6092E-07 3.9172E-07 1.5600E-07 7.0782E-08 3.8378E-08
944 5.8818E-07 4.1149E-07 1.6293E-07 7.4699E-08 3.9267E-08
945 6.3823E-07 4.4746E-07 1.7757E-07 8.0653E-08 4.1520E-08
946 6.7558E-07 4.7372E-07 1.8385E-07 8.3245E-08 4.3680E-08
947 7.0135E-07 4.9104E-07 1.8650E-07 8.3124E-08 4.2106E-08
948 7.3939E-07 5.1497E-07 1.9471E-07 8.4956E-08 4.3475E-08
949 8.1115E-07 5.6448E-07 2.1320E-07 9.5124E-08 4.5995E-08
950 9.1138E-07 6.3598E-07 2.4466E-07 1.0915E-07 5.4865E-08
951 9.9063E-07 6.8924E-07 2.6828E-07 1.2064E-07 5.9593E-08
952 9.7330E-07 6.7204E-07 2.5462E-07 1.1220E-07 5.3977E-08
953 8.8957E-07 6.0659E-07 2.2093E-07 9.4134E-08 4.6272E-08
954 7.9196E-07 5.3384E-07 1.8388E-07 7.6410E-08 3.6734E-08
955 7.0544E-07 4.6691E-07 1.5496E-07 6.3299E-08 2.8755E-08
956 6.3834E-07 4.1623E-07 1.3193E-07 5.1301E-08 2.4837E-08
957 5.8897E-07 3.7788E-07 1.1524E-07 4.3108E-08 2.0824E-08
958 5.5592E-07 3.5218E-07 1.0377E-07 3.8867E-08 1.9101E-08
959 5.3625E-07 3.3322E-07 9.6026E-08 3.4250E-08 1.5709E-08
960 5.2259E-07 3.2096E-07 9.0063E-08 3.2373E-08 1.5851E-08
961 5.1859E-07 3.1357E-07 8.6511E-08 2.9952E-08 1.4672E-08
962 5.2261E-07 3.1017E-07 8.3832E-08 3.0456E-08 1.4093E-08
963 5.3454E-07 3.1267E-07 8.3276E-08 2.9689E-08 1.2848E-08
964 5.5936E-07 3.2156E-07 8.3278E-08 2.8589E-08 1.3699E-08
965 5.9883E-07 3.3811E-07 8.7800E-08 2.9575E-08 1.4005E-08
966 6.5798E-07 3.6565E-07 9.3538E-08 3.2892E-08 1.4069E-08
967 7.4640E-07 4.1086E-07 1.0597E-07 3.7510E-08 1.7810E-08
968 8.6104E-07 4.6722E-07 1.2366E-07 4.3427E-08 2.1074E-08
969 9.6608E-07 5.1627E-07 1.3670E-07 4.8484E-08 2.4423E-08
970 1.0279E-06 5.3837E-07 1.4083E-07 5.0101E-08 2.2991E-08
971 1.0715E-06 5.4958E-07 1.4160E-07 4.9541E-08 2.4101E-08
972 1.1003E-06 5.5170E-07 1.4043E-07 4.9461E-08 2.3857E-08
973 1.0946E-06 5.3501E-07 1.3218E-07 4.6843E-08 2.2610E-08
974 1.0833E-06 5.1371E-07 1.2176E-07 4.3123E-08 2.0030E-08
975 1.1095E-06 5.1321E-07 1.1707E-07 4.1763E-08 2.0210E-08
976 1.2287E-06 5.5119E-07 1.2385E-07 4.2071E-08 2.0403E-08
977 1.5588E-06 6.8517E-07 1.5235E-07 5.3665E-08 2.5496E-08
978 2.3519E-06 1.0306E-06 2.4185E-07 8.8119E-08 4.3496E-08
979 3.7935E-06 1.6909E-06 4.4851E-07 1.7271E-07 8.4299E-08
980 4.4389E-06 1.9614E-06 5.4239E-07 2.1369E-07 1.0662E-07
981 3.2832E-06 1.3859E-06 3.6073E-07 1.3827E-07 6.8685E-08

982 1.9503E-06 7.8853E-07 1.8839E-07 7.0607E-08 3.5371E-08
983 1.2454E-06 4.8953E-07 1.1390E-07 4.1020E-08 2.1933E-08
984 9.4401E-07 3.6547E-07 8.5259E-08 3.0188E-08 1.6633E-08
985 8.0676E-07 3.0870E-07 7.2721E-08 2.8153E-08 1.4251E-08
986 7.6417E-07 2.8773E-07 6.9175E-08 2.5237E-08 1.3241E-08
987 8.1754E-07 3.0657E-07 7.4053E-08 2.8654E-08 1.6097E-08
988 9.8124E-07 3.6672E-07 9.0424E-08 3.5446E-08 1.9769E-08
989 1.1923E-06 4.4265E-07 1.1173E-07 4.3761E-08 2.3476E-08
990 1.6234E-06 6.1037E-07 1.6231E-07 6.5766E-08 3.5406E-08
991 2.7048E-06 1.0421E-06 3.0464E-07 1.2980E-07 6.7539E-08
992 3.8678E-06 1.5002E-06 4.6228E-07 1.9881E-07 1.0525E-07
993 3.6996E-06 1.4083E-06 4.2464E-07 1.8209E-07 9.3670E-08
994 2.5984E-06 9.6666E-07 2.7265E-07 1.1422E-07 5.9449E-08
995 1.7401E-06 6.4481E-07 1.7754E-07 7.3116E-08 3.8590E-08
996 1.2382E-06 4.6288E-07 1.2680E-07 5.2706E-08 2.9317E-08
997 9.5692E-07 3.6162E-07 1.0104E-07 4.2214E-08 2.4010E-08
998 7.8665E-07 3.0192E-07 8.5674E-08 3.5387E-08 2.1823E-08
999 6.8177E-07 2.6702E-07 7.6985E-08 3.3336E-08 2.0379E-08